THE EFFECT OF COAL SYN GAS CONTAINING HYDROGEN SULFIDE ON THE OPERATION OF A PLANAR SOLID OXIDE FUEL

A thesis presented to

the faculty of the

Fritz J. and Dolores H. Russ

College of Engineering and Technology

of Ohio University

In partial fulfillment

of the requirements for the degree

Master of Science

Jason P. Trembly

March 2005

This thesis entitled

THE EFFECT OF COAL SYN GAS CONTAINING HYDROGEN SULFIDE ON THE OPERATION OF A PLANAR SOLID OXIDE FUEL CELL

by

Jason P. Trembly

has been approved

for the Department of Chemical Engineering

and the Russ College of Engineering and Technology by

David J. Bayless

Associate Professor of Mechanical Engineering

Dennis Irwin

Dean, Russ College of Engineering and Technology

Trembly, Jason P. March 2005. Chemical Engineering

The Effect of Coal Syn Gas Containing Hydrogen Sulfide on the Operation of a Planar Solid Oxide Fuel Cell (153pp.)

Director of Thesis: David Bayless

Planar solid oxide fuel cell (PSOFC) research at Ohio University has shown that the PSOFC may be used to produce electrical energy using gasified Ohio coal. Electrolyte supported PSOFCs with an anode containing nickel, yttria stabilized zirconium, and cerium oxide were operated for over 500 hours. PSOFCs were tested by supplying the fuel cell with a simulated coal syn gas and assessing the performance of the fuel cell by operating it under a load of 14 Amps and measuring the fuel cell's potential and area specific resistance (ASR). PSOFCs used in the research were found to have a potential of 0.74±0.01 Volts under a load of 0.21±0.01 Amps/cm^2 and an ASR increase of 0.10±0.16 percent per 100 hours of operation with out H_2S and have a potential of 0.66±0.01 Volts under a load of 0.21±0.01 Amps/cm^2 and an ASR increase of 5.4±2.8 percent per 100 hours of operation with 249±9 ppm H_2S.

Approved:

David Bayless

Associate Professor of Mechanical Engineering

Acknowledgements

I would like to express my full gratitude to my advisor Dr. David Bayless for encouragement, mentoring, time, and financial assistance. I am also very grateful to my other committee members Dr. Gerardine Botte who has made electrochemistry very enjoyable for me, Dr. Gregory Kremer, and Dr. Ben Stuart for all their time and help during my research work. Thanks are also needed for Dr. Andres Marquez who has been very helpful answering my questions when I have been in doubt. I would like to acknowledge and thank the Ohio Coal Research Center coordinators Shyler Switzer and Patrick Curran and the undergraduate staff for their time and effort in the development of the PSOFC testing systems and SOFCo EFS for providing valuable research space. Also I would like to thank my family and friends who have always encouraged me to achieve my goals.

Table of Contents

Abstract……...iii

Acknowledgements……iv

List of Tables……viii

List of Figures……ix

Chapter – 1 Introduction 1

1.1. Introduction 1

1.2. PSOFC Construction 6

1.3. Significance of Research 13

1.4. Goals and Objectives 14

Chapter – 2 Literature Review 16

2.1. Introduction 16

2.2. Literature Review 16

Chapter – 3 Experimental Plan 26

3.1. Planned Approach 26

Chapter – 4 Experimental Methods 35

4.1. Test Cell Characteristics 35

4.2. Mass Flow Controller Calibration 35

4.3. Ambient Pressure Experimental Setup 37

4.4. Single Cell Test Stand Heating 49

4.5. Electrochemical Measurements 50

4.6. Material Analyses 59

4.6.1. SEM and EDXS Analyses 59

4.6.2. XRD Analyses 59

Chapter – 5 Experimental Results 61

5.1. Introduction 61

5.2. Testing Difficulties 61

5.3. Research Test Matrix 61

5.4. Trial Four 62

5.4.1. Trial Four Initial PSOFC Operation 63

5.4.2. Trial 4 PSOFC Operation with Baseline Simulated Coal Syn Gas 69

5.4.3. Material Analysis of PSOFC KS1S040318-1 76

5.4.4. Baseline Anode Material Analysis 76

5.4.5. Trial 4 Anode Material Analyses 83

5.5. Trial 5 88

5.5.1. Trial 5 Initial PSOFC Operation 89

5.5.2. Trial 5 Operation with Simulated Coal Syn Gas 93

5.5.3. Trial 5 Anode Material Analyses 99

5.6. Trial Six 105

5.6.1. Trial 6 Initial PSOFC Operation 105

5.6.2. PSOFC Operation with Simulated Coal Syn Gas Containing H_2S 108

5.6.3. Trial 6 Anode Mateial Analyses 113

5.7. Overview of Results 118

Chapter – 6 Conclusions 123

6.1. Introduction 123

6.2. Operation of PSOFC Utilizing Simulated Baseline Coal Syn Gas 123

6.3. Operation of PSOFC Utilizing Simulated Coal Syn Gas Containing H_2S . 125

6.4. Recommendations 126

6.4.1. ASR Degradation Determination 126

6.4.2. PSOFC Testing Setup 127

6.4.3. Operation of Single Cell Test Stand 129

6.4.4. Pressurized PSOFC Testing Chamber 130

6.4.5. Sulfur Tolerant Anode Materials 130

References……132

Appendix 1……..135

Appendix 2……...136

List of Tables

Table 1.1 Comparison of Emissions Produced by Conventional Power Generation and PSOFCs. 5

Table 3.1 Fuel Gas and Oxidant Molar Compositions. 27

Table 4.1 MFC Gains and Errors. 36

Table 4.2 Accepted MFC Errors. 36

Table 5.1 Completed Research Test Matrix. 62

Table 5.2 Initial Anode Gas Composition. 62

Table 5.3 Calculated PSOFC ASRs Using H_2/N_2 Anode Gas. 68

Table 5.4 SCGS Composition Comparison. 70

Table 5.5 O_2 Blown Pittsburgh No.8 Syn Gas Composition. 70

Table 5.6 Calculated PSOFC ASRs Using Simulated Coal Syn Gas. 73

Table 5.7 Trial 4 Initial Anode Gas Composition 89

Table 5.8 Calculated PSOFC ASRs Using H_2/N_2 Anode Gas. 92

Table 5.9 Trial 5 Simulated Baseline 94

Table 5.10 Trial 5 Calculated PSOFC ASRs. 97

Table 5.11 Trial 6 Simulated Coal Syn Gas Composition 108

Table 5.12 Trial 6 Calculated PSOFC ASRs 108

Table 5.13 Simulated Coal Syn Gas 109

Table 5.14 Trial 6 Calculated PSOFC ASRs Utilizing Simulated Coal Syn Gas Containing H_2S. 111

List of Figures

Figure 1.1 PSOFC Diagram 7

Figure 2.1 Sulfur Adsorption onto Nickel at the PSOFC Anode Interface. 21

Figure 3.1 PSOFC Testing Apparatus. 26

Figure 4.1 Placement of Anode Manifold into Single Cell Test Stand. 38

Figure 4.2 Positioning of Manifold Thermocouple. 38

Figure 4.3 Layer of NiO Ink Being Applied to Anode Manifold. 39

Figure 4.4 Nickel Foam Prepared with NiO Ink. 40

Figure 4.5 Placement of Incanel Ribbon onto Nickel Foam. 40

Figure 4.6 Application of NiO Ink to the PSOFC Anode. 41

Figure 4.7 Placement of PSOFC onto Anode Manifold. 42

Figure 4.8 Application of 0.8 PrO_8 Ink to PSOFC Cathode. 42

Figure 4.9 Silver Mesh Cathode Current Collector with Voltage Tap. 43

Figure 4.10 Rolling 0.8 PrO_8 Ink onto Silver Mesh. 44

Figure 4.11 Placement of Silver Mesh onto PSOFC Cathode. 45

Figure 4.12 Cathode Voltage Tap Taped into Position. 45

Figure 4.13 Positioning of Cathode Manifold. 46

Figure 4.14 Final Placement of Cathode Manifold. 47

Figure 4.15 Anode Gas Line Connection. 48

Figure 4.16 Cathode Gas Line Connection. 48

Figure 4.17 Single Cell Test Stand Ready to be Closed. 49

Figure 4.18 Electrochemical Test Geometry. 51

Figure 4.19 Agilent N3300A Potentiostat. 53

Figure 4.20 Single Cell Test Stand Indicators. 53

Figure 5.1 Trial 4 Initial VI Scan. 64

Figure 5.2 Initial PSOFC ASR Regression. 66

Figure 5.3 Initial ASR Regression with Simulated Coal Syn Gas. 71

Figure 5.4 ASR Comparison of Trial 4. 72

Figure 5.5 Trial 4 ASR History 75

Figure 5.6 Baseline PSOFC Cross Section. 77

Figure 5.7 PSOFC Anode Surface at 550X. 78

Figure 5.8 PSOFC Anode Surface at 1430X. 79

Figure 5.9 PSOFC Anode Cross Section EDS Spectrum. 80

Figure 5.10 PSOFC Anode Surface EDXS Spectrum. 81

Figure 5.11 XRD Spectrum of Baseline PSOFC Anode. 82

Figure 5.12 Trial 4 SEM Image Comparison with Baseline Anode SEM Image 84

Figure 5.13 Trial 4 SEM Image at 1510X. 86

Figure 5.14 EDXS Spectrum from Trial 4 Anode. 87

Figure 5.15 XRD Spectrum from Trial 4 Anode. 88

Figure 5.16 Trial 5 Initial VI Scan. 90

Figure 5.17 Trial 5 Initial PSOFC ASR Regression. 91

Figure 5.18 Trial 5 ASR Regression with Simulated Coal Syn Gas. 95

Figure 5.19 PSOFC ASR Comparison for Trial 5. 96

Figure 5.20 PSOFC KS1S040210-43 ASR History. 98

Figure 5.21 PSOFC Anode SEM Images 100

Figure 5.22 SEM Image of Trial 5 Anode at 1430X. 101

Figure 5.23 Anode EDXS Spectrums 103

Figure 5.24 Trial 5 PSOFC Anode XRD Spectrum. 104

Figure 5.25 Trial 6 Initial VI Scan. 106

Figure 5.26 Trial 6 Initial ASR Regression. 107

Figure 5.27 Initial ASR Regression After Injection of H_2S 110

Figure 5.28 ASR History of Trial 6. 112

Figure 5.29 Trial 6 PSOFC Anode at 570X. 113

Figure 5.30 High Magnification SEM Images of PSOFC Anodes 115

Figure 5.31 Trial 6 Anode EDXS Spectrum. 116

Figure 5.32 Trial 6 Anode XRD Spectrum. 117

Figure 5.33 VI Scans for PSOFCs Utilizing H_2/N_2 and Simulated Coal Syn Gases 119

Figure 5.34 InDEC PSOFC ASR History Comparison. 120

Figure 5.35 Trial 4 Through 6 ASR History Comparison. 121

Chapter - 1

Introduction

1.1. Introduction

Coal is the most abundant fossil fuel in the United States and the country possesses one fourth of the world's total reserves. These reserves are spread out across the nation allowing easy transportation of coal to various destinations. Coal is also the lowest cost fossil fuel per unit of energy in the United States. Coal averages approximately $1.30/MBtu, compared to natural gas at $5.60/MBtu and No. 2 heating oil at $5.76/MBtu [1]. Because of these reasons coal is used for more than 50 percent of the electrical energy production in the United States. The electric power production industry reported that electric production through the burning of coal, which accounts for over half of the electric production in the United States, used 1004.3 million short tons of coal in 2003 [2]. Because of coal's availability and its price it is also very likely that coal will be the power production fuel of choice for years to come.

However there are many problems associated with the traditional combustion processes. The first problem with coal combustion based electrical power generation is the efficiency of the process. The efficiency of electrical power production process by burning coal to produce steam is limited by the Carnot Cycle efficiency, shown in Equation 1.1.

$$CarnotCycleEfficiency = \left(1 - \frac{T_C}{T_H}\right) \times 100 \qquad \text{Equation 1.1}$$

where T_C and T_H are the maximum and minimum temperatures of the cycle in Kelvin. For most combustion processes the temperature of the boiler is kept around 600K and the heat sinks, which are normally rivers and lakes, is approximately 300K and so the practical limit to the thermal efficiency of a boiler is approximately 50 percent. In 2002 the world's most efficient power plant found in Germany had an efficiency of 43 percent, due to its ultra-supercritical operation, while most power plants still operate in the 33-37 percent efficiency range [3]. This inefficiency results in most of the heat produced in the combustion of the coal to be wasted as steam evaporating from the cooling towers of a power plant.

Another problem with using coal combustion to produce electricity is the emission of pollutants, such as nitrous oxides (NO_X), sulfur dioxides (SO_X), and particulate matter. These pollutants are known to be precursors to the production of ground level ozone in the case of NO_X, acid rain in the case of NO_X and SO_X, and respiratory problems in humans in the case of particulate matter which are emitted and formed in the atmosphere by NO_X and SO_X in the form of fine sulfate and nitrate particles [4,5]. In 2000 coal burning power plants emitted over 11.5 million tons of SO_2 and over 5.6 million tons of NO_X, which accounted for nearly two thirds and a quarter of the nation's total emissions respectively [6]. The U.S. EPA has placed regulations on these pollutants through the 1990 Clean Air Act Amendments (CAAA). The goal of the Acid Rain Program which was a part of the 1990 CAAA, was to reduce the amount of

SO_2 emitted by power plants to a level of 2.5 lbs/MBtu and to reduce the amount of NO_X by two millions tons from the 1980 emission levels [7]. The SO_X regulations were complied with in 1995 and the NO_X reductions were made in two phases, the first phase beginning in 1997, and the second phase in 2000. In order for the power companies to comply with these regulations great investments were made into pollution control technologies such as scrubbers for sulfur removal and Selective Catalytic Reactors for NO_X reductions. Because of the CAAA and more environmental legislation that is sure to come it will only become more costly to produce electricity from the combustion of coal.

Another problem associated with the emission of pollutants produced from the combustion of coal for the production of electricity is the health effects on the people of the United States. NO_X when mixed with volatile organic compounds and sunlight produce ground level ozone [4]. People with asthma or are frequently outside can sustain lung tissue damage when exposed to high ozone levels. Sulfur dioxide also can cause lung damage to those who have prolonged exposure.

Particulate matter that is emitted and formed in the atmosphere by other pollutants produced in the combustion of coal has the largest and most detrimental effect on the United States population. One study completed by Wilson, Richard, and Spengler in 1998 estimates that nearly 60 thousand premature deaths are caused every year by particulate matter, while the Harvard School of Public Health estimates that approximately 15 thousand premature deaths are caused each year by particulate matter [5]. The cost for the treatment of the effects suffered from coal combustion power plants

is enormous. A study was completed to find the monetary benefit that would be seen if all power plants were upgraded to today's emissions standards. The savings from avoided health care services was found to be over 100 billion dollars per year [8].

Since coal will likely be a major fuel for electrical power production in the future more efficient and environmentally friendly production methods must be used. One technology that has shown great potential to replace the traditional production means are fuel cells, specifically planar solid oxide fuel cells (PSOFC). A PSOFC is a device that directly converts chemical energy into electrical energy much like a battery. PSOFC's, as well as solid oxide fuel cells in general, show great potential as a replacement for electricity produced by the combustion of coal for multiple reasons. These reasons are the high power generation efficiency, ultra low production of regulated emissions, applicability as a source of distributed generation, and ability to be used for the production of electricity and heat (cogeneration) [9]. The results from a study that was completed that compared the amount of regulated emissions that are produced by traditional generation of electric power by the combustion of coal and the pollutants produced by solid oxide fuel cells using natural gas as fuel are shown in Table 1.1 [10-12].

Table 1.1 Comparison of Emissions Produced by Conventional Power Generation and Solid Oxide Fuel Cells.

Regulated Emissions	NOx (g/kWh)	SOx (g/kWh)	CO (g/kWh)	Particulate Matter (g/kWh)
Conventional Generation	1.02	0.33	0.43	0.01
SOFC Generation	0.06	0.013	0.012	0

Because of the high operating efficiency of a PSOFC system and almost negligible emission of pollutants, as can be seen in Table 1.1, the PSOFC should be considered as the replacement for current methods of producing electricity through the combustion of coal.

PSOFC's also offer the possibility of being effectively used in distributed power generation. PSOFC's are excellent for this type of electric power production since the units can be installed at or near the end user's site due to their low emissions and noise. An average PSOFC operates at a sound level typically below 60 dB [9]. Also the deregulation of the electric power industry that has and will continue to take place will allow the solid oxide fuel cell to become even more competitive. The reasons for this are due to the fact that PSOFC's do not require expensive transmission lines, distribution costs, and electromotive force problems associated with transmission lines [9]. These advantages will allow the PSOFC to be competitive in the small residential and commercial sector (< 500kW) and the medium commercial and industrial sectors (0.5-5.0MW) [13].

Cogeneration is another reason that the PSOFC will be a potential replacement for the combustion of coal for electric power production. This type of energy production is very important so that energy resources are conserved. PSOFC's are capable of high efficiency electrical power generation, and also produce high quality heat from their exiting gases, typically 1000˚C, which can be used for the production of steam for heating of homes and businesses. PSOFC's also operate efficiently at part load compared to internal combustion engines, which operate most efficiently at full load and have a rapid decline in efficiency at part load. Also the electric and thermal characteristics of solid oxide fuel cells systems meet the requirements for home use much better than internal combustion systems. The reason for this is because on average the residential thermal to electric energy (T/E) ratio is in the range of 0.6-1.0. A PSOFC system operates with an approximate T/E ratio of 1.0, while internal combustion cogeneration systems operate anywhere from 2.7 when electric is in high demand, to 17.4 when thermal energy is more needed [9]. This makes the PSOFC a good match for the field of home cogeneration.

1.2. PSOFC Construction

A PSOFC contains two planar shaped electrodes that sandwich a planar electrolyte. The anode is typically made of a Ni/ZrO_2 cermet, the cathode is made of a doped lanthanum manganite, and the electrolyte is made of a yttria stabilized ZrO_2 (8 mol% YSZ) [14]. The PSOFC converts chemical energy into electrical energy through the following two reactions shown in Figure 1.1, and in Equation 1.2 and 1.3 [15].

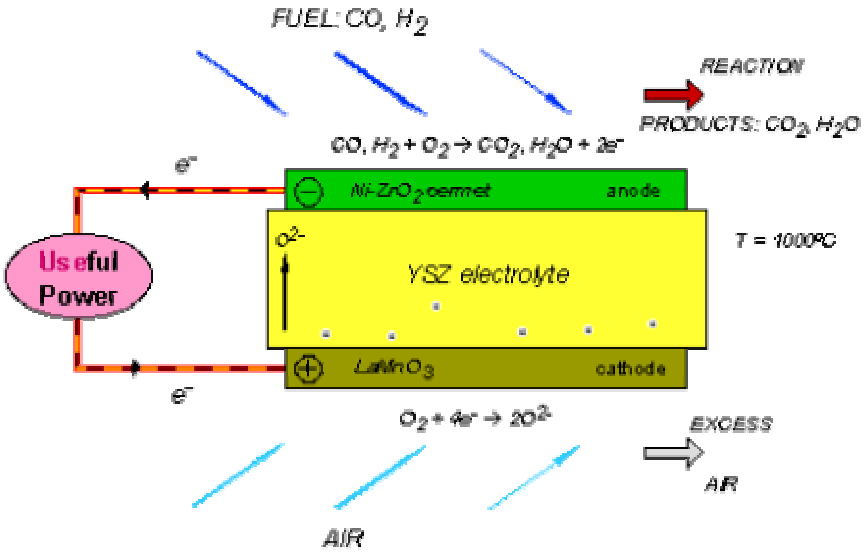

Figure 1.1 PSOFC Diagram

$$H_2 + 0.5\,O_2 \rightarrow H_2O \qquad \text{Equation 1.2}$$

$$CO + 0.5\,O_2 \rightarrow CO_2 \qquad \text{Equation 1.3}$$

Coal can be used as the fuel source for the PSOFC by converting the coal into a gaseous product containing hydrogen (H_2) and carbon monoxide (CO). The fuel gas which may contain H_2, CO, or a combination of the two are sent to the anode of the PSOFC and oxygen in the form of air is sent to the cathode side of the PSOFC. The H_2 and CO that enter the anode are then oxidized. The oxidation of each H_2 and CO molecule produces two electrons that travel to the cathode of the PSOFC through an external circuit, shown in equations 1.4 and 1.5.

$$H_2 + O^{2-} \rightarrow H_2O + 2e^- \qquad \text{Equation 1.4}$$

$$CO + O^{2-} \rightarrow CO_2 + 2e^- \qquad \text{Equation 1.5}$$

At the cathode the oxygen in the form of air is reduced by the electrons flowing from the external circuit coming from the anode shown in Equation 1.6.

$$0.5O_2 + 2e^- \rightarrow O^{2-} \qquad \text{Equation 1.6}$$

The oxygen ions are transported through the ceramic electrolyte to the surface of the anode where the ions oxidize the H_2 and CO as shown in Equations 1.4 and 1.5.

The PSOFC operates at a high temperature compared to other types of fuel cells, typical units operate at 1000˚C. These high temperatures allow for faster travel of oxygen ions across the electrolyte. Also expensive catalyst such as platinum are not needed to speed the oxidation and reduction reactions that take place at the electrodes due to the high operation temperature [16]. The PSOFC is also very flexible in the fuels which it can use. Hydrocarbons such as methane (CH_4) may also be used. The high temperature of the PSOFC allows the hydrocarbons to be internally reformed to H_2 and CO in the anode compartment of the fuel cell when steam is added. This is very attractive since it saves money and space because a fuel reformer is not needed for the operation of a PSOFC. This hydrocarbon reformation takes place by the water-gas shift that is shown in Equation 1.7.

$$CH_4 + H_2O \rightarrow 3H_2 + CO \qquad \text{Equation 1.7}$$

The ideal performance of a PSOFC is defined by the Nernst equations, which measures the potential of the cell, for the reactions that take place. The Nernst equation allows the ideal operating potential to be found by providing a relationship between the standard potential (E°), at 1 atm and 25°C, and the ideal equilibrium potential (E) for other temperatures and pressures. The Nernst equations for the two reactions that take place in the anode of the PSOFC are shown in Equations 1.8 and 1.9.

$$E = E^{\circ} + \left(\frac{RT}{2F}\right)\ln\left[\frac{P_{H_2}}{P_{H_2O}}\right] + \left(\frac{RT}{2F}\right)\ln\left[P_{O_2}^{0.5}\right] \qquad \text{Equation 1.8}$$

$$E = E^{\circ} + \left(\frac{RT}{2F}\right)\ln\left[\frac{P_{CO}}{P_{CO_2}}\right] + \left(\frac{RT}{2F}\right)\ln\left[P_{O_2}^{0.5}\right] \qquad \text{Equation 1.9}$$

where E° is 1.18 volts with H_2O as a gaseous product, P is partial pressure of the respective component, R is the universal gas constant, T is in Kelvin, and F is the Faraday constant [14]. The effect of changing temperature and pressure have on the ideal potential of a PSOFC can be found by studying the changes in Gibb's free energy (ΔG) for temperature and pressure. Equations 1.10 and 1.11 show the effects of changing the temperature or pressure has on a PSOFC.

$$\left(\frac{\partial E}{\partial T}\right)_P = \frac{\Delta S}{nF} \qquad \text{Equation 1.10}$$

$$\left(\frac{\partial E}{\partial P}\right)_T = \frac{-\Delta V}{nF} \qquad \text{Equation 1.11}$$

Since the entropy change for both of the reactions that take place in equations 1.3 and 1.4 are negative the ideal potential of the PSOFC decreases as temperature increases [14]. Since the volume change for an increase in fuel pressure causes the reaction volume to become smaller then the PSOFC potential increases [16].

However the actual performance of a PSOFC is not the same as the ideal performance that is found by the Nernst equations. This is caused by the irreversible losses that take place when current is drawn from a fuel cell [14]. These losses are known as polarizations and there are three main types: activation polarization, ohmic polarization, and concentration polarization. Activation polarization is the potential loss caused by the limited speed of charge and ion transport across the PSOFC [16]. It is present when slow electrochemical rates of reaction are present at the electrodes of the fuel cell [14]. Ohmic polarization is not caused by any chemical process, but is a result of resistances to the flow of ions in the electrolyte and electrode materials[16]. Concentration polarization is caused by pressure and concentration gradients that occur between the electrode and bulk fluid as a reactant is consumed [16]. The potential losses in a PSOFC are mainly caused by ohmic polarization and the ohmic polarization is primarily caused by cathode polarizations. Although the electrolyte and cell

interconnections have higher resistances, it has a shorter conduction path through the electrolyte than in the plane of the cathode [14].

It is possible to reduce the amount of polarization and improve the performance of a fuel cell by modifying the operating conditions; however this can cause a problem with cell stability. One method that may be used to improve the performance of a PSOFC is to increase the operating temperature of the fuel cell. The increased temperature increases the reaction rate, causes a higher mass-transfer rate, and lowers the resistances of the materials [14]. An empirical model, Equation 1.12, has been formulated which gives the change in cell potential due to changes in the operating temperature of a solid oxide fuel cell at a given current density [14].

$$\Delta V = 0.008(T_2 - T_1) \times J \qquad \text{Equation 1.12}$$

where V is the change of the cell potential in mV, T is in Kelvin, and J is the current density of the fuel cell (mA/cm^2). However this has not always been found to be the case since the operational efficiency is reduced due to differences in material expansion at such high temperatures. This leads to poorer charge and ion transfer as well as sealing issues. Another way to increase the performance of a fuel cell is to increase the oxygen (O_2) concentration in the cathode chamber. Tests have shown that as the cell potential difference between pure O_2 and air increases as the cell's current density increases. This would suggest that concentration polarization is present in the reduction of O_2 on the anode. However there are practical limits to the pressures that fuels and oxidizers can be processed in PSOFC's due to material strengths. The sealants used in the construction of

a PSOFC stack are only capable of withstanding fuel and oxidant gas pressures that are inches of H_2O greater than atmospheric pressure. Fuel and oxidant gas pressures that are greater than inches of H_2O gauge will rupture the seals of the PSOFC stack and begin to leak from the sides of the fuel cells disrupting the operation of the stack and lowering its operation efficiency. However it is possible to operate a single PSOFC with higher fuel and oxidant gas pressures because no seals are needed in the operation of a single fuel cell. It is known that the overpotential of a PSOFC increases with increasing fuel and oxidant gas pressures. Equation 1.13 is used to approximate the increase in a solid oxide fuel cell's overpotnetial operating at 1000°C [14].

$$\Delta V_p(mV) = 59\log\left(\frac{P_2}{P_1}\right) \qquad \text{Equation 1.13}$$

where ΔV_p is the change in the PSOFC overpotential in millivolts, P_1 and P_2 are the different PSOFC fuel and oxidant gas pressures.

Another cause for the reduction of PSOFC operation efficiency is due to pollutants in the fuel gas. The main pollutant that has been found to cause degradation in the performance of a PSOFC is hydrogen sulfide (H_2S). H_2S hinders the operation of a PSOFC by increasing the resistance of the anode with the formation of nickel sulfide, increasing the ohmic polarization of the PSOFC, and blocking reactions sites at the anode interface with the formation of nickel sulfide, increasing the activation polarization of the PSOFC. H_2S can also affect the operating efficiency of a PSOFC by causing degradation of the PSOFC materials because the gas is highly corrosive. The effect of H_2S on the operation of a PSOFC has been found to be related to the operating temperature of the

fuel cell. It has been determined experimentally that the operating efficiency of a PSOFC is more easily affected by H_2S at lower temperatures. The higher the operating temperature of a PSOFC the greater its tolerance of H_2S becomes. This reduction in efficiency can be eliminated by reducing the amount of H_2S in the fuel gas to levels below the cell's toleration limit [17].

Because of the reasons that have been stated above the factors effecting the performance of a PSOFC need to be investigated more thoroughly. Especially the effect of pressure and H_2S has on the performance of the PSOFC since these two parameters seem to have the greatest effect on the operation of a PSOFC.

1.3. Significance of Research

The problem to be solved by this research is to find the effect that coal syn gas containing H_2S at a pressure greater than ambient pressure has on the operation of a single PSOFC. The solution to this problem is important for the development of future PSOFC systems for distributed power generation using coal as its fuel source. This method of electrical power production will play a key role in the production of the United States' future energy needs due to its higher operation efficiency and much lower production of pollutants compared to today's methods of energy production. The unique elements of this proposed research are the testing of fuel gas without H_2S with a pressure greater than ambient pressure effect on the operation of a single PSOFC and fuel gas containing H_2S with a pressure greater than ambient pressure effect on the operation of a single PSOFC. The effect of fuel and oxidant gas pressurization and the effect of fuel gas containing H_2S at a pressure greater than ambient pressure have not been investigated

before on a PSOFC. The results of this research will increase the engineering knowledge base by showing the effect that these test parameters have on the operation of a single PSOFC and also establish if the pressurization of fuel gas will be a beneficial way to increase the overall operation efficiency of the PSOFC.

1.4. Goals and Objectives

The goal of this project is to determine the effect that pressurizing fuel gas containing H_2S has on the operation of a single PSOFC. This will be done by studying the areas of fuel gas composition, i.e. fuel gas with and without H_2S, and the pressurization of the fuel gas being supplied to a PSOFC. Two tasks and two objectives are to be completed to arrive at the goal of this project. The first task is to establish repeatable operation of the single PSOFC by supplying the fuel cell with fuel gas without H_2S and oxidant gas at ambient pressure. The second task will be to establish the repeatable operation of a single PSOFC by supplying the fuel cell with fuel gas that does not contain H_2S and oxidant gas at pressures of approximately 50 psig. The first objective will be to determine the effect H_2S at ambient pressure has on a single PSOFC by supplying the fuel cell with fuel gas containing H_2S and oxidant gas at ambient pressure. The second objective will be to determine the effect of fuel gas with H_2S at higher than ambient pressure will have on a single PSOFC by supplying the fuel cell with fuel gas containing H_2S and oxidant gas at approximately 50 psig. The intellectual products that are expected to be found is percent difference between the PSOFC area specific resistance (ASR) operating at ambient pressures with fuel gas with and without H_2S. The percent difference between the PSOFC ASR while operating with fuel gas with

and without H_2S at approximately 50 psig. The three intellectual products that are expected to be found from the completion of this research will be used to decide if fuel and oxidant gas pressurization research needs to be investigated further.

Chapter - 2

Literature Review

2.1. Introduction

PSOFC technology has become an emerging distributed power generation technology over the past decade. Many scientists and engineers have conducted research to improve the PSOFC so it may become a viable energy alternative. The main areas of research of interest are improving the current density of PSOFCs, reducing electrode polarizations, improving the ionic conductivity of the electrolyte, and finding anode materials that are resistant to sulfur. The following section will review research that has been conducted that is of interest to PSOFCs that utilize coal syn gas as a fuel.

2.2. Literature Review

One of the most important characteristics and advantages of the PSOFC is its ability to use CO as a fuel, which allows fuels that contain both carbon and hydrogen to be used as feed stock for the fuel cell. However there are many problems associated with using CO as a fuel, including diffusivity problems, slow reaction kinetics, and unwanted side reactions involving the species. Research has shown that the electrochemical performance of a PSOFC with a CO/CO_2 anode atmosphere is not as efficient compared to a H_2/H_2O atmosphere due to higher anodic concentration polarization and slower electrochemical oxidation of CO at the anode compared to H_2 [18]. The main cause of the high anodic concentration polarization is the diffusion of the species into the anode of the PSOFC. Jiang and Virkar (2003) determined that the Knudsen diffusion for the CO/CO_2 atmosphere was 1.41 cm^2/s while for the H_2/H_2O

atmosphere was found to be 13.3 cm^2/s. This reveals that a longer period of time is required for CO to travel to a nickel reaction site and for CO_2 to diffuse back to the surface of the anode than for H_2 and H_2O [18]. Yakabe et al. (2000) also reported that the polarization over potential of the CO/CO_2 system is large compared to the H_2/H_2O system since the diffusion rate of CO is lower than that of H_2 [19].

Another major cause of the problems associated with using CO as a fuel for the PSOFC is the slow reaction kinetics of CO on the anode of the PSOFC. Jiang and Virkar determined through their research that the anodic activation polarization with the CO/CO_2 mixture at 0.25 A/cm^2 was approximately 0.173 V greater than its equivalent H_2/H_2O system which lead them to the conclusion that nickel-based anodes along with CO alone as fuel are not a viable source of energy when high power density is a requirement [18]. Matasuzaki and Yasuda (2000) have reported from their research that the ratio of the oxidation rate of H_2 to CO at the anode of a PSOFC at 1023K and 1273K was greater than 1.9-2.3 and 2.3-3.1 respectively with a constant oxygen partial pressure at the anode which also shows that the electrochemical oxidation of CO at the PSOFC anode is slower than the electrochemical oxidation for H_2. The authors also discovered that the rate of the anodic oxidation reaction is caused by a mass-transfer process which includes the dissociative adsorption of the reacting species onto the anode surface and the diffusion of the adsorbed reactant on the surface of the anode to the nickel reaction site [20].

Although CO has been found not to be as promising of a PSOFC fuel as H_2 research that was completed did not show that reformed hydrocarbons such as coal could

not be used as a practical fuel source. When hydrocarbon fuels are reformed a product gas containing a mixture of H_2 and CO based on the elemental composition of the reformed fuel will be produced. In order to determine the effect of reformed hydrocarbon fuels on the operation of PSOFCs several engineers have conducted research investigating different CO/H_2 ratios as well as the effect of directly injecting gaseous hydrocarbons to the anode of the PSOFC. Weber et al. (2002) investigated the effect of fuel gas with varying CO/H_2 ratios on the operation of a PSOFC. The authors found no significant difference in the operation of the PSOFC using a fuel gas made of pure H_2 and a fuel gas with 25 mole percent CO and the balance H_2. Also the authors investigated several different CO/H_2 fuel gas ratios and found no severe effect on current density until the CO composition in the fuel gas reached 85 mole percent or greater [21]. Research conducted by Jiang and Virkar found that PSOFC performance comparable to a fuel gas containing pure H_2 was achievable if the H_2 content of the fuel gas was greater than 50 mole percent [18]. Both Weber et al. and Jiang and Virkar concluded that the favorable performance of the PSOFC was due to the water-gas shift reaction as shown in Equation . 1.7. Sasaki et al. also investigated the effect of the CO/H_2 fuel gas ratio on the operation of a PSOFC and found the H_2O vapor concentration of the fuel gas to be an important operational parameter. They found that a greater H_2O vapor concentration in the fuel gas was found to increase the H_2/CO ratio from the water-gas shift reaction for fuels that were rich in CO [22].

Other research has been conducted to determine the effect of using gaseous hydrocarbons at the anode as a fuel for the PSOFC. Gaseous hydrocarbons may be

utilized as a fuel for the PSOFC because the reformation of the hydrocarbon at the anode into CO and H_2 is possible due to the operational temperature of the PSOFC. Also it has been found that the direct electrochemical oxidation of hydrocarbon fuels in PSOFCs is possible but leads to the deposition of carbon onto the surface of the anode at operational temperatures greater than 800ºC when nickel anodes are used [23]. This is caused by nickel's ability to break carbon to carbon bonds which leads to coking of the anode. Murray and Barnett (1999) completed research with a PSOFC anode made of ceria oxide and nickel that was operated at 650ºC and found the direct electrochemical oxidation of dry methane at the anode was possible and generated up to 0.35 W/cm^2 at a temperature of 650ºC. Also the post trial XRD and SEM materials analyses of the anodes revealed that no carbon had deposited onto the surface of the anode [24]. Park, Vohs, and Gorte (2000) conducted PSOFC research with an anode made of 40 weight percent copper and 20 weight percent CeO_2 that was held in place by a YSZ matrix. The authors used copper as the anode reaction catalyst due to nickels propensity to cause coking. The authors used n-butane and toluene hydrocarbons as the fuel and found that the PSOFC operation was stable at a power density of 0.12 W/cm^2 at 975ºC over a 48 hour period. However when toluene was used as the fuel gas the performance of the PSOFC rapidly decreased caused by heavy carbon deposition on the anode. The PSOFC recovered its performance when n-butane was again used as the fuel gas [25].

H_2S is known as a fuel gas contaminant that causes degradation in the performance of PSOFCs. The degradation in the performance of the PSOFC is caused by the sulfur that is produced by the equilibrium reaction shown in Equation 2.1 [26].

$$2H_2S \longleftrightarrow S_2 + 2H_2 \qquad \text{Equation 2.1}$$

The sulfur present at the surface of the Nickel cermet then adsorbs onto the nickel sites of the cermet to form Ni_2S_3 [27]. The adsorption of sulfur onto the nickel sites of the cermet blocks reaction sites for the oxidation of the H_2 and CO to take place. This degradation is seen as an increase in the polarization resistance.

The concentration of the H_2S in the fuel gas of a SOFC has also been found to affect the amount of degradation that takes place. As the concentration of H_2S in the fuel gas increases there is also an increase in the amount of S_2 that is present in the anode of the PSOFC system. The greater the concentration of S_2 at the anode/fuel gas interface the more sulfur that will be available to adsorb onto the nickel sites of the anode, blocking reaction sites and hindering the flow of electrons through the anode. This increases the polarization of the PSOFC in two ways. First the formation of the nickel sulfide at the anode increases the resistance of the anode material inhibiting electron flow therefore increasing the ohmic polarization of the anode of the PSOFC. Second is that a thin layer of nickel sulfide that builds on the anode interface acts a as barrier to the fuel gas increasing the activation polarization of the PSOFC. Figure 2.1 shows a basic schematic of the process that takes place at the anode/fuel gas interface.

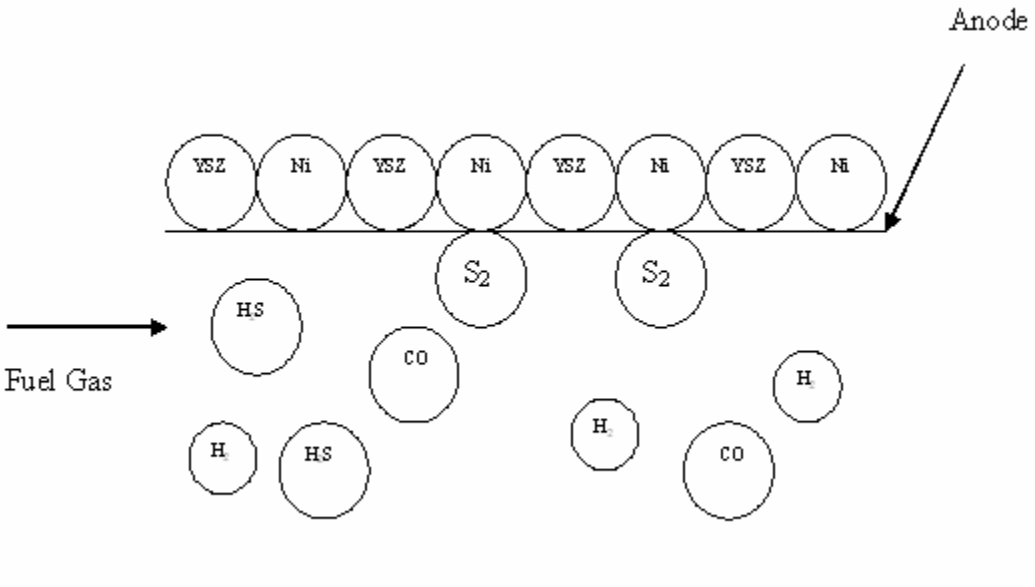

Figure 2.1 Sulfur Adsorption onto Nickel at the PSOFC Anode Interface.

Maskalisk and Ray (1992) found that a simulated coal-derived fuel gas containing 1 ppm of H_2S caused the open cell potential in a tubular SOFC operating at 1000°C to decrease after 24 hours of operation. However no voltage decline was seen in the fuel cell when a fuel gas containing 0.1 ppm was tested [28]. Another study testing the kinetics of a Ni/YSZ anode by Geyer et al. (1996) found that the anode could be artificially poisoned by H_2S [29]. The SOFCo Corporation (1999) tested their PSOFC's tolerance toward H_2S. The studies showed that the fuel cell's did not incur any degradation in performance when fuel gas containing 5 and 50 ppm H_2S was used. Fuel gas streams with H_2S concentrations of 500 and 1000 ppm were found to cause a 50 mV decrease in the fuel cell's voltage, however stable operation was maintained [30]. A 10 kW tubular SOFC was tested by Iritani, Kougami, and Komiyama (2001) and was found that 1 ppm of H_2S caused a rapid drop in fuel cell potential [31]. Sulzer Hexis (2001) tested the

SOFCs produced by their company by an integrated process and was found to operate well with 100 ppm H_2S in the fuel gas. All tests that were completed found that all losses in fuel cell potential were reversible once H_2S was removed from the fuel gas.

Another factor that affects the amount of anode degradation that takes place when H_2S is present is the operation temperature of the SOFC. SOFC's have a higher H_2S tolerance as the operation temperature is increased. Maskalisk and Ray (1992) found that a tubular SOFC suffered less potential degradation by 1 ppm H_2S at an operational temperature of 1025°C than at 1000°C [28]. Matsuzaki and Yasuda (2000) tested the effect of temperature on a PSOFC's H_2S tolerance. Their research revealed that the fuel cell began to experience potential losses at H_2S concentrations of 0.05, 0.5, and 2 ppm at temperatures of 1023K, 1173K, and 1273K respectively [28]. However Primdahl and Mogensen (1999) found that the operational temperature of a solid oxide fuel cell had no effect on the fuel cell potential loss caused by 35 ppm H_2S [32].

The amount of time that fuel gas containing H_2S is utilized by a PSOFC has also been found to have an effect on the operation of the fuel cell. Maskalisk and Ray (1992) found that when fuel gas with H_2S is supplied to a SOFC an initial potential drop takes place after the initial 24 hours of operation. After this period a fuel cell potential drop that is linear with time was then found to take place [28]. Matsuzaki and Yasuda (2000) also tested the amount of time that a PSOFC's potential will decline once H_2S is added to the fuel gas. The testing revealed that the amount of time that a PSOFC will experience potential degradation is also dependent upon the operational temperature. At an operating temperature of 1273K it was found that the PSOFC stopped experiencing

potential degradation at a time between 3600 and 4800 seconds once H_2S was added to the fuel, while at 1173K it was found to be 9000 seconds, and at 1023K it was found to be 90000 seconds. This testing revealed that the higher the operating temperature of a PSOFC, the shorter the potential degradation time will occur due to the anodes greater resistance to sulfur degradation at higher temperatures [26].

Due to the loss of power associated with the operation of PSOFCs with fuel gas containing H_2S work is being completed to develop a PSOFC anode material that is resistant to H_2S. Mukundan et al. (2004) are developing an anode made of a peroviskite metal oxide structured material. The metal oxides in the perovskite material have been found to be less reactive to sulfur than metals such as nickel and copper and also have a good chemical compatibility to zirconium oxide electrolytes. The authors prepared PSOFCs with an anode composition of $Sr_{0.6}$ $La_{0.4}TiO_3$ (LST/YSZ) and compared their performance to a Ni/YSZ anode with fuel gases containing different H_2S concentrations for 24 hours at 1273K [33]. Using a fuel gas with 10 ppm H_2S and the balance being H_2 the authors found negligible effect on the LST/YSZ anode while the Ni/YSZ anode was affected as other authors had reported. A fuel gas containing 100 ppm H_2S was found to cause a six percent decrease in the PSOFC potential at a current density of 0.25 A/cm^2. Also it was found that the LSZ/YSZ anode suffered a 7 percent loss in cell potential while operating with a fuel gas containing 1000 ppm H_2S. Surprisingly the performance of the LSZ/YSZ anode was found to significantly improve as fuel gas containing 5000 ppm H_2S was used. While operating at a current density of 0.6 A/cm^2 an increase in cell potential of 180 mV was observed corresponding to a 20 percent increase in performance

of the PSOFC [33]. Even though the LST/YSZ anode material exhibits a dramatically better tolerance towards H_2S compared to Ni/YSZ anode the overall performance of the cell needs to be improved to compete with the Ni/YSZ cells. The authors believe this will be possible by tailoring the composition and morphology of the LST/YSZ anode [33].

Another condition that has been found to affect the operation of a PSOFC is the pressure of the fuel gas. Increasing the pressure of the fuel gas being utilized by a PSOFC will increase the fuel cell's potential. This can be seen in Equations 1.8 and 1.9. This can be explained by the change in the Gibb's free energy, which is shown in Equation 1.11. An increase in the pressure of the fuel gas will cause the reacting volume to become smaller and this will cause the PSOFC's potential to increase [34]. To determine the effect of pressurized conditions Kikuchi et al. (2003) investigated the anodic reaction under pressurized conditions of a Ni-YSZ/YSZ half cell operated at 900ºC and 1000ºC with AC impedance spectroscopy. The authors also calculated the thermodynamic conditions that favor the deposition of carbon at 1 atm and 15 atm. The authors first examined the effect of fuel gas with constant oxygen partial pressure at total anode gas pressures of 1 atm, 4atm, and 10 atm. Kikuchi found that the low frequency arc of the Nyquist plot shrunk as total pressure increased as the low frequency arc expanded. The authors explained that the shrinking of the high frequency arc was caused by the increase in collision frequency of H_2 with the anode, increasing the oxidation rate of H_2, which decreased the resistance characterized by the high frequency arc. Overall the authors determined the high frequency arc expanded as temperature decreased due to slower reaction kinetics at the anode surface and the low frequency arc was dependent

upon the H_2/H_2O fuel gas mixture and also independent of temperature. The authors also reported the operation of the PSOFC under high pressure conditions would be favorable for the prevention of carbon deposition [35].

It is expected that further development of PSOFC materials will allow higher pressure fuel gases to be used, increasing the PSOFC's potential [35,36]. Aguiar, Chadwick, and Kershenbaum (2001) modeled the operation of a SOFC. Through the modeling that was completed it was found that increasing the fuel gas pressure from 5 bar to 10 bar increased the operational efficiency of the fuel cell from 53.1 percent to 55.5 percent. The research also revealed that increasing the pressure reduced the temperature difference across the anode, which reduced the amount of stress caused by differences in material expansion.

Singhal (1999) conducted research with a 250 kW pressurized tubular SOFC. Comparing the operation of the system using pressurized fuel gas to fuel gas at atmospheric pressure revealed many positive aspects. It was found that operating the system at elevated pressures yielded a higher fuel cell potential at any current density. This was due to the increased Nernst potential and reduced cathode polarization. Operating at the elevated fuel gas pressures allowed the tubular SOFC to operate at a higher efficiency and have a greater power output. Also if SOFCs are operated at higher pressures the fuel cells can then be used as replacements for combustors in gas turbines [37].

Chapter - 3

Experimental Plan

3.1. Planned Approach

The planned experiments are designed to test the effect of pressurized fuel gas, oxidant gas, and H_2S on the operation of a planar solid oxide fuel cell (PSOFC). Figure 3.1 is a basic schematic of the PSOFC testing apparatus. Table 3.1 illustrates the fuel gas and oxidant gas compositions to be used in the testing.

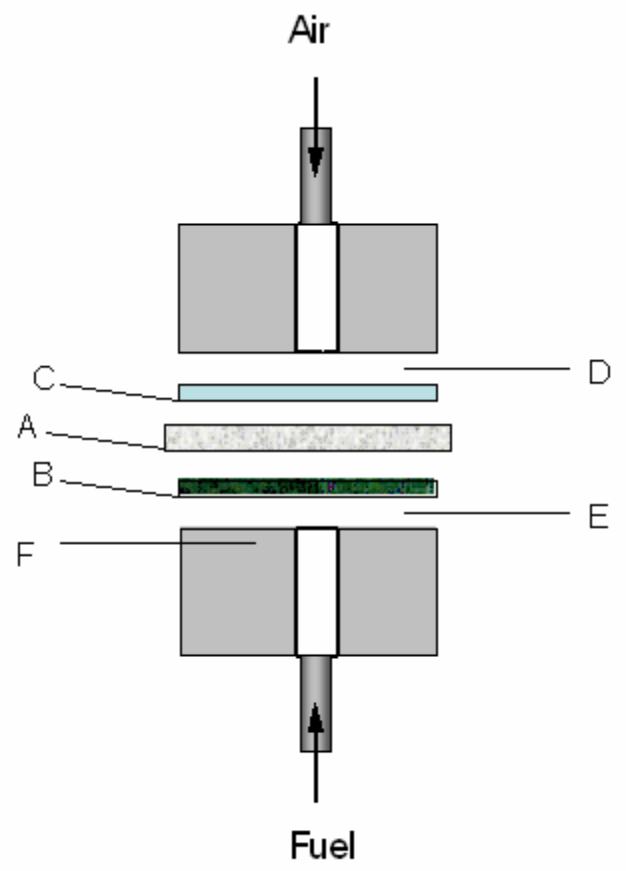

Figure 3.1 PSOFC Testing Apparatus.

Where A is the PSOFC, B is a nickel foam anode current collector, C is the silver mesh cathode current collector, D is cathode voltage tap, E is the anode voltage tap, and F is the fuel manifold. An electronic load will be attached at the ends of the fuel manifolds to control the operation of the PSOFC. The inputs to the PSOFC are the fuel and oxidant gases shown in Figure 3.1 and have the compositions as shown in Table 3.1 below. The PSOFC will be operated galvanostically under a total load of 14 Amps [38 SOFCo]. The electronic load and data acquisition system will be used to collect the PSOFC's voltage and current data to monitor the operation of the PSOFC.

Table 3.1 Fuel Gas and Oxidant Molar Compositions.

Component	Trials 1 and 2 (mole %)	Trials 3 and 4 (mole %)	Trial 5 (mole %)	Trial 6 (mole %)
Fuel Gas				
Carbon Monoxide	40.0	40.0	40.0	40.0
Hydrogen	26.3	26.3	26.3	26.3
Nitrogen	33.7	33.7	33.7	33.7
Hydrogen Sulfide	0	0	300 ppm	300 ppm
Water	2% R.H.*	2% R.H.*	2% R.H.*	2% R.H.*
Oxidant Gas				
Nitrogen	79.0	79.0	79.0	79.0
Oxygen	21.0	21.0	21.0	21.0

- R.H. – Relative Humidity

Each trial will use a single SOFCo EFS PSOFC that has an electrode surface area of 68.1 cm^2. The fuel cells will be operated in a test stand constructed by SOFCo EFS and will collect the voltage and current data of the PSOFC so the area specific resistance (ASR) may be calculated. The ASR will be calculated by completing a V-I scan approximately

every 24 hours. The V-I scan will be completed by operating the PSOFC over the current density range of (0.00 to 0.35 Amps/cm^2) and measuring the resulting PSOFC potential. The ohmic region data (0.05 to 0.35 Amps/cm^2) will then plotted as the PSOFC potential against the corresponding current density. A least squares linear regression will be completed on the data and the negative of the slope will be accepted as the PSOFC ASR at that point in time.

Trials 1 and 2 will be used to establish the repeatability of the baseline operation of the PSOFC. The trials will be carried out with a fuel gas rate of 428 mL/min and an oxidant gas rate of 2.6 L/min with the compositions shown in Table 3.1 at a pressure of 8 inches of H_2O gauge. The experimental error for the fuel and oxidant gas flow rates will be calculated taking into account the error associated with each MFC. Assuming that three mass flow controllers all having a maximum flow rate of 200 mL/min and with an accuracy of ±1 percent of the maximum flow rate range, and using propagation of error to account for the error associated with all three mass flow controllers, the flow rate of the fuel gas that will be supplied to the test stand will be 428 ± 6 mL/min. Also assuming a mass flow controller with a maximum flow rate of 5 sL/min of air would make the flow rate of oxidant gas to be supplied to the test stand to be 2.60 ± 0.03 sL/min. The gas flow rate ranges were chosen because it is a SOFCo EFS standard to supply their circular PSOFC with an electrode surface area of 68.1 cm^2 with 428 mL/min of fuel gas containing 50 mole percent H_2 and the balance being N_2 and 2.6 L/min of oxidant gas made of air. Each trial will be carried out at 850˚C for at least 500 hours. The operation temperature of the PSOFC has also been chosen from previously conducted trials by

SOFCo EFS. This temperature has been found to be the lowest temperature that will allow optimal oxygen ion transfer across the ceramic electrolyte. The trial length of 500 hours was chosen because it is an industry standard for solid oxide fuel cell testing. The PSOFC potential (Volts) and current (Amperes) will be collected every 10 minutes through the test stand's DAQ to track the potential of the PSOFC over time. The error of the SOFCo EFS electronic load (Agilent N3300A) is 0.05 percent and ±3 mA with respect to PSOFC current and ±3 mV with respect to PSOFC potential. Voltage/Current (VI) scans will be completed on the PSOFC once a day to measure the ASR of the PSOFC. The potential of the PSOFC will be measured over the current density range of 0.00 to 0.35 Amps/cm^2. The ohmic region data (0.05 to 0.35 Amps/cm^2) will then be used to calculate the ASR of the PSOFC by carrying out a least squares linear regression of the data. The error associated with the regression will be reported as the confidence interval found by calculating sigma mean from the data. The negative of the slope found from the data will then be accepted as the ASR of the PSOFC at that point in time. The PSOFC ASR (Ohms·cm^2) will then be plotted against time (hours). It is known that the degradation of a PSOFC's ASR is approximately 3 percent per 1000 hours of operation from previously tested 68.1 cm^2 circular PSOFC's by SOFCo EFS. If the degradation of the PSOFC's ASR is found to be less than 0.6 percent less than the initial cell's ASR after 200 hours of testing then operation repeatability will be assumed to have been established and the trial will be discontinued, followed by a second trial of 200 hours in length. Repeatable operation of the PSOFC will be assumed to have been established if the final PSOFC ASR values over the 200 hour trial lengths are within ±30 percent of

each other which is the criteria used by SOFCo EFS. If however the final PSOFC ASR of the second trial is not found to be within ±30 percent of the final PSOFC ASR value found in the first trial, then the second trial will be carried out for the full 500 hour trial length. If the two trials are unable to establish repeatable operation, final ASR values within ±30 percent of each other, then more trials will be carried out so repeatability may be established. The reason for only two trials being planned to establish repeatable operation of the PSOFC is due to the long trial lengths of 500 hours, shortening of these initial trials will enable more time to be spent researching the effect of the presence of H_2S in fuel gas and fuel gas pressurization. This data will allow the PSOFC ASR within ±30 percent of the value over time while operating at 850°C and ambient pressure to be established using fuel and oxidant gas compositions as shown in Table 3.1 at the flow rate of 428 ± 6.0 mL/min and 2.6 ± 0.3 L/min respectively to be known.

The third and fourth trials to be conducted will be used to establish the repeatability of the PSOFC operating with fuel and oxidant gas pressures at 50 psig. This pressure was chosen because it is the largest pressure that a test stand built by SOFCo EFS can withstand. The error that is associated with the pressure of the fuel and oxidant gases will be found by taking into account the accuracy of the gas pressure regulators (±0.5 psig) that are used to supply the mass flow controllers. For this case the accuracy of the regulators ±0.5 psig, which would make the pressure of the fuel gas and oxidant gas being supplied to the test stand to be 50.0 ± 1.5 psig, due to the mixture of three gases and 50.0 ± 0.5 psig respectively. Both trials will be carried out with fuel gas and oxidant

compositions as shown in Table 3.1. The fuel gas and oxidant gas will be supplied at rates of 428 ± 6 mL/min and 2.60 ± 0.03 L/min respectively to the PSOFC at a pressure of 50 ± 1.5 psig for the fuel gas and 50.0 ± 0.5 psig for the oxidant gas at 850˚C and 500 hours each. As in trial one if the final PSOFC's ASR value is found to be less than 0.6 percent of the initial PSOFC ASR then the trial will be carried out for 200 hours since it would be in agreement with trial data that has been supplied by SOFCo EFS, if it is not then the full 500 hour trial length will be used. As in trial two the fourth trial will be carried out for 200 hours if the PSOFC ASR value at that time is within ±5 percent of the PSOFC ASR found at that time for the third trial, if this is not the case then the full 500 hour trial length will be used. If at the end of trials three and four the final PSOFC ASR values are not found to be within ±5 percent of each other then more trials will be carried out until repeatable operation of the PSOFC with fuel gas with the composition as shown in Table 1 at an operating pressure of 50 ± 1.5 psig is established. This data will then be plotted as PSOFC ASR (Ohms·cm^2) versus time (Hours). The average PSOFC ASR degradation in percent difference for trials one through four will then be found by using Equation 3.1.

$$ASRDegradation = \frac{\left(ASR_{initial} - ASR_{final}\right)}{ASR_{initial}} \times 100 \qquad \text{Equation 3.1}$$

where ASR Degradation is in percent. The average PSOFC ASR degradation in trials three and four will then be compared to the average PSOFC ASR degradation from trials one and two by finding the percent difference between the two values. This value will

allow the effect of pressurizing the fuel and oxidant gas on the PSOFC ASR to be established.

The fifth trial is designed to allow the effect of H_2S on the PSOFC ASR at ambient pressure conditions to be found. The fuel and oxidant gas will be supplied at rates of 428.0 ± 6.0 mL/min and 2.60 ± 0.03 L/min respectively and have the compositions as shown in Table 3.1 at a pressure of 8 inches of H_2O gauge, at operating temperature of 850˚C, and an operation time of 500 hours. The experimental errors associated with the fuel and oxidants gases as well as their pressure will be done as explained above in trials one through four except the experimental error from the addition of H_2S into the fuel gas will also be accounted for. PSOFC VI scans will be approximately every 24 hours using the test stand's electronic load so the PSOFC ASR can be calculated using including its experimental error. The H_2S concentration in the coal syn gas mixture will be calculated by using the open cell potential of the PSOFC along with the Nernst equation for the PSOFC to determine the H_2O content of the simulated coal syn gas which will then be used to complete a mass balance to determine the H_2S content of the fuel gas. The H_2S composition including the error that is associated with the gas mixture will be accepted as the true H_2S concentration of the fuel gas. The trial data will then be plotted as PSOFC ASR ($Ohms/cm^2$) versus time (hours). The PSOFC ASR degradation for trial five will then be calculated using Equation 3.1. This will allow the PSOFC ASR within ±5 percent of its true value at the conditions specified for trial five over time to be established. The PSOFC ASR degradation of trial five will then be compared to the average PSOFC ASR degradation from trials one and

two by finding the percent difference between the two values. This will allow the effect of fuel gas containing H_2S at ambient pressure to be established.

The sixth trial is designed to demonstrate the effect of fuel gas containing H_2S at 50 psig on the operation of a PSOFC. The fuel gas and oxidant gas will be supplied at rates of 428.0 ± 6.0 mL/min and 2.60 ± 0.03 L/min respectively at the compositions shown in Table 1 and at a pressure of 50.0 ± 2.0 psig. The higher uncertainty in the gas pressure is caused by the addition of the H_2S. The PSOFC will be operated at 900˚C for 500 hours. PSOFC voltage and current data will be collected every ten minutes by the test stand's data acquisition system. The error associated with the fuel and oxidant gas flow rates and pressures will be completed as explained in the earlier trials. The H_2S composition of the gas will be determined in the same procedure as explained in trial five. The PSOFC ASR over time will be calculated using the least squares method using the data collected from the trial. This will allow the PSOFC ASR over time within ±5 percent of its true value to be known at the operating conditions specified for trial six. This data as in the previous trials will then be plotted as PSOFC ASR ($Ohms \cdot cm^2$) versus time (hours). The PSOFC degradation of trial six will then be calculated using Equation 3.1. The PSOFC ASR degradation of trial six will then be compared to the average PSOFC ASR degradation of trials three and four by calculating the percent difference between the two values. This will allow the effect of H_2S in a fuel gas at 50.0 ± 2.0 psig on PSOFC ASR to be established.

Once all six trials have been completed the overall effect that pressurized fuel gas containing H_2S has on PSOFC ASR will be found. This comparison will be done by

finding the percent difference between the average PSOFC ASR degradation value found from trials one and two and the PSOFC ASR degradation value from trial six. This value will then establish the general effect that the parameters of fuel gas containing H_2S and the pressurization of the fuel gas have on the operation of a PSOFC. The PSOFC ASR data from trials one and two and trial six will be plotted as PSOFC ASR ($Ohms \cdot cm^2$) versus time (hours). Also in effort to explain the effects that are seen from the variation of the experimental parameters the PSOFC's used in each trial will have XRD and SEM analyses completed on the anodes of the PSOFCs. These two analyses will allow the anode facial composition and its structure to be known and seen. Due to the uncertainty of the results from these tests, the results will not be relied upon to help explain the trends that are found from the planned experiments. The results from the XRD and SEM will only be used if the results are found to be of use in explaining the trends that are found.

Chapter - 4

Experimental Methods

4.1. Test Cell Characteristics

Electrolyte supported PSOFCs produced by InDEC were used in the experimental trials that were completed. Each PSOFC had an active area of 68.1 cm^2 under the gas delivery manifolds. The electrolyte was made of 3 mole percent yttria doped fully stabilized zirconium (YSZ), the cathode of the PSOFC is made was made of a strontium doped lanthanum manganite (LSM) peroviskite, and the anode was made of a proprietary blend that consisted of gadolinium doped cerium oxide (GDC) and nickel (Ni). The cathode was made of a strontium doped lanthanum manganite (LSM) peroviskite.

4.2. Mass Flow Controller Calibration

In order to supply the PSOFC with simulated coal syn gas to the anode and air to the cathode mass flow controllers (MFCs) from Porter Instruments were used. The simulated coal syn gas was produced through the use of three different MFCs; H_2, CO, and N_2 with maximum flow rates of 0.40 sLpm, 0.30 sLpm, and 0.50 sLpm respectively. An air mass flow controller with a maximum flow rate of 3.0 sLpm was used to control the cathode air flow rate. The manufacturer reported that the MFCs have an error of 1.5 percent of the maximum flow rate. To ensure that the MFCs were operating within the expected error reported by the manufacturer each MFC was calibrated individually with a bubble meter and stop watch. Flow rates and times were recorded for control voltages of 1.0 V, 2.0 V, 3.0 V, 4.0 V, and 5.0 V respectively. The calibration charts for each MFC

is attached in the appendix. Table 4.1 lists each gas' MFC gain and error found from the calibration testing.

Table 4.1 MFC Gains and Errors.

MFC	Gain (sLpm/%)
Hydrogen	$4.07x10^{-3} \pm 0.01x10^{-3}$
Carbon Monoxide	$3.15x10^{-3} \pm 0.01x10^{-3}$
Nitrogen	$5.25x10^{-3} \pm 0.04x10^{-3}$
Air	$3.00x10^{-2} \pm 0.01x10^{-2}$

At the time when MFC calibrations were completed a bubble meter large enough for the testing of the air MFC was not available, because of this the manufacturer calibration chart and error of 1.5 percent of the maximum flow rate was accepted as the error associated with the air MFC. Calibration charts for each gas' MFC are attached in the appendix. Since the error reported by the manufacturer was greater than the error found during calibration trials the 1.5 percent of the maximum flow rate was accepted as the error of each respective MFC to be conservative.

The errors that have been accepted for each gas' MFC are shown in Table 4.2.

Table 4.2 Accepted MFC Errors.

MFC	Error sLpm
Hydrogen	0.006
Carbon Monoxide	0.005
Nitrogen	0.008
Air	0.05

The error associated with the MFCs is important because it allows the known effect on the operation of a PSOFC by a simulated coal syn gas to be quantified. However since gas sampling is not an option at the anode of the SOFCo single cell test stand the effect that each individual gas in the simulated coal syn gas can not be found. Because there are two possible reacting species contained in the simulated coal syn gas, H_2 and CO, and the possibility of reforming reactions taking place at the anode of the PSOFC individual gas effects on the operation of the PSOFC can not be quantified in this research.

4.3. Ambient Pressure Experimental Setup

In order to operate the single cell test stand properly and ensure the data acquired from the trials are accurate an experimental set up procedure has been developed for both the ambient and pressurized trials. The first step in ambient pressure trial procedure is to prepare the anode side of the PSOFC for insertion into the single cell test stand. First the anode manifold is cleaned with acetone so that no contaminants are present on its surface. Next the anode manifold is placed into the annulus sleeve of the single cell test stand as shown and the manifold thermocouple is inserted as shown Figure 4.1 and Figure 4.2.

Figure 4.1 Placement of Anode Manifold into Single Cell Test Stand.

Figure 4.2 Positioning of Manifold Thermocouple.

As can be seen in Figure 4.1 the surface of the anode manifold has been cleaned so that no contaminants are present. Next a layer of NiO ink is rolled onto the surface of the anode manifold shown in figure 4.3.

Figure 4.3 Layer of NiO Ink Being Applied to Anode Manifold.

Next the nickel foam current collector is prepared by rolling a layer of the anode ink onto each side so that the pores of the foam are clogged with the ink but are not saturated. Then a second layer of NiO ink is brushed onto the outer edge of the nickel foam so the outer region becomes saturated. This is done to help seal the outer edge of the PSOFC while the cell is being operated. Figure 4.4 shows the nickel foam current collector after it has been prepared with the NiO ink.

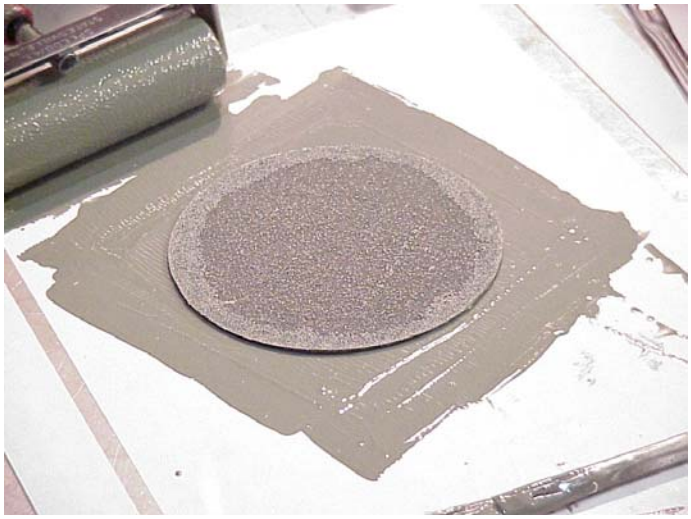

Figure 4.4 Nickel Foam Prepared with NiO Ink.

Next the nickel foam current collector is placed onto the anode gas manifold while a piece of 5 mill Incanel ribbon is placed on top of the nickel foam as shown in Figure 4.5. The Incanel ribbon is used as an anode voltage tap for the Agilent electronic load.

Figure 4.5 Placement of Incanel Ribbon onto Nickel Foam.

The Incanel ribbon is then taped to the side of the single cell test stand furnace so that it does not come into contact with any other metal materials on the test stand. The anode of the PSOFC is then prepared by applying a thin layer of the NiO ink onto the anode of the PSOFC with an acid free brush as shown in Figure 4.6.

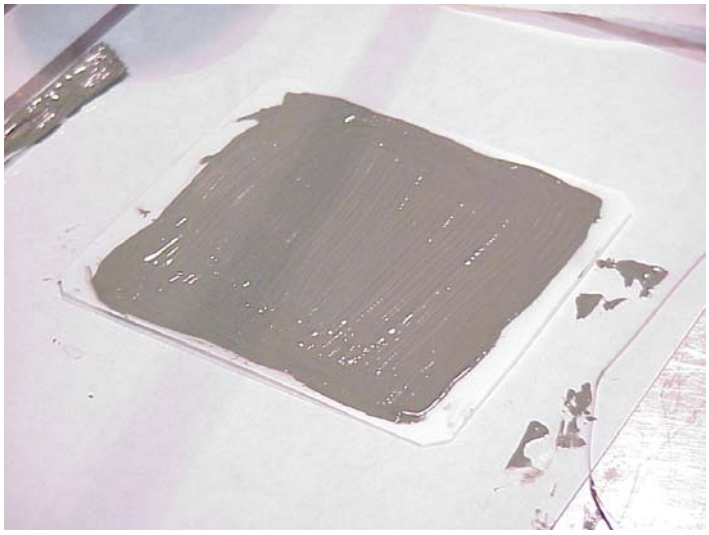

Figure 4.6 Application of NiO Ink to the PSOFC Anode.

As can be seen from Figure 4.6 great care must be taken to make sure that no NiO ink is present on the outside edge of the PSOFC. The presence of NiO ink on the outside edge of the PSOFC may lead to a short circuit during the PSOFC heating process. After the anode of the PSOFC has been prepared it is then placed on top of the nickel foam so that the circular surface of the nickel foam is evenly distributed across the anode surface of the PSOFC shown in Figure 4.7.

Figure 4.7 Placement of PSOFC onto Anode Manifold.

Next the cathode of the PSOFC is prepared for the single cell test stand. The first step in the PSOFC cathode preparation is to apply a thin layer of 0.8 PrO8 ink onto the PSOFC cathode with an acid free brush shown in Figure 4.8.

Figure 4.8 Application of 0.8 PrO_8 Ink to PSOFC Cathode.

As in the case of the PSOFC anode great care must taken to make sure that no 0.8 PrO_8 touches the edge of the PSOFC so that a short circuit does not occur during warm up. Next the silver mesh current collector for the cathode of the PSOFC is prepared by weaving a piece of 2 mill Cromel ribbon into the silver mesh as a voltage tap and spot welding the ribbon several times as shown in Figure 4.9

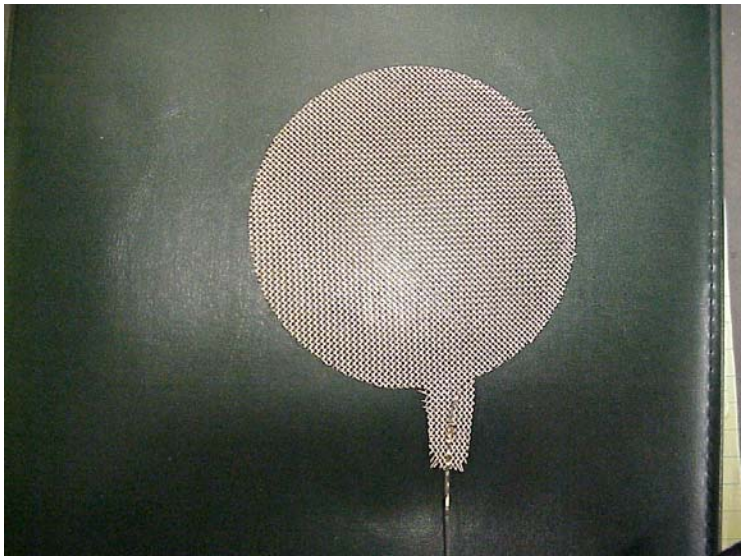

Figure 4.9 Silver Mesh Cathode Current Collector with Voltage Tap.

Next 0.8 PrO_8 ink is rolled onto the silver mesh so that the open areas of the mesh are clogged with the ink as shown in Figure 4.10.

Figure 4.10 Rolling 0.8 PrO_8 Ink onto Silver Mesh.

The silver mesh current collector and voltage tap is then placed on top of the cathode of the PSOFC so that it is centered around the cathode of the PSOFC. The Cromel ribbon is taped to the opposite side of the single cell test stand as the anode voltage tap shown in Figure 4.11 Figure 4.12.

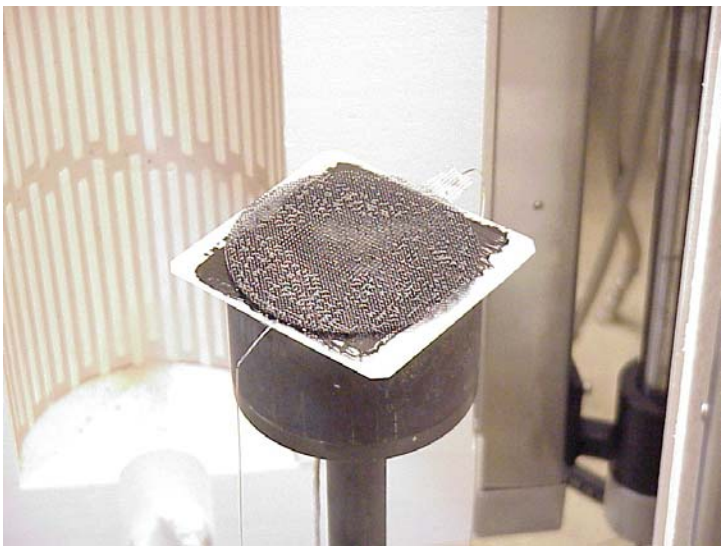

Figure 4.11 Placement of Silver Mesh onto PSOFC Cathode.

Figure 4.12 Cathode Voltage Tap Taped into Position.

Once the silver mesh and cathode voltage tap have been placed onto the cathode of the PSOFC the cathode manifold is then prepared for installation. First the cathode manifold is thoroughly cleaned with acetone in the same manner as the anode manifold. Next a

thin layer of 0.9 PrO_8 ink is rolled onto the surface of the cathode manifold. Then the cathode manifold is carefully placed so that it sits directly above the anode manifold so that an even distribution of the manifold's weight across the PSOFC is achieved shown in Figure 4.12 and Figure 4.13.

Figure 4.13 Positioning of Cathode Manifold.

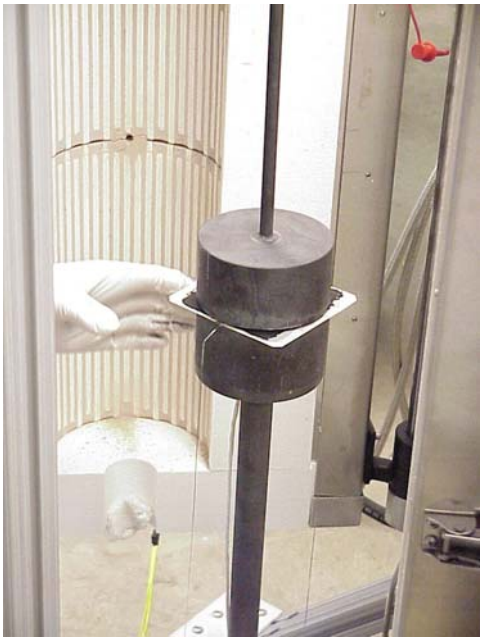

Figure 4.14 Final Placement of Cathode Manifold.

Next the voltage taps and the anode and cathode gas lines are connected to Agilent electronic load and the single cell test stand system respectively as shown in Figure 4.15 and Figure 4.16.

Figure 4.15 Anode Gas Line Connection.

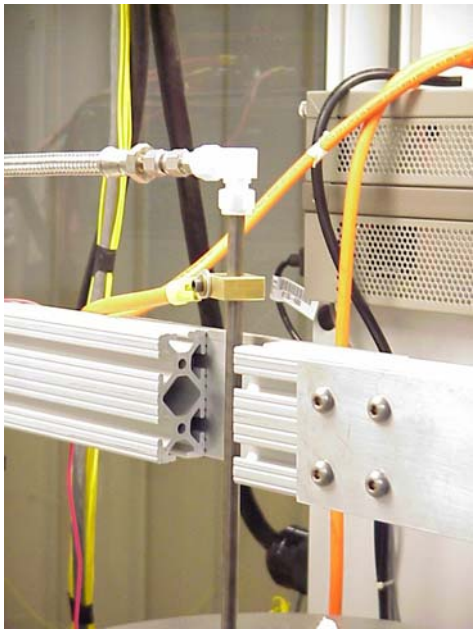

Figure 4.16 Cathode Gas Line Connection.

After all of the connections have been made and checked the single cell test stand is then closed shown in Figure 4.17.

Figure 4.17 Single Cell Test Stand Ready to be Closed.

The last task of the single cell test stand procedure is to fill the H_2O bubbler column located on the side of the single cell test stand.

4.4. Single Cell Test Stand Heating

During the initial operation of the PSOFC the fuel cell must first be provided with both anode and cathode gases that will allow the heating of the fuel cell to take place evenly. SOFCo EFS standard single cell testing flow rates of 214.0±6.0 mL/min H_2 and 214.0±7.5 mL/min N_2 to the anode and 2500±45 mL/min to the cathode, which is equivalent to 10 stoichs of air are provided to the single cell test stand. The PSOFC is slowly increased up to the operational temperature of 850°C by two different heating cycles that are used and allow the PSOFC to be heated evenly across its surface so that cracking does not take place. The first heating cycle which is controlled by software on

the single cell test stands heats the PSOFC from room temperature to 600°C at a rate of 0.7°C/min. The second heating procedure then heats the PSOFC from 600°C to 850°C at a rate of 1.5°C/min. Once the PSOFC has reached its operational temperature the fuel cell is then subjected to electrochemical measurements. The temperature of the PSOFC is measured with a type-K thermocouple with an error of ±1.5°C that is located approximately 0.25 inches below the anode of the fuel cell as shown in Figure 4.2. To ensure that the temperature of the PSOFC is nearly the same as the measurement from the thermocouple the fuel cell is allowed to warm for approximately three to four hours once the operational temperature of 850°C is established at the anode manifold thermocouple. SOFCo EFS believes that little error is involved in accepting the anode manifold temperature as the true temperature of the PSOFC as long as the three to four hour warm up time is observed between the end of the furnace heating cycles and the beginning of the electrochemical measurements.

4.5. Electrochemical Measurements

Figure 4.18 shows the test geometry used for the PSOFC electrochemical measurements.

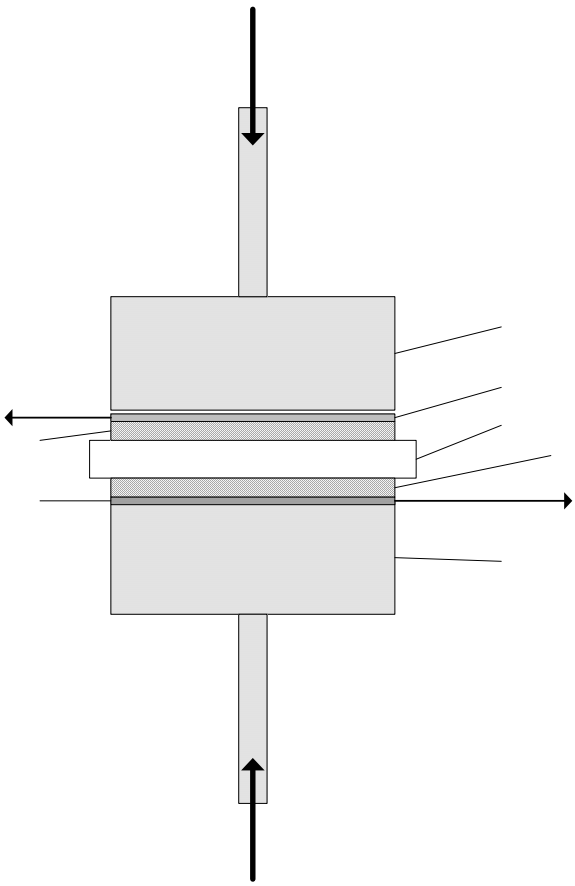

Figure 4.18 Electrochemical Test Geometry.

Where A is the cathode manifold, B is the silver mesh cathode current collector, C is the PSOFC cathode, D is the PSOFC electrolyte, E is the PSOFC anode, F is the nickel foam anode current collector, and G is the anode manifold. The cathode voltage tap is placed spot welded onto the silver mesh current collector as shown in Figure 4.18 and the anode voltage tap is placed between F and G. The anode and cathode manifolds used in the test setup are made of Incal Alloy 80.

The anode and cathode voltage taps are connected to an Agilent Model N3300A potentiostat that is used to operate the PSOFC under load and collect the potential and

current data from the PSOFC. The error associated with the voltage and current collection devices ±0.05 percent of the value displayed on the electronic load and ±3mA in the case of current and ±3mV in the case of potential. The errors associated with the voltage and current will allow the actual operation of the PSOFC with various anode and cathode gas conditions to be quantified very well. This will allow the effect of various anode fuel gas compositions on the operation of the PSOFC to be determined with minimal instrument uncertainty.

In order to determine if the PSOFC is operating properly the fuel cell is first tested to determine if it operates according to prior SOFCo EFS test data. In order to do this the PSOFC is first supplied an anode gas made of 350±6mL/min of H_2 and 350±6mL/min of N_2 and a cathode gas flow rate of 2500±45mL/min of air [1]. The single cell test stand is then heated through the two cycles that were explained in detail in section 4.4. Once the PSOFC reached its operational temperature and the three to four hour PSOFC soak time was completed a voltage/current (VI) scan was then taken to determine the area specific resistance (ASR) of the PSOFC. A VI scan is completed by operating PSOFC is operated galvanostatically through a range of electrical loads from 0 to 22.00±0.01Amps in 2Amp increments. The load that the PSOFC is operated under is selected by first pressing the current button located on the Agilent N3300A potentiostat located on top of the single cell test stand. Then a current load in Amps is then inputted into the potentiostat using the numeric keypad and then the enter button is pressed as shown in Figure 4.19 and Figure 4.20.

Figure 4.19 Agilent N3300A Potentiostat.

Figure 4.20 Single Cell Test Stand Indicators.

After the enter button has been pressed the PSOFC is then operated under the load that was inputted into the potentiostat. Once the PSOFC reached a steady state potential which typically occurred after 20 seconds upon the change of the load. The potential of

the PSOFC is recorded from the instrumentation on the front of the single cell test stand as shown in Figure 4.19. Once the steady state potential for the current load has been recorded a load increase of 2 Amps is inputted into the potentiostat and the same procedure is once again repeated. The same method of increasing the load by 2 Amps and recording the respective steady state PSOFC potential is repeated until a load of 22 Amps is reached. No more data points are taken after a current load of 22 Amps because the PSOFC then approaches the concentration polarization range and only the ohmic region data that has been collected will be used to correlate the linear ASR slope. The ASR of the PSOFC is determined by plotting the PSOFC potential (Volts) against current density (Amps/cm^2) and then calculating the linear slope of the ASR line ($\Omega \cdot cm^2$) with the ohmic region data (0 to 0.35±0.01 Amps/cm^2) by the method of least squares linear regression. The confidence interval of the slope was calculated by finding σ_{mean} for each set of ohmic region data. This confidence interval will show the range of the ASR value and will allow an appreciable change in the ASR to be seen if further VI scans result in ASR values that do not lie within the confidence intervals of each other. This slope represents the total losses (anodic, electrolyte, and cathodic) of the PSOFC as explained in section 1.1. Because the losses in the PSOFC below 0.05 Amps are considered to be the activation losses of the fuel cell these data points are not used in the calculation of the PSOFC's ASR. Since the activation losses of the PSOFC are considered to be negligible because of the high operational temperature of the PSOFC they are ignored when determining the performance of the PSOFC. Once the initial ASR for the PSOFC has been determined the fuel cell is operated under a load of 14 Amps (0.21 Amps/cm^2). The

load of 14 Amps was chosen to keep with SOFCo EFS single cell testing practices. A VI scan is taken approximately every 24 hours and the respective ASR including its confidence interval is calculated from each set of data. In order to protect the PSOFC from damage when VI scans are taken the load on the PSOFC is slowly decreased at a 2 Amp interval with a period of at least 30 seconds between each load decrease. In order to determine if the PSOFC is operating according to SOFCo EFS standards the PSOFC ASR values are plotted against time to determine if the values have remained in an acceptable ASR range of ±30 percent of the 1.22 $\Omega \cdot cm^2$ after 24 hours of operation or if a high rate of ASR degradation has taken place. If no apparent ASR changes are seen and the final ASR value that has been calculated for the PSOFC is with in ±30 percent of 1.22 $\Omega \cdot cm^2$ then the PSOFC is considered to be operating properly.

After the PSOFC has been determined to be operating properly a baseline coal syn gas mixture is then provided as the fuel for the PSOFC. The simulated baseline coal syn gas mixture contained 40.0 mole percent CO, 23.7 mole percent H_2, and the balance being N_2. This was achieved by setting the MFCs for the anode gas so that 212.1±4.5 mL/min CO, 139.2±6.0 mL/min H_2, and 175.6±7.5 mL/min N_2 are mixed in the anode gas manifold of the gas delivery system and then delivered to the anode of the PSOFC. These gas flow rates yield a total simulated coal syn gas flow rate of 526.9±18.0 mL/min. The error associated with each gas' MFC yielded the following ranges in composition; 40.0±2.1 mole percent CO, 23.7±4.3 mole percent H_2, and 33.3±4.3 mole percent N_2. These flow rates were chosen so that the normal fuel that is provided by SOFCo EFS (214 mL/min H_2) is replaced by CO. The error associated with the simulated baseline

coal syn gas composition and flow rate is considered to be insignificant. The reason the anode gas' composition error is considered insignificant is that the composition of a coal syn gas produced by a gasifier changes to some extent due to slight changes in the composition of the coal being gasified and in the flow rates of the coal, steam, and oxygen that are supplied to the gasifier. Also the reason that the error associated with the flow rate of the simulated baseline coal syn gas is considered to be insignificant is due to the fact that the fuel utilization of the PSOFC during steady state operation and VI scans is no greater than 50 percent. Since the fuel utilization of the PSOFC is in this range problems associated with concentration polarization will not take place.

The PSOFC was operated with the simulated baseline coal syn gas mixture for approximately 4 hours under a load of 14 Amps before the first VI scan was completed. After the first VI scan was completed the PSOFC was operated under the steady state galvanostatic condition once again. Additional VI scans were then taken approximately every 24 hours and the ASR and confidence interval with each set of data was calculated. The PSOFC was operated under this condition for at least one week. However the overall goal of the trials was to operate the PSOFC under the simulated baseline coal syn gas for at least 500 hours. However this was unable to be reached due to problems with the loss of electricity at the SOFCo EFS facility, problems associated with the electrical backup, and coking that was taking place in the anode manifold inlet tube. After the simulated baseline coal syn gas trial was completed the overall trend in the ASR of the PSOFC was calculated to determine the percentage difference from the initial PSOFC ASR for 1000 hours of operation. The successfulness of the trial is determined according

to a SOFCo EFS standard of an increase in the ASR of the PSOFC of approximately 3 percent or less for every 1000 hours of operation.

In order to establish reproducibility and due to the excessively lengthy trials one trial has been replicated for reproducibility. This trial was carried out in the same manner as explained above and was considered to be credible evidence of reproducibility due to past SOFCo EFS trial data which is shown in Appendix 1. SOFCo EFS considers a trial to be reproducible if the increase in the ASR of the PSOFC is approximately 3 percent per 1000 hours of operation and if the final and initial ASR values including error are within ±30 percent of each other. Although this range of acceptance seems to be very large SOFCo EFS has explained that due to the state of the technology at this time trials can not be carried out with exceedingly high levels of precision. After the repeatability of the simulated baseline coal syn gas was established the next level of testing was completed.

The next trial that was completed established the effect of H_2S on the operation of the PSOFC. This was done by using a premixed bottle of CO containing 758±4ppm H_2S. This mixture of CO and H_2S was chosen so that the CO MFC may be used to control the level of H_2S that is in the simulated coal syn gas and also reduce the amount of H_2S that would be contained in the cabinet at any moment for safety purposes. The error associated with the H_2S composition was accepted from the calibration data from the AGA gas company that produced the gas mixture. This mixture was originally chosen so that a simulated coal syn gas containing approximately 300ppm H_2S could be produced. However because of the coking problem in the anode manifold inlet tube in the first trial

a heating strip was added to the H_2O bubbler of the single cell test stand. This heating strip was used to increase the H_2O temperature from 25°C to 70°C which increased the H_2O content of the simulated coal syn gas as it traveled through the bubbler column. This increased H_2O content was used to prevent coking problem that was taking place. However the additional H_2O in the simulated coal syn gas effected the H_2S composition that could be produced. In order to determine the new concentration of H_2O in the simulated coal syn gas the open cell potential of the PSOFC while using 50 mole percent H_2 and balance N_2 anode gas was used along with the Nernst equation to calculate the new H_2O concentration of the simulated coal syn gas. Little error is associated in using this method to calculate the H_2O content of the simulated coal syn gas since the calculation used the open cell potential of the PSOFC and the well known Nernst equation. This calculation is discussed in more detail in Chapter 5.

After the initial VI scan was taken from the PSOFC the simulated baseline coal syn gas that was used in the previous trials was then provided to the PSOFC. This was done so that the PSOFC ASR utilizing the baseline coal syn gas mixture could be established and allow the effect of the H_2S contaminant to be seen upon its addition to the system. The baseline coal syn gas mixture was provided to the PSOFC for approximately 72 hours when the CO portion of the baseline coal syn gas mixture was switched to the CO/H_2S mixture. The PSOFC was operated utilizing the simulated coal syn gas mixture containing H_2S for approximately 460 hours.

4.6. Material Analyses

After the completion of each trial material analyses (SEM, EDXS, and XRD) were completed on the PSOFC used in the trials and on a PSOFC that had not been used in testing. The materials testing was used to determine if there were any noticeable changes in the structure or composition of the PSOFC anode after each trial compared to the unused PSOFC anode. The following sections will explain the methods and settings that were used in each testing method.

4.6.1. SEM and EDXS Analyses

A Cambridge S240 SEM was used to capture images of the PSOFC anodes. SEM images were taken from several areas of the PSFOC anode to determine the homogeneity of the anode after utilizing the various anode fuels. SEM images were taken at magnifications of approximately 550X, 1430X of each anode so comparisons could be made. A NORAN Instruments energy dispersive x-ray spectrometer (EDXS) system used for testing. EDXS was used to determine the elemental composition of the PSOFC anode surface. Multiple EDXS spectrums were taken to ensure the homogeneity of the surface of the PSOFC anode. Upon the completion of the SEM and EDXS analyses the results were compared to one another.

4.6.2. XRD Analyses

X-ray diffraction (XRD) analyses were completed with a Ringaku Incorporated x-ray generator. All of the XRD spectrums were obtained using an RS slit of 0.3 and a SS slit of 1.0°. The spectrums were completed over a theta to theta range of 15° to 90° with a scan rate of 1.5°/min. Although the theta to theta range was completed from 15° to 90°

the range of interest was 20° to 60° for the components of the PSOFC. The main components that were searched for in the PSFOC anode were cerium oxide, zirconium oxide, nickel, carbon, and nickel sulfide (Ni_2S_3). Multiple XRD spectrums were taken over each PSOFC anode to ensure the homogeneity of the anode surface. Upon the completion of all of the XRD spectrums the results were compared to one another.

Chapter - 5

Experimental Results

5.1. Introduction

A modified test matrix containing three trials investigating the effects of a simulated coal syn gas and a simulated coal syn gas containing H_2S has been completed. The original test matrix proposed in Chapter 3 was not completed due to many complications associated with testing and planning that were outside the control of the Ohio Coal Research Center. A brief overview of the difficulties that were encountered during the testing will be presented as well as the results from the three trials that were completed. The intellectual information that has been gained from these trials will be presented in the following sections.

5.2. Testing Difficulties

The first three trials that were completed with the SOFCo EFS single cell test stand encountered many problems associated with the operation of the test stand and the gas delivery system including incorrectly wired solenoid valves, incorrectly sized MFCs, and power outages. The data obtained from these trials was deemed unacceptable and so the data will not be presented or used to draw conclusions upon.

5.3. Research Test Matrix

Table 5.1 presents the test matrix of the research that was completed.

Table 5.1 Completed Research Test Matrix.

	Date	Testing Parameter
Trial 4	5-25-04 to 6-9-04	Baseline Coal Syn Gas
Trial 5	6-25-04 to 7-7-04	Baseline Coal Syn Gas
Trial 6	7-20-04 to 8-16-04	Coal Syn Gas Containing H_2S

From Table 5.1 it may be seen that two trials were completed using the baseline coal syn gas mixture and one trial using the same coal syn gas mixture with H_2S contaminant. The results from the trials 4 through 6 will be presented in the following sections.

5.4. Trial Four

Trial four was designed to test the PSOFCs ability to utilize a simulated coal syn gas as fuel. The PSOFC is initially operated in every trial with an anode fuel gas flow rate of 771±14 smL/min with the composition shown in Table 5.2 and a cathode air flow rate of 2500±45 smL/min.

Table 5.2 Initial Anode Gas Composition.

SOFCo Anode Gas Composition (Mole %)
48.4±0.8 H_2
48.4±1.1 N_2
3.1±1.9 H_2O

The anode gas composition shown in Table 5.2 was used to match standard SOFCo EFS anode gas composition and flow rate to determine if the PSOFC was operating properly according to SOFCo EFS standards. According to SOFCo EFS a PSOFC is considered to

be operating properly if the area specific resistance (ASR) of the PSOFC is within ±30 percent of 1.20 $\Omega \cdot cm^2$. The large percentage variation in the initial PSOFC ASR value is caused by part to part variation that is seen in the PSOFCs. Although all of the PSOFCs are produced in the same manner large differences in the ASRs of the PSOFCs have been seen as shown in the past SOFCo EFS InDEC PSOFC data attached in Appendix 1.

5.4.1. Trial Four Initial PSOFC Operation

The operation of InDEC ESC PSOFC KS1S040318-1 was started by increasing the temperature of the PSOFC from room temperature to its operational temperature of 850°C through the two heating cycles that were explained in section 4.4. Once the PSOFC reached its operating temperature of 850°C it was allowed to operate in open cell condition, no electrical load was applied, for approximately 1 hour. The initial open cell potential of the PSOFC was found to be 1.020±0.004 Volts compared o a theoretical open cell potential of 1.05 Volts for the anode gas mixture shown in Table 5.2. The theoretical open cell potential calculations are shown in Appendix 2. The difference between the theoretical and the measured potential of the PSOFC is caused by the activation polarization that is present in all fuel cells but due to the high operating temperature of the PSOFC little difference is found between the theoretical and the measured open cell potentials. After the PSOFC was allowed to reach a steady state open cell operating condition the initial VI scan was completed by applying a current (Amperes) and measuring the resultant PSOFC potential (Volts). Currents in the range of 0-22 Amps in two Amp intervals were applied to the PSOFC and the resulting steady state PSOFC potentials were then recorded. Once the data from the initial VI scan was

recorded the data was used to graph the characteristic operating curve of the PSOFC by plotting the potential of the PSOFC (Volts) against the current density of the PSOFC (Amps/cm^2). The current density of the PSOFC was found by dividing the total applied load (Amps) by the active area of the fuel cell (68.1 cm^2) which is equal to the area of one of the gas manifolds adjacent to the electrodes of the PSOFC at a temperature of 850°C as shown in Figure 4.18. No error is associated with the area of the gas manifold since SOFCo EFS has determined that the area of the fuel manifolds has little variation. The resulting characteristic curve resulting from the initial VI scan on PSOFC KS1S040318-1 is shown in Figure 5.1.

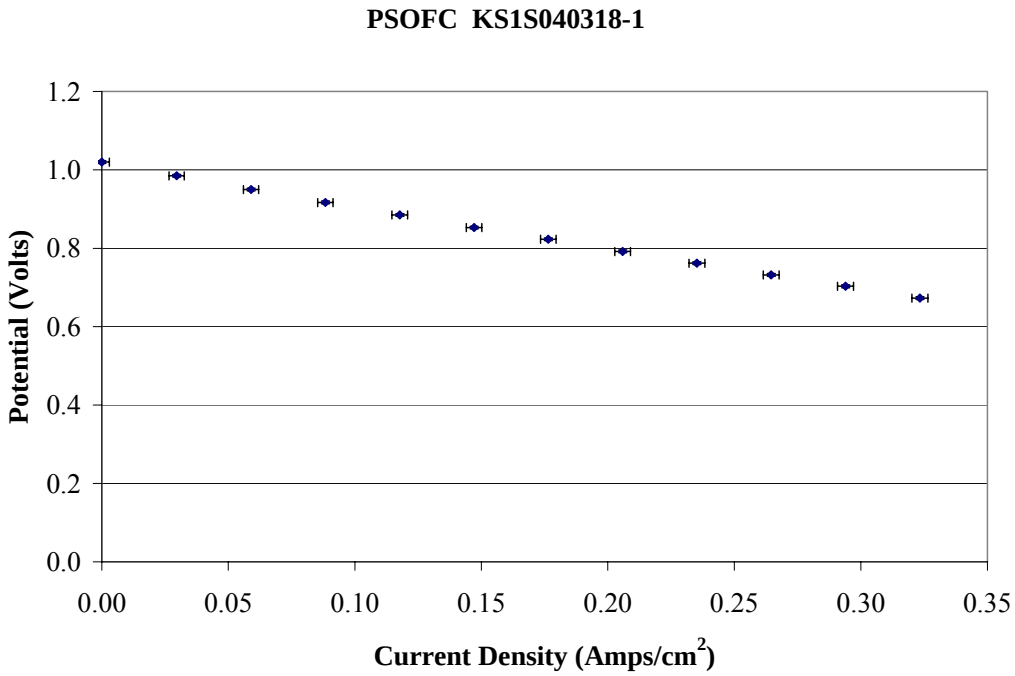

Figure 5.1 Trial 4 Initial VI Scan.

The error bars associated with the PSOFC current density and potential represent the measurement error associated with the Agilent N3300A potentiostat that was used to

control the PSOFC. The error associated with the Agilent N3300A is 0.05 percent of the current and potential value shown on the potentiostat and ±3 mA in the case of current or ±3 mV in the case of potential. In order to determine the operational condition of the PSOFC the ASR of the PSOFC was measured by determining the slope of the data present in the ohmic loss region of the PSOFC's characteristic curve. Although the ASR of the PSOFC represents all the resistances (anodic, cathodic, and electrolyte) the value is mainly composed of the cathodic losses [14]. The ohmic loss region of the InDEC ESC PSOFCs that were used is this research is considered to be in the current density region of 0.05±0.01 Amps/cm^2 to 0.35±0.01 Amps/cm^2 according to SOFCo EFS fuel cell engineers. This was verified by completing a least squares linear regression using the first three VI scan data points. This regression yielded an ASR of 1.18±0.03 Ω·cm^2 while the slope of the line associated with the ohmic loss region of the PSOFC characteristic curve yielded a slope of 1.04±0.02 Ω·cm^2 indicating a transition point between the activation and ohmic loss region takes place at a current density of approximately 0.0590±0.003 Amps/cm^2 as was measured from the PSOFC. The data associated with the activation losses of the PSOFC is not considered to be as important as the losses associated with the ohmic resistance of the PSOFC since this region accounts for the majority of the polarizations in the PSOFC. Activation losses are very small for PSOFCs in general due to the high operational temperature. Data for current densities greater than the ohmic loss region (> 0.35 Amps/cm^2) is not considered to be as important as the ohmic region because the losses are caused by concentration differences that take place when there is high fuel utilization which can not be avoided. In order to determine the

ASR of the PSOFC the VI data recorded in the ohmic loss current density region is plotted as the PSOFC potential (Volts) against the PSOFC current density (Amps/cm^2). A least squares linear regression is completed on the ohmic loss data fitting it to a simple linear equation and the negative of the slope of the line is equivalent to the ASR of the PSOFC ($\Omega \cdot cm^2$). The simple linear equation, least squares regression equations, statistical equations, and methods used are shown in Appendix 2. Figure 5.2 shows the initial ohmic loss region data and resulting regression for PSOFC KS1S040318-1.

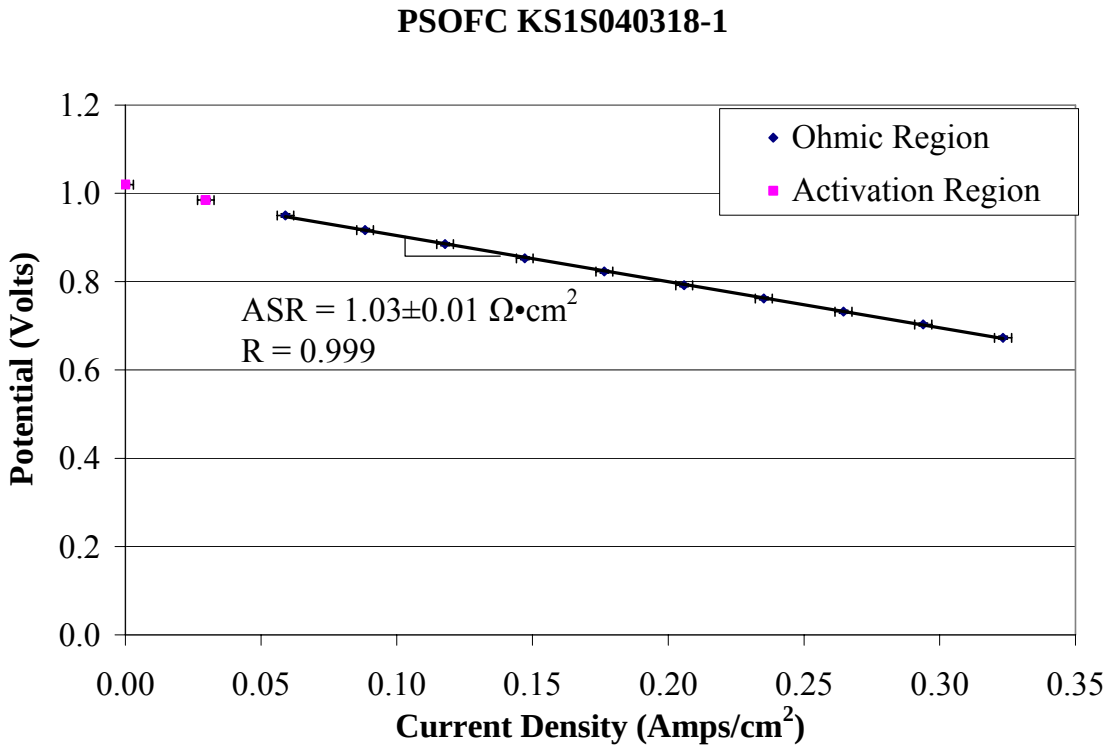

Figure 5.2 Initial PSOFC ASR Regression.

From the least squares linear regression the ASR of PSOFC KS1S040318-1 was found to be 1.03±0.01 $\Omega \cdot cm^2$. The correlation coefficient, R, from the regression was found to be

0.999 showing that the regression resulted in a very linear line. The regression coefficient R is the square root of the coefficient of determination, R^2, which represents the fraction of total variation response that is explained by the predictable part of the data. Since R is very close to 1 this means there is very little difference between the actual ohmic resistance data and the values predicted by the model. The small confidence interval that resulted from the linear regression revealed that little variability is present in the current and potential data that was recorded from the Agilent N3300A potentiostat. The PSOFC was determined to be operating normally according to SOFCo EFS conditions described previously. The initial ASR value was determined to be within 14.8±1.6 percent of the accepted SOFCo EFS initial ASR value of 1.20 $\Omega \cdot cm^2$ so the PSOFC was determined to be operating properly.

After the initial ASR value of PSOFC KS1S040318-1 was calculated the PSOFC was operated under an electrical load of 14.00± 0.01 Amps for approximately 159.8 hours with the same anode and cathode gas compositions and flow rates stated above. Three additional VI scans were completed over the specified time period and the ASR of the PSOFC was calculated in the same manner as explained above. The results from VI scans two through four that were completed on PSOFC KS1S040318-1 are shown in Table 5.3.

Table 5.3 Calculated PSOFC ASRs Using H_2/N_2 Anode Gas.

VI Scan	Operation Time (Hours)	ASR ($\Omega \cdot cm^2$)
2	23.0	1.22±0.01
3	113.5	1.16±0.01
4	159.8	1.17±0.01

From the regressed ASR values shown in Table 5.3 it can be seen that an initial increase in the ASR of 17.3±1.9 percent of the PSOFC KS1S040318-1 took place over the first 160 hours of operation. The increase of the PSOFC's ASR was expected based on past SOFCo EFS data for the InDEC PSOFCs that are being used for this research. A plot of past ASR data from several SOFCo EFS trials is attached in Appendix 1. SOFCo EFS' data indicates that ASR values are typically within ±30 percent of 1.20 $\Omega \cdot cm^2$. Also past SOFCo EFS PSOFC data shows that the InDEC ESC PSOFCs used in the previous testing show a behavior of having an ASR value lower than 1.20 $\Omega \cdot cm^2$ and quickly increasing to approximately 1.20 $\Omega \cdot cm^2$ after the first 24 hours of operation and then operating steadily. The PSOFC was concluded to be operating normally based on the results obtained from VI scans one through four and with personal communication with SOFCo EFS fuel cell engineers.

In order to determine the degradation rate of the PSOFC over time a least squares linear regression was completed on the data obtained while using the H_2/N_2 anode gas mixture. The slope of the line resulting from the regression is equivalent to the degradation of the PSOFC ASR over time. Two least squares linear regressions were completed. The first regression was completed with ASR values from VI scans 1 through

four that resulted in a slope whose confidence interval spanned zero revealing that the parameter was statistically insignificant. The second regression was completed using VI scans 2 through 4 since the ASR value resulting from the second VI scan was accepted as the initial steady state value of the PSOFC. However this regression also resulted in a statistically insignificant slope. Equation 3.1 was then used to determine the ASR degradation of the PSOFC using VI scan 2 as the initial ASR value and VI scan 4 as the final ASR value that resulted in a degradation rate of -3.00 percent per 100 hours of operation. Because it is impossible to for the ASR of the PSOFC to improve over long periods of operation more effective methods to determine the ASR degradation rate of the PSOFC will be discussed in the recommendations section of this thesis.

5.4.2. Trial 4 PSOFC Operation with Baseline Simulated Coal Syn Gas

Once PSOFC KS1S040318-1 was determined to be operating normally a simulated coal syn gas mixture was sent to the single cell test stand immediately after VI scan four was completed. The coal syn gas mixture that was used contained a mixture of 212.1±4.5 smL/min CO, 139.2±6.0 smL/min H_2, and 175.6±7.5 smL/min N_2 and a cathode air flow rate of 2500±45 smL/min. The flow rate of CO was chosen so that the H_2 fuel that was utilized in typical SOFCo EFS trials, 214 smL/min H_2, would be replaced with approximately the same amount of the lesser quality fuel. The flow rates of the other baseline coal syn gases were then chosen so that the baseline coal syn gas mixture proposed in Table 3.1 could be achieved. Table 5.4 presents the simulated coal syn gases (SCSG) produced in the gas delivery system (GDS) and after the H_2O bubbler that is utilized by the PSOFC.

Table 5.4 SCGS Composition Comparison.

Component	GDS Composition (Mole %)	Anode Fuel Gas Composition (Mole %)
H_2	26.4±4.3	25.6±1.4
CO	40.3±2.1	39.0±0.8
N_2	33.3±4.3	33.2±2.3
H_2O	0	2.2±0.7

The error associated with the H_2O content of the simulated baseline coal syn gas was found by taking into account the variability of the open cell potential of the PSOFC measured by the potentiostat. The simulated coal syn gas mixture was used to model a Pittsburgh No.8 O_2 blown gasified coal. Table 5.5 shows the composition of the coal syn gas produced by O2blown coal gasification.

Table 5.5 O_2 Blown Pittsburgh No.8 Syn Gas Composition.

Species	Mole %
CO	37.73
CO_2	15.38
H_2	24.9
H_2O	16.21
CH_4	4.53
H_2S	0.95
COS	0.02
NH_3	0.27
HCN	0.02

PSOFC KS1S040318-1 was operated utilizing the simulated coal syn gas mixture under a load of 14.00± 0.01 Amps for approximately 0.5 hours when another VI scan was completed. The same method was used to calculate the ASR of the PSOFC as discussed above. The results from the least squares regression is shown in Figure 5.3.

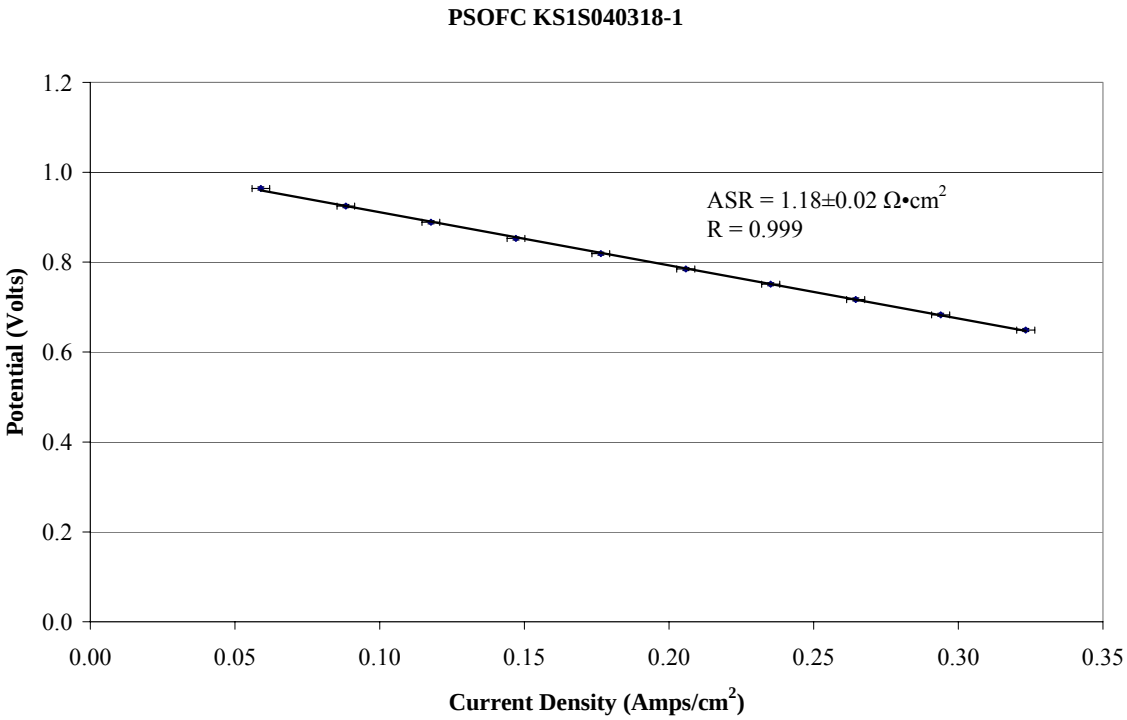

Figure 5.3 Initial ASR Regression with Simulated Coal Syn Gas.

The regression revealed an ASR value of 1.18±0.02 Ω·cm^2 as shown in Figure 5.3. Based upon the correlation coefficient that resulted from the linear regression it was concluded that a very linear line resulted from the regression as explained previously in Figure 5.2. The small confidence interval found from the least squares linear regression showed little variability in the data that was collected from the Agilent N3300A potentiostat. Figure 5.4 shows an ASR comparison of the PSOFC up to VI scan 5.

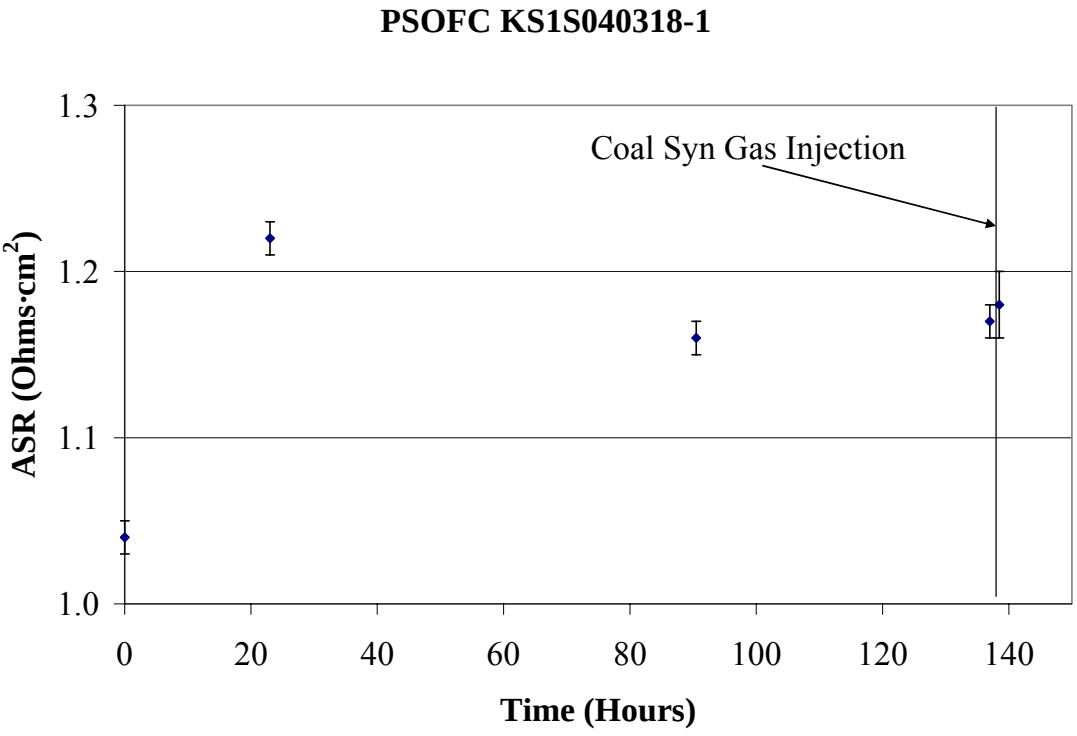

Figure 5.4 ASR Comparison of Trial 4.

Figure 5.4 shows a small increase in the ASR of the PSOFC of 0.9±1.7 percent when the anode gas was switched from the H_2/N_2 mixture to the baseline coal syn gas mixture. Since the confidence intervals of the ASR values that were found from VI scan four and five lie within one another the values may be considered to be statistically the same.

After VI scan five was completed the PSOFC was operated with an electrical load of 14.00±0.01 Amps. Four additional VI scans were completed on PSOFC KS1S040318-1. The PSOFC ASR values that resulted from VI scans 6 through 9 are shown in Table 5.6.

Table 5.6 Calculated PSOFC ASRs Using Simulated Coal Syn Gas.

VI Scan	Operation Time (Hours)	ASR ($\Omega \cdot cm^2$)
6	118.9	1.21±0.04
7	142.9	1.25±0.02
8	166.9	1.24±0.02
9	190.9	1.22±0.01

From the results shown in Table 5.6 it may be seen that the PSOFC KS1S040318-1 ASR increased 3.3±1.7 percent in only 24 hours for VI scans 6 and 7. This sudden increase in the ASR of the PSOFC was the result of a local power outage. The power outage caused the compressor that provides the cathode air to shut down. Because of this shut down the PSOFC was operated under a load of 14.00± 0.01 Amps without sufficient cathode air. The lack of available oxygen to be reduced at the cathode of the PSOFC is believed to have caused this increase in the ASR of the PSOFC. However as can be seen from the results shown in Table 5.6 the ASR of the PSOFC began to recover back towards the ASR value found when simulated coal syn gas was first utilized by the PSOFC anode. 24 hours after VI scan nine was completed the PSOFC developed a backpressure of 20 psig at the anode and the trial was shut down to investigate the cause. Upon inspection of the PSOFC setup it was found that coking had taken place in the inlet tube of the anode fuel manifold. The coking was assumed to have caused the increase in the back pressure.

Once trial 4 was shut down due to high anode back pressure the ASR history of PSOFC KS1S040318-1 was studied. Upon review it was determined that no measurable degradation of the PSOFC's ASR had taken place over the 311.9 hours of operation.

This was concluded by accepting the ASR value found from VI scan two (1.22±0.02 $\Omega \cdot cm^2$) as the initial steady state ohmic resistance of the PSOFC. The acceptance of the ASR determined from the second VI scan as the initial value was done for two reasons. The first reason is that 1.22±0.02 $\Omega \cdot cm^2$ is within the typical SOFCo EFS reported initial ASR values, which are in the range of 1.18 $\Omega \cdot cm^2$ to 1.24 $\Omega \cdot cm^2$ as can be seen in the plot of past SOFCo EFS data attached in Appendix 1. The second reason is that only a small difference is seen between the ASRs calculated between VI scan two and three, whereas a large difference was seen between the ASRs calculated between VI scan one and two showing that a steady state ASR value had been attained. The ASR history of trial four is presented below in Figure 5.5.

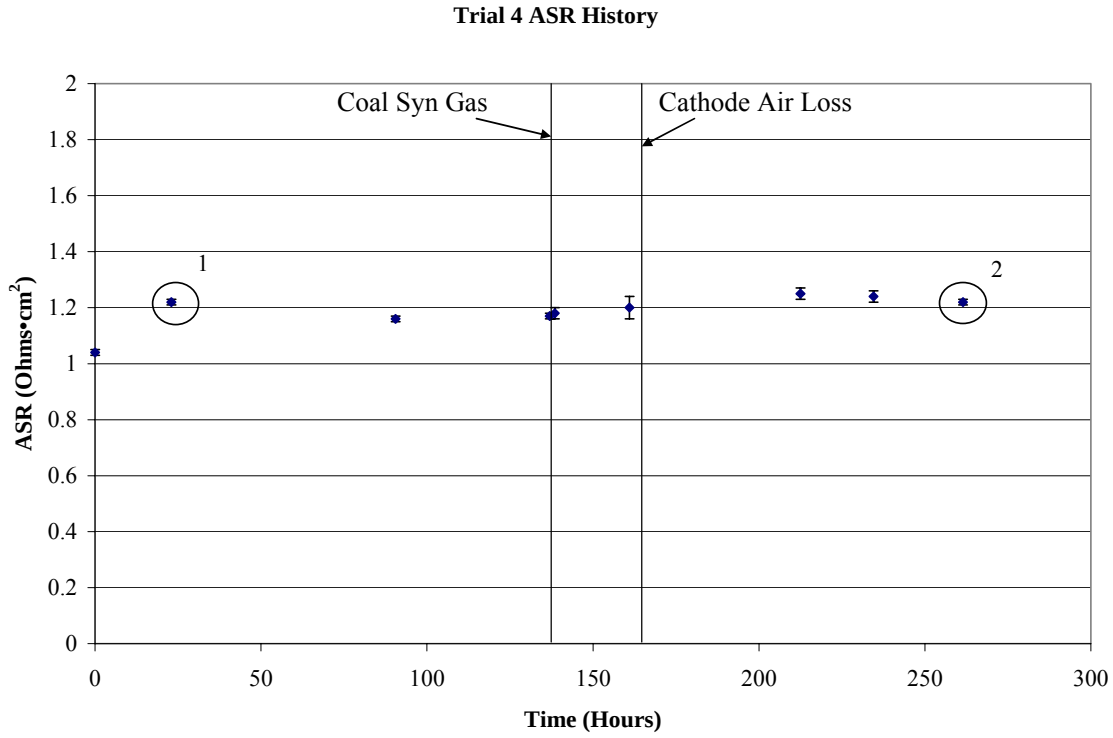

Figure 5.5 Trial 4 ASR History.

The most important characteristic to notice is that little to no degradation in the performance of the PSOFC took place when the fuel gas was switched from H_2 to the simulated baseline coal syn gas mixture. The confidence intervals from VI scans four and five lie within one another so the values can be considered to be statistically the same. The second important trend is shown after VI scan 6 was completed. The PSOFC showed good recovery back towards its original operating performance after the power outage caused insufficient air to be supplied to the cathode. The overall degradation of PSOFC KS1S040318-1 was found to be -0.11±0.08 percent per 100 hours of operation using the points labeled 1 and 2 in Figure 5.5. The percent difference between the two ASRs over the operation period between the two was used to extrapolate the degradation

of the PSOFC over 1000 hours of operation. A least squares linear regression was also completed on the data obtained while operating the PSOFC with the simulated coal syn gas. Again as with the H_2/N_2 anode gas mixture the ASR degradation slope of the line was found to be statistically insignificant. More accurate methods to determine the ASR degradation of the PSOFC will be discussed in the recommendations section.

5.4.3. Material Analysis of PSOFC KS1S040318-1

In order to better determine the effect that simulated coal syn gas has on the anode of the PSOFCs that were used in the research material testing techniques x-ray diffraction (XRD), scanning electron microscopy (SEM), and energy dispersive x-ray spectroscopy (EDXS) were used. These techniques were used to determine any changes the simulated coal syn gas may have caused to the anode structure or anode composition of the PSOFC. This was done by first completing an in depth material analysis of two PSOFCs that had not been operated and then comparing the results to PSOFCs that have been exposed to baseline simulated coal syn gas and simulated coal syn gas containing H_2S.

5.4.4. Baseline Anode Material Analysis

The first material analyses were conducted to characterize a baseline InDEC PSOFC that had not been operated. The tests that were completed on the PSOFC included SEM, EDXS, and XRD. The tests were used to determine the anode thickness, electrolyte thickness, and cathode thickness, determine if the anode of the PSOFC was porous, and determine the material components of the anode. These baseline results would then be used to compare with the results obtained from PSOFCs that have been operated utilizing various simulated coal syn gases.

The SEM was used to determine the approximate thicknesses of the anode, electrolyte, and cathode by obtaining images of the PSOFC cross section so that all three sections of the PSOFC could be viewed. The thicknesses were found by measuring the thicknesses of each respective section in several places from the SEM images and then accepting the average of these measurements as the respective thickness of each PSOFC component. Figure 5.6 is an image that was used to determine the thicknesses of the anode and electrolyte at magnification of 200X.

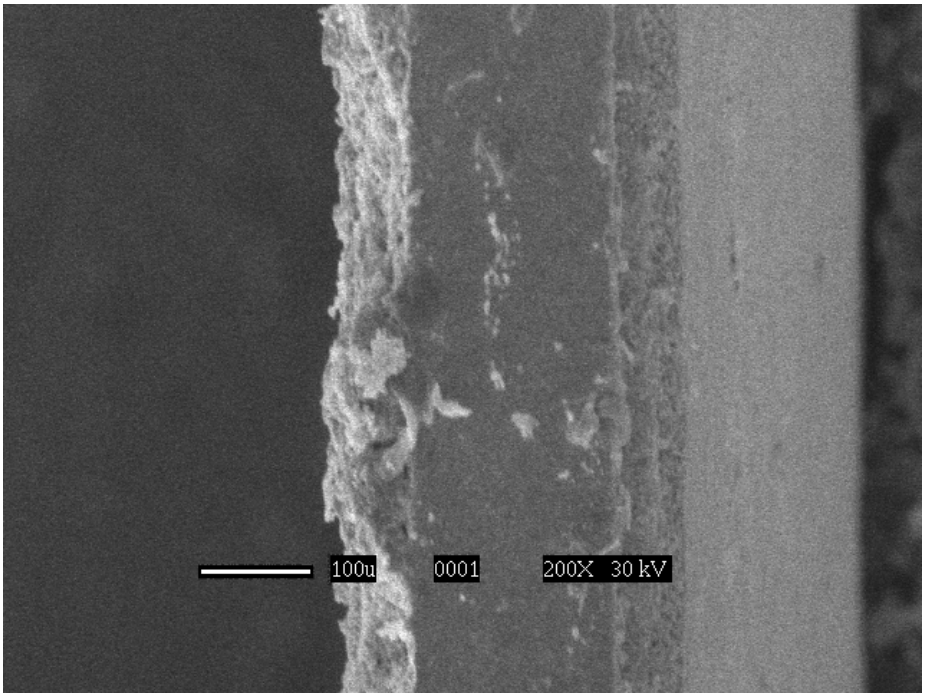

Figure 5.6 Baseline PSOFC Cross Section.

From the SEM images of the PSOFC cross section it was determined that the thicknesses of the anode, electrolyte, and cathode were 250±5 μm, 165±5 μm , and 70±5 μm

respectively. Figure 5.6 was not used to determine the thickness of the cathode since it is not shown in the SEM image.

Once the respective thicknesses of each PSOFC section was determined the SEM was then used to determine if the anode of the PSOFC was porous. This was done by focusing the SEM onto the surface of the anode and then studying the resulting images. Figure 5.7 presents an SEM image of the anode surface at a magnification of 550X.

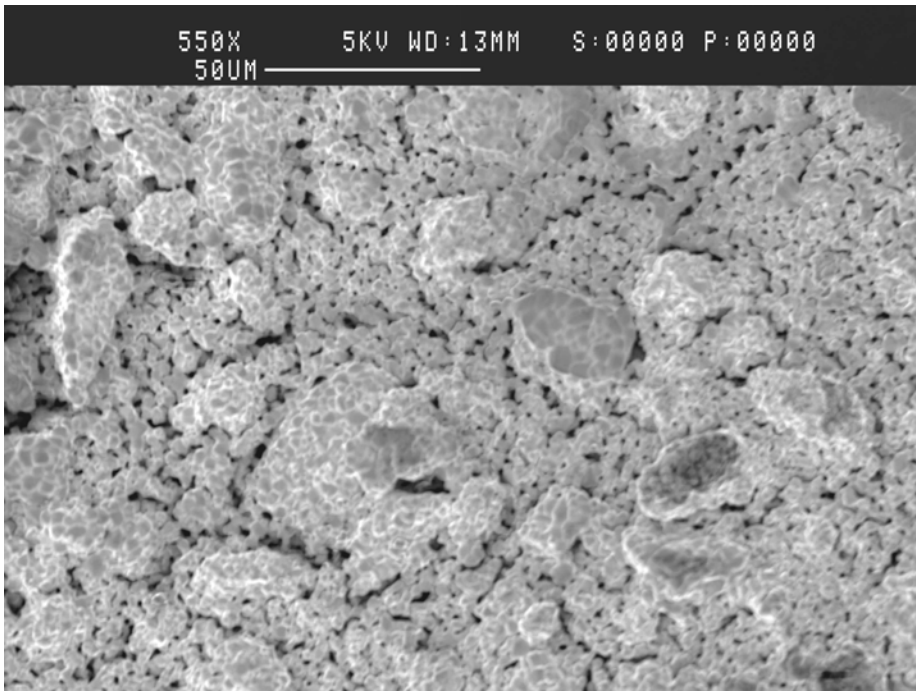

Figure 5.7 PSOFC Anode Surface at 550X.

The image shown in Figure 5.7 shows a surface containing many pores and leads to the conclusion that the anode surface of the PSOFC is very porous. A technique to actually quantify the porosity of the anode surface is not available in the Ohio Coal Research Center at this time so the porosity of the anode can only be defined by visual inspection

with the SEM. Also the anode material of the PSOFC was determined to be homogenous by inspecting several areas of the PSOFC anode and finding the same basic anode structure to be present at each site that was inspected. In Figure 5.8 another area of the baseline PSOFC anode is shown at a magnification of 1430X.

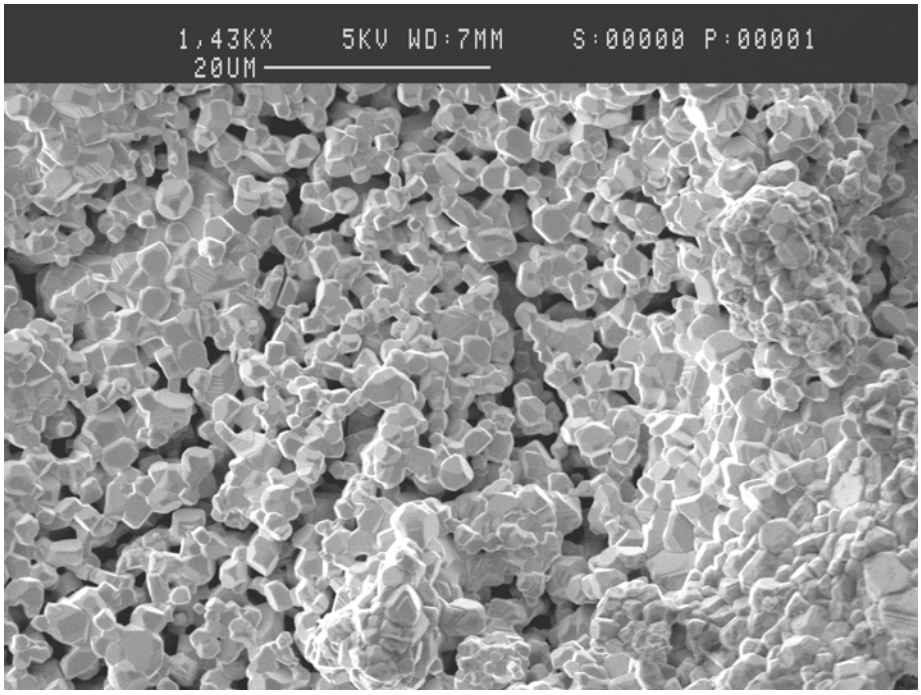

Figure 5.8 PSOFC Anode Surface at 1430X.

From Figure 5.8 the surface of the PSOFC anode can again be seen to be very porous but also contain varying surface heights and many channels for gases to travel through.

EDXS was used to determine the elemental components of the PSOFC anode. This test was completed on several areas of the PSOFC anode including the surface and the cross section of the anode. Figure 5.9 shows the typical EDXS spectrum that was found from the cross section of the PSOFC Anode.

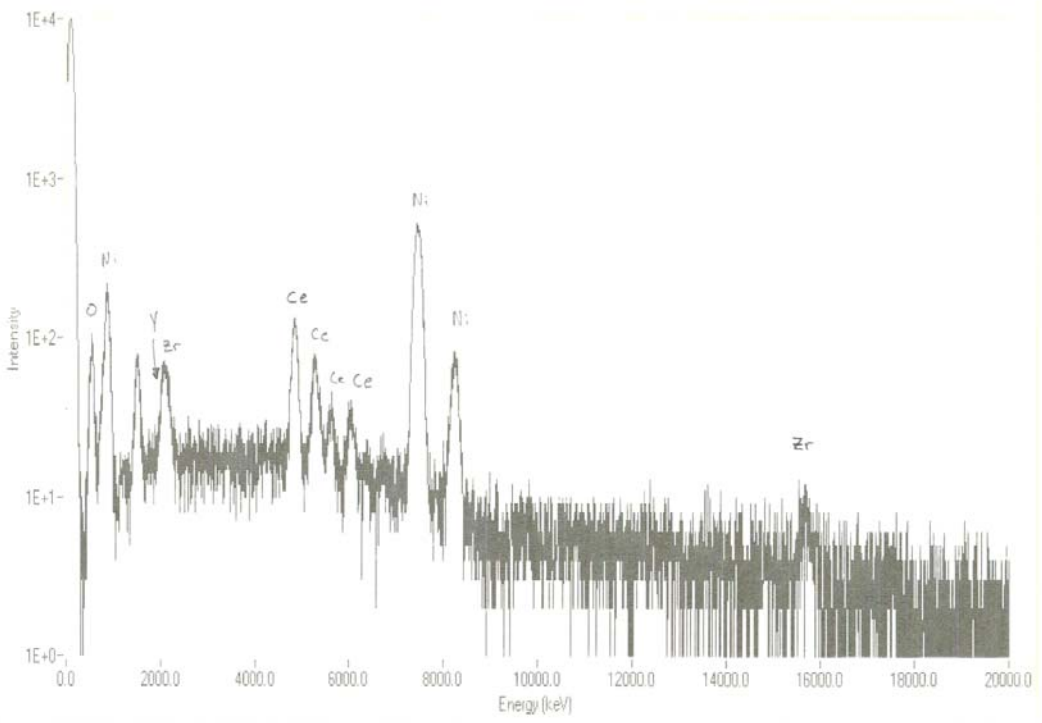

Figure 5.9 PSOFC Anode Cross Section EDS Spectrum.

From Figure 5.9 it may be seen that the main elemental components of the PSOFC anode are nickel (Ni), cerium (Ce), zirconium (Zr), yttrium (Y), gadolinium (Gd), and oxygen (O). The oxygen present in the EDXS spectrum is due to the ceramic oxides (NiO, CeO_2 and ZrO_2) that are present. EDXS analysis was also completed on the anode surface of the PSOFC. Figure 5.10 presents a typical EDXS spectrum that was found from the anode surface of the PSOFC.

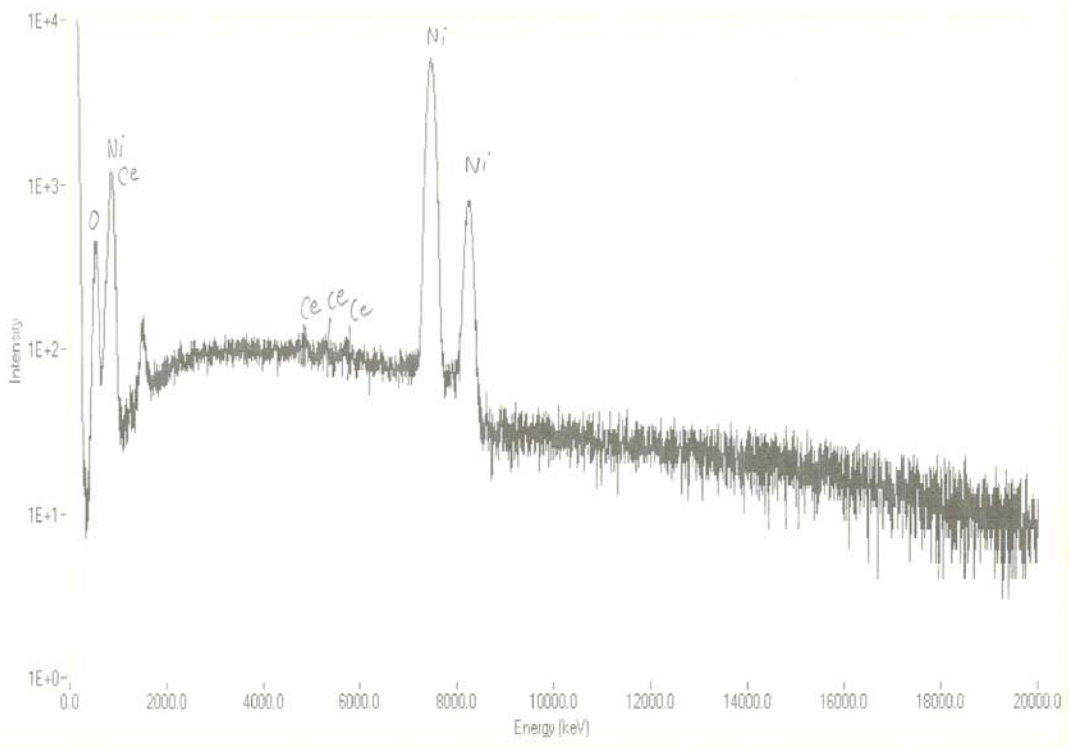

Figure 5.10 PSOFC Anode Surface EDXS Spectrum.

From Figure 5.10 it can be seen that the main components of the anode surface are Ni, Ce, and O. Comparing Figure 5.9 and 5.10 it can be seen that the nickel peaks are much higher at the surface of the PSOFC than in the cross section of the PSOFC anode. The high concentration of nickel serves as a current collector for the electrons that are produced from the electrochemical oxidation of H_2 and CO at the PSOFC anode.

XRD analyses were also completed on the surface of the PSOFC to determine the type of compounds present at the anode interface. The main difference between the EDXS and XRD analysis is that the EDXS will only confirm what elements present in the material being tested whereas XRD testing will reveal the actual compounds in the materials being tested. For example the EDXS spectrums show that oxygen is present in

the PSOFC anode while the XRD spectrums will show that ceramic oxides are present in the PSOFC anode. The XRD equipment was used with an RS slit of 0.3, an SS slit of 1.0°, a trial range of 15° to 90°, and a scan rate of 1.5°/min. Figure 5.11 shows the XRD spectrum that was found from the baseline PSOFC anode.

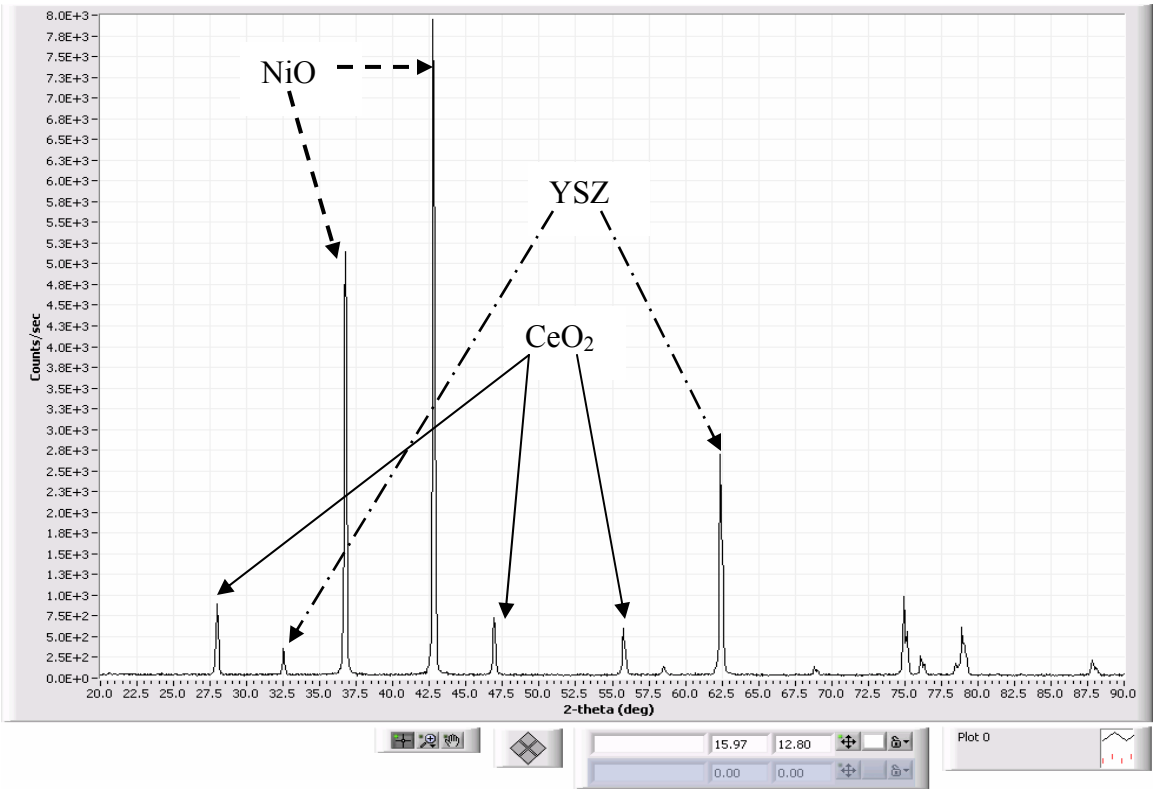

Figure 5.11 XRD Spectrum of Baseline PSOFC Anode.

The XRD spectrum shown in Figure 5.11 shows that the anode of the PSOFC is made of CeO_2, YSZ, and NiO. The NiO in the anode of the PSOFC is initially reduced to Ni during heating and being exposed to the anode fuel gas.

5.4.5. Trial 4 Anode Material Analyses

Once trial 4 was completed material analyses (SEM, EDXS, and XRD) were completed on PSOFC KS1S040318-1. SEM was the first material analysis to be completed on the anode of the PSOFC KS1S040318-1. The SEM was used to inspect the anode of the PSOFC for any visual changes or defects that occurred to the anode of the PSOFC after utilizing the baseline simulated coal syn gas. The main objectives were to inspect the anode of PSOFC KS1S040318-1 for any signs of cracking or blockage of the porous anode surface. Figure 5.12 shows an SEM image of the anode of PSOFC KS1S040318-1 at a magnification of 552X.

(a)

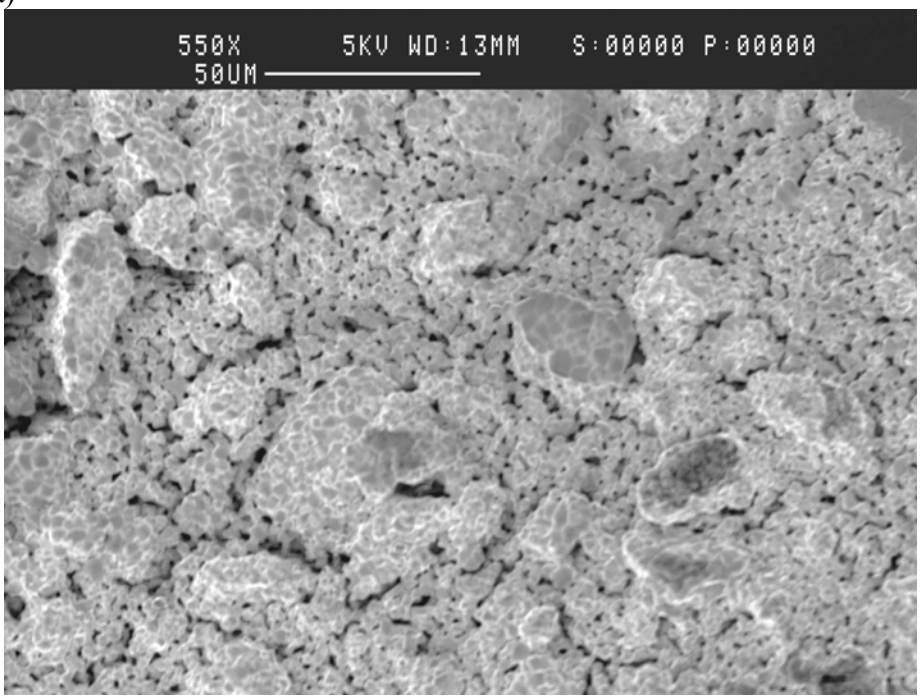

(b)

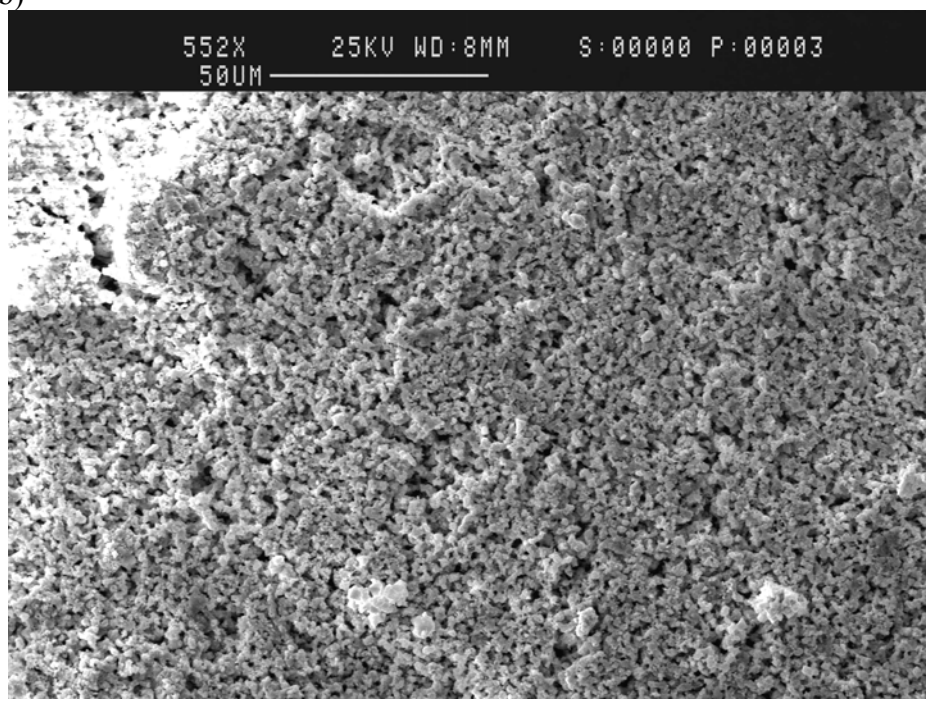

Figure 5.12 Trial 4 SEM Image Comparison with Baseline Anode SEM Image (a) Baseline PSOFC Image at 550X and (b) Trial 4 Anode SEM Image at 552X.

Inspecting Figure 5.11 it can easily be seen that the anode of PSOFC KS1S040318-1 is still very porous after utilizing coal syn gas. After inspection of several areas of the PSOFC the anode was determined to be homogeneous. One difference that can be seen between Figure 5.7 and 5.11 are the white areas of the image. These white areas are believed to be caused by Ni agglomerates that formed from the NiO ink that was painted onto the anode surface. During the heating of the PSOFC the NiO in the ink is transformed into Ni as in the PSOFC anode forming a good current collector. This Ni deposited from the ink formed areas of higher elevation causing these areas to become out of focus compared to the lower portions of the image. Comparing Figure 5.7 to Figure 5.12 it can be seen that both anode surfaces are very porous. Another SEM image of the PSOFC at a magnification of 1510X is shown in Figure 5.13.

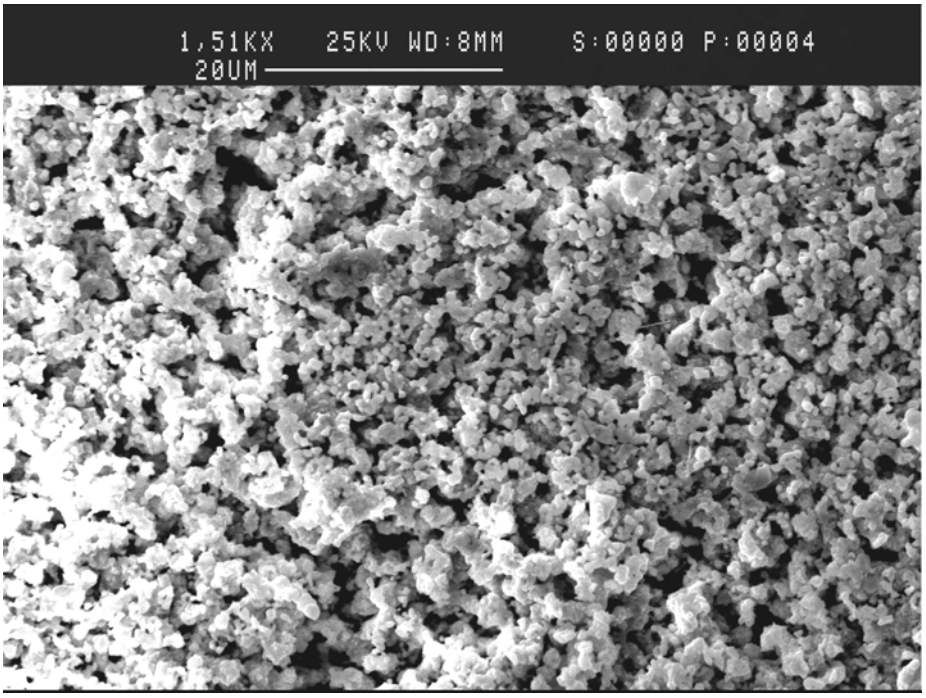

Figure 5.13 Trial 4 SEM Image at 1510X.

From Figure 5.13 the anode surface of the PSOFC can be seen to have remained porous while utilizing the simulated coal syn gas allowing for diffusion of the fuel through the anode of the PSOFC.

After the SEM analyses were completed the anode of PSOFC KS1S040318-1 underwent EDXS to determine the elemental composition of the anode. EDXS analysis was completed on several areas of the PSOFC KS1S040318-1. A representative spectrum is shown in Figure 5.14.

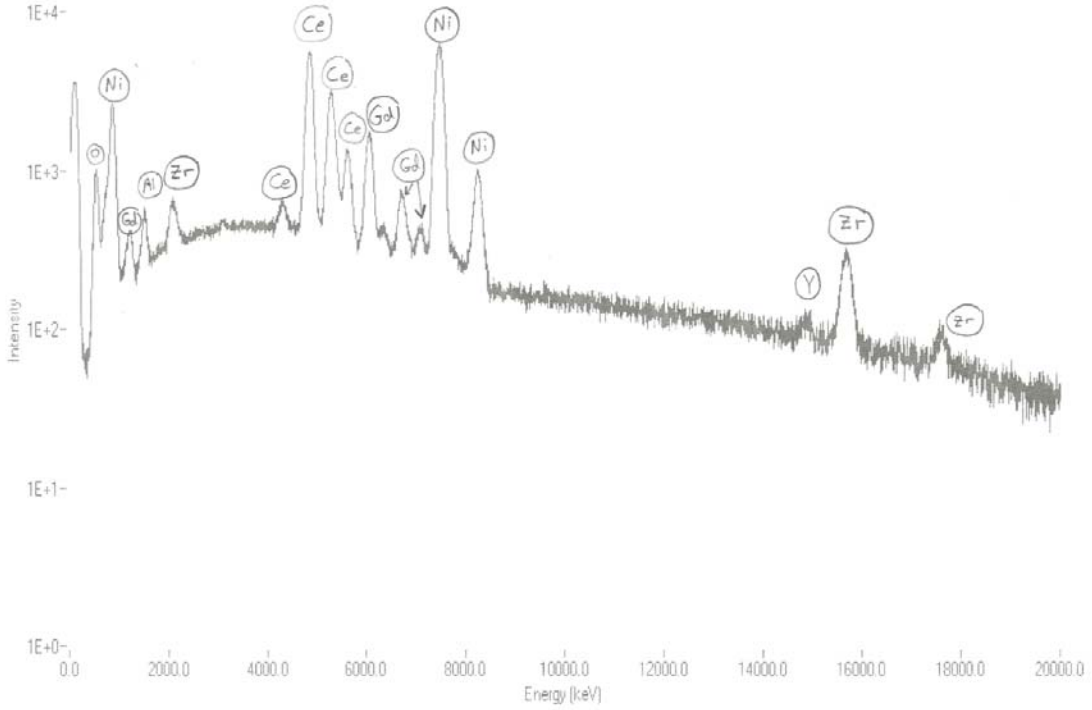

Figure 5.14 EDXS Spectrum from Trial 4 Anode.

From Figure 5.14 it can be seen that the anode of PSOFC KS1S040318-1 also contains Ni, Ce, Gd, O, Y, and Zr which were all found in the baseline PSOFC. One important element that does not appear in the EDXS spectrum above is carbon. This allows the conclusion that little coking at the surface of the PSOFC anode occurred while utilizing the simulated coal syn gas.

The final material analysis that was conducted on the anode of PSOFC KS1S040318-1 was XRD. Several XRD analyses were conducted using the same testing parameters described in section 5.3.3 on the anode of PSOFC. A representative spectrum is shown in Figure 5.15.

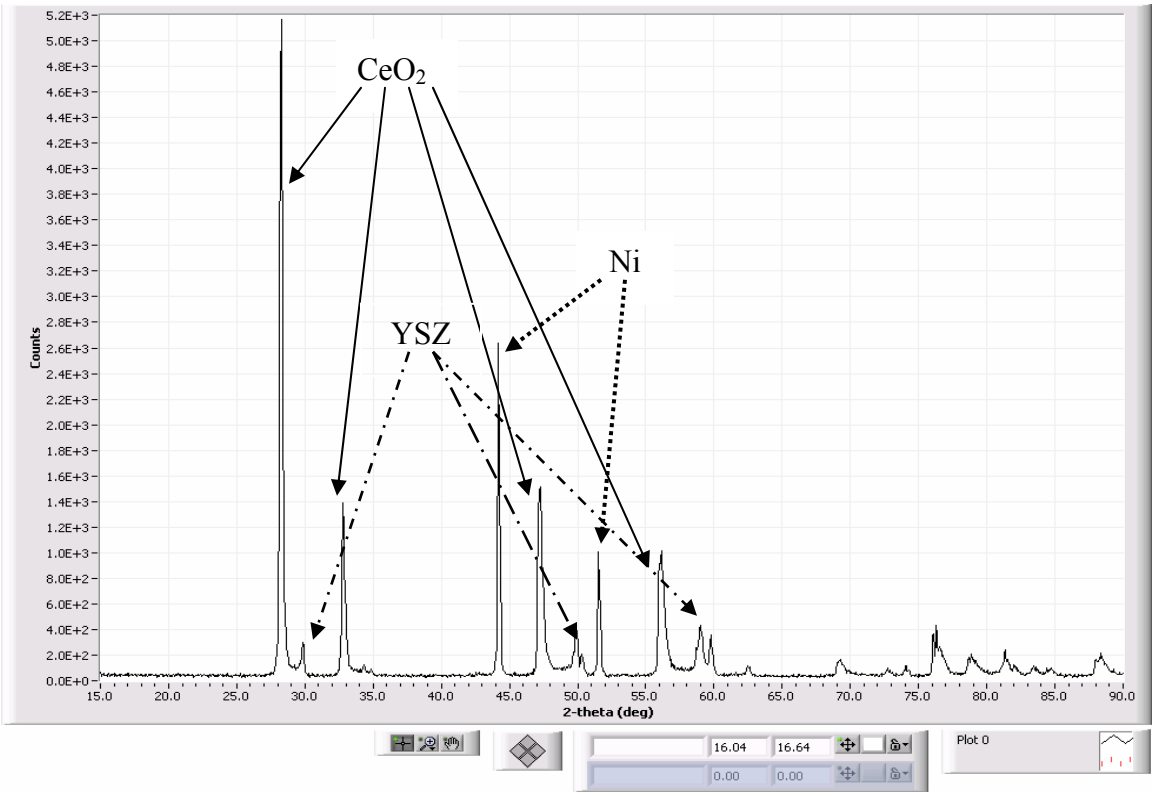

Figure 5.15 XRD Spectrum from Trial 4 Anode.

From Figure 5.15 the XRD spectrum showed the anode of PSOFC KS1S040318-1 contained Ni, CeO_2, and YSZ. These compounds coincide with the elements that were found from the EDXS spectrum shown in Figure 5.13. The only element that was not accounted for was gadolimium (Gd). This is believed to be caused by the fact that the XRD spectrums for cerium oxide (CeO_2) and gadolinium doped cerium oxide (GDC) are very similar. Because of this it has been assumed that the spectrums are one in the same and the Gd in Figure 5.13 is accounted for by the CeO_2 in Figure 5.14.

5.5. Trial 5

Trial 5 was operated with the same GDS compositions as in trial 4 but with an increased H_2O content to prevent the coking that was found to have caused the increase

in the anode back pressure of trial 4. This was done by increasing the H_2O bubbler temperature from 25°C to 70°C. The results from Trial 5 are presented below.

5.5.1. Trial 5 Initial PSOFC Operation

The operation of InDEC ESC PSOFC KS1S040210-43 was begun increasing the temperature of the PSOFC from room temperature to its operational temperature of 850°C through the two heating cycles that were explained in section 4.4. Once the PSOFC reached its operating temperature of 850°C it was allowed to operate in open cell condition, no electrical load was applied, for approximately 1 hr. The initial open cell potential of the PSOFC was found to be 0.956±0.004 Volts compared to a theoretical open cell potential of 0.93 Volts. Because it is impossible for the actual open cell potential of a PSOFC to be greater than the theoretical open cell potential the assumption that the partial pressure of the H_2O is equivalent to the saturated partial pressure at 70°C was incorrect and the actual partial pressure of H_2O in the anode fuel gas was then calculated. This was done by using the same Nernst equations used in trial 4 except using the measured open cell potential of the PSOFC to calculate the actual H_2O content of the anode fuel gas. The composition of the initial anode fuel gas found from the calculation is shown in Table 5.7.

Table 5.7 Trial 4 Initial Anode Gas Composition.

Anode Gas Composition (Mole %)
39.5±0.7 H_2
39.5±0.9 N_2
21.0±1.6 H_2O

The error associated with the H_2O content was found by taking into account the variability of both the H_2 and N_2 flow rates. After the PSOFC was allowed to reach a steady state open cell operating condition the initial VI scan was completed by applying a current (Amperes) and measuring the resultant PSOFC potential (Volts). Once the data from the initial VI scan was recorded the data was used to plot the characteristic operating curve of the PSOFC by plotting the potential of the PSOFC (Volts) against the current density of the PSOFC (Amps/cm^2). The resulting characteristic curve resulting from the initial VI scan on PSOFC KS1S040210-43 is shown in Figure 5.16.

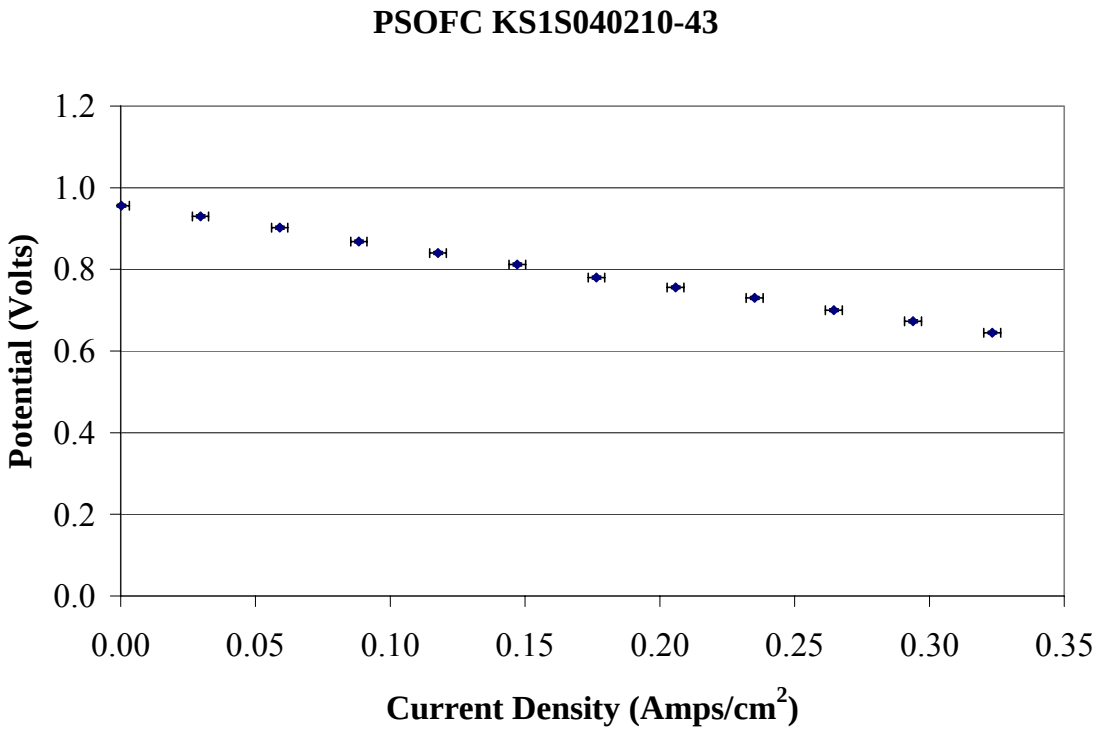

Figure 5.16 Trial 5 Initial VI Scan.

The error bars associated with the PSOFC current density and potential were found using the measurement error associated with the Agilent N3300A potentiostat that was used to control the PSOFC. The ASR of the PSOFC was then calculated in the same manner as explained in 5.4.1. Figure 5.17 shows the initial ohmic loss region data and results from the ASR calculation for PSOFC KS1S040210-43 in trial 5.

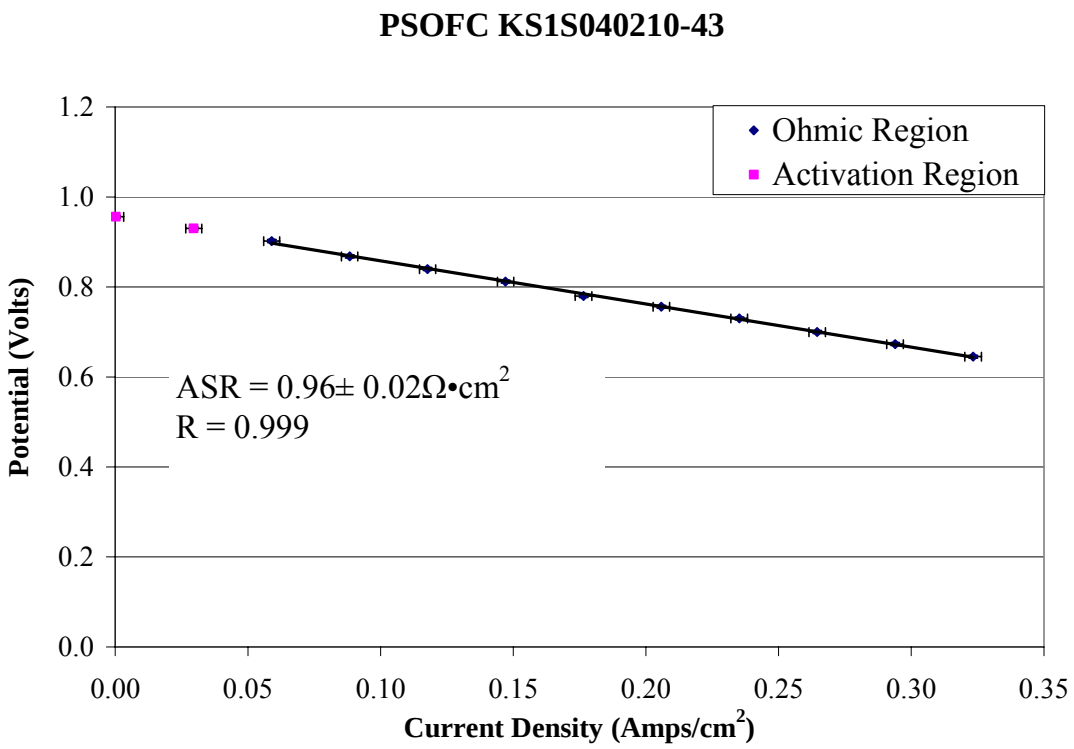

Figure 5.17 Trial 5 Initial PSOFC ASR Regression.

From the least squares linear regression the ASR of PSOFC KS1S040210-43 was found to be 0.96±0.02 $\Omega \cdot cm^2$ with a coefficient of regression of 0.999. The PSOFC was determined to be operating normally according to the SOFCo EFS conditions described

above due to part by part variation in the PSOFCs. The initial ASR value was determined to be within 21.3±1.6 percent of the accepted SOFCo EFS initial ASR value of 1.20 $\Omega \cdot cm^2$.

After the initial ASR value of PSOFC KS1S040210-43 was determined the PSOFC was operated under an electrical load of 14.00±0.01 Amps for approximately 71.2 hours with the same anode and cathode gas compositions and flow rates stated above. Two additional VI scans were completed on the PSOFC over the specified time period and the ASR of the PSOFC was calculated in the same manner as explained previously. The results from VI scan two and three that were completed on PSOFC KS1S040210-43 are shown Table 5.8.

Table 5.8 Calculated PSOFC ASRs Using H_2/N_2 Anode Gas.

VI Scan	Operation Time (Hours)	ASR ($\Omega \cdot cm^2$)
2	23	1.04±0.02
3	71.2	1.08±0.02

From the regressed ASR values shown in Table 5.8 it can be seen that an initial increase in the ASR of 12.5±2.1 percent of the PSOFC KS1S040210-43 took place over the first 71.2 hours of operation. The increase of the ASR of the PSOFC was expected based on past SOFCo EFS data for the InDEC ESC PSOFCs that are being used for this research and shown in Appendix 1. From the past PSOFC EFS results it was concluded PSOFC KS1S040210-43 was operating normally based upon past SOFCo EFS data and with

personal communication with SOFCo EFS fuel cell engineers. Based on communications with SOFCo EFS fuel cell engineers the second ASR value calculated ($1.04\pm0.02\ \Omega\cdot cm^2$) for PSOFC KS1S040210-43 was accepted as the fuel cell's initial ASR value.

The same procedures as used in trial 4 to determine the ASR degradation of the PSOFC over time were completed on the data obtained from the PSOFC while using the H_2/N_2 anode gas mixture. Once again the least squares linear regression yielded ASR degradation slopes that were statistically insignificant. Using Equation 3.1 the ASR degradation of the PSOFC while using the H_2/N_2 anode gas mixture was found to be 8.0±3.9 percent per 100 hours of operation.

5.5.2. Trial 5 Operation with Simulated Coal Syn Gas

Once PSOFC KS1S040210-43 was determined to be operating normally a the same coal syn gas mixture was produced in the single cell gas delivery system listed in Table 5.2. However because of the increased H_2O bubbler temperature, 25°C to 70°C, the composition of the anode fuel gas after passing through the H_2O bubbler was different from trial 4. Table 5.9 shows the anode fuel gas composition that was calculated using the H_2O content that was determined during the initial operation of trial 5 above.

Table 5.9 Trial 5 Simulated Baseline Coal Syn Gas Composition.

Anode Gas Composition (Mole %)
20.9±0.9 H_2
31.8±0.7 CO
26.3±1.2 N_2
21.0±2.7 H_2O

Again the error associated with the H_2O content of the simulated coal syn gas was taken into account using the variability of the other fuel gas species. The cathode air flow rate provided to the cathode of the PSOFC was 2500±45 smL/min.

PSOFC KS1S040210-43 was operated with the simulated coal syn gas mixture shown in Table 5.9 under a load of 14±0.01 Amps for approximately 19.7 hours when VI scan four was completed the results from the least squares regression is shown in Figure 5.18.

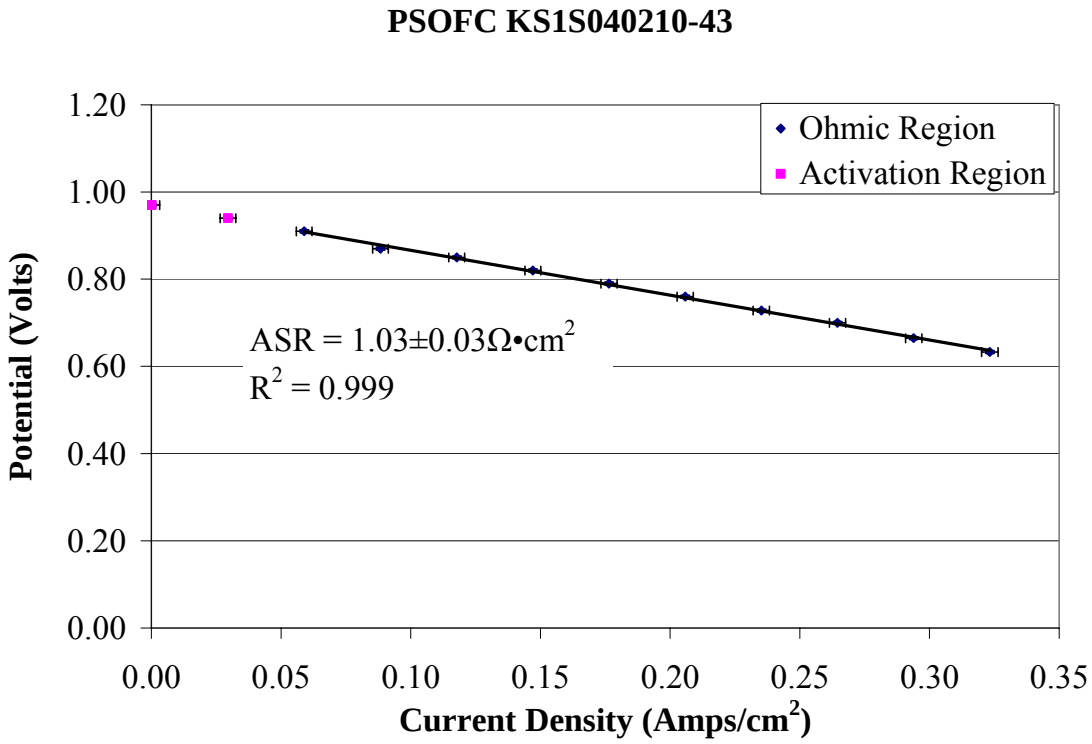

Figure 5.18 Trial 5 ASR Regression with Simulated Coal Syn Gas.

The least squares linear regression that was completed revealed the ASR of PSOFC KS1S040210-43 to be 1.03±0.03 $\Omega \cdot cm^2$ when baseline simulated coal syn gas was utilized by the PSOFC anode. A decrease of 5.4±2.7 percent in the ASR of PSOFC KS1S040210-43 was seen when the anode gas was switched from the H_2/N_2 mixture to the baseline simulated coal syn gas mixture as shown in Figure 5.19.

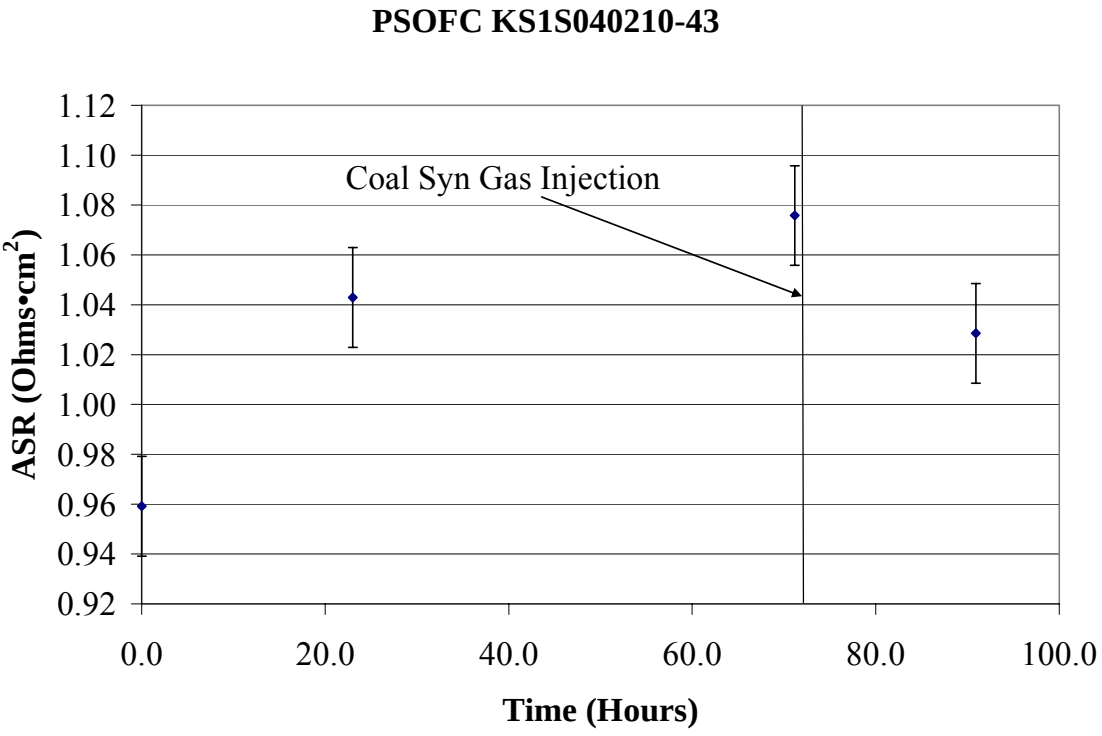

Figure 5.19 PSOFC ASR Comparison for Trial 5.

After VI scan four was completed the PSOFC was operated with an electrical load of 14.00±0.01 Amps. Five additional VI scans were taken from PSOFC KS1S040210-43. The PSOFC ASR values that resulted from VI scans 5 through 9 are shown in Table 5.9.

Table 5.10 Trial 5 Calculated PSOFC ASRs Using Baseline Simulated Coal Syn Gas.

VI Scan	Operation Time (Hours)	ASR ($\Omega \cdot cm^2$)
5	115.2	1.05±0.01
6	142.1	1.03±0.01
7	164.3	1.03±0.01
8	256.0	1.02±0.04
9	286.3	1.03±0.04

From the results shown in Table 5.9 it can be seen that PSOFC KS1S040210-43 showed no signs of appreciable degradation after 286 hours of operation. Although the ASR of the PSOFC was showing no signs of deterioration the trial had to be shut down due to a power outage that damaged PSOFC KS1S040210-43. The backup power unit for the entire testing system did not work properly and so the trial was lost.

After trial five was shut down due to the power outage the ASR history of PSOFC KS1S040210-43 was plotted as shown in Figure 5.20.

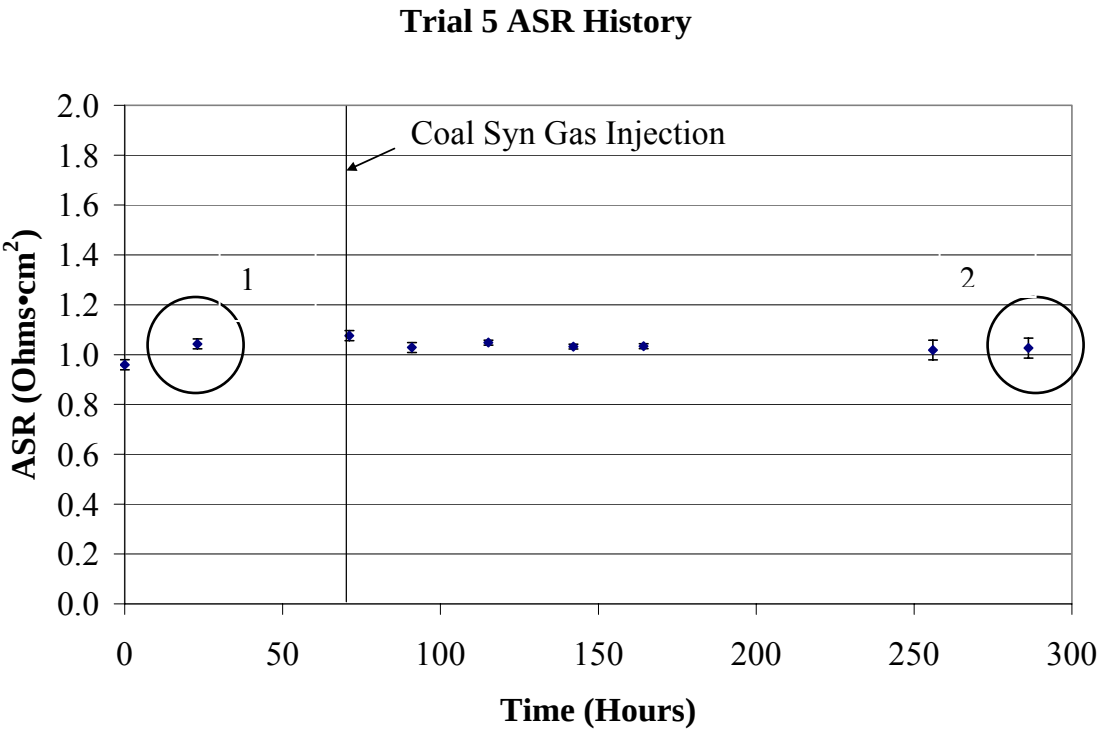

Figure 5.20 PSOFC KS1S040210-43 ASR History.

After reviewing the ASR history of PSOFC KS1S040210-43 it was concluded that no appreciable degradation in the ohmic resistance of the PSOFC had taken place over the 286.3 hours of operation. A degradation rate of -6.0±3.9 percent per 1000 hours of operation was calculated for trial 5. This was concluded by accepting the ASR value found from VI scan two (1.04±0.02Ω·cm^2) labeled as 1 in Figure 5.20 as the initial steady state ASR of the PSOFC and the final ASR value labeled 2 in Figure 5.20 (1.03±0.04Ω·cm^2). Also an important characteristic to be noticed from the ASR history of trial five is the slight increase in the ASR of the PSOFC when simulated coal syn gas is initially utilized. Although the ASR of the PSOFC increased to 1.08±0.02 Ω·cm^2 the

fuel cell quickly recovered towards its initial ASR value of 1.04±0.02Ω·cm^2 after approximately 20 hours of operation with the simulated coal syn gas.

The degradation rate of the PSOFC while utilizing the baseline coal syn gas was again determined by completing a least squares linear regression on the ASR values obtained from VI scans 5 through 9. Once again the least squares linear regression of the ASR data revealed a statistically insignificant ASR degradation rate due to its confidence interval spanning zero. Equation 3.1 was then used with ASR values from VI scan 5 and 9 as the initial and final ASR values respectively which revealed an ASR degradation rate of 0.2±0.1 percent per 100 hours of operation. Again better methods to determine the ASR degradation rate of the PSOFC will be discussed in the recommendations section of the thesis.

5.5.3. Trial 5 Anode Material Analyses

Once trial 5 was completed material analyses (SEM, EDXS, and XRD) were completed on PSOFC KS1S040210-43. The SEM was used to inspect the anode of the PSOFC for any visual changes or defects that occurred to the anode of the PSOFC after utilizing the baseline simulated coal syn gas. The main objectives were to inspect the anode of PSOFC KS1S040210-43 for any signs of cracking or blockage of the porous anode surface and compare the images to those of the baseline and trial 4 PSOFC anode. Figure 5.21 shows an SEM image of the anode of PSOFC KS1S040210-43 at a magnification of 500X.

(a)

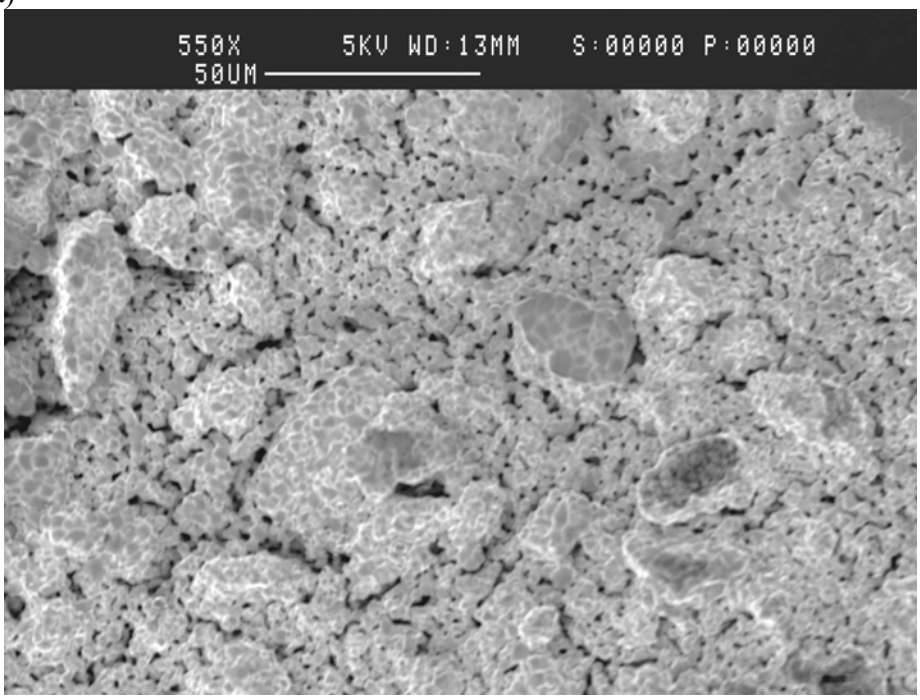

(b)

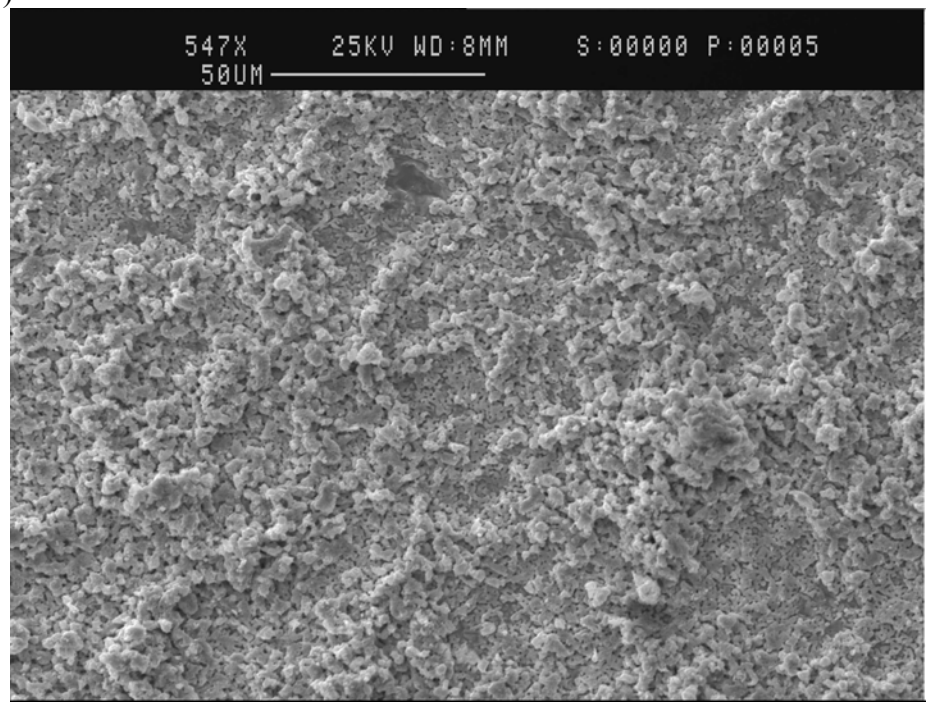

Figure 5.21 PSOFC Anode SEM Images

(a) Baseline PSOFC Anode at 550X and (b) Trial 5 Anode at 547X.

Inspecting Figure 5.21 it may be seen that the anode of PSOFC KS1S040210-43 is still very porous after utilizing the simulated coal syn gas. After inspection of several areas of the PSOFC the anode was determined to be homogeneous. Comparing anodes of the baseline PSOFC and trial 5 PSOFC anodes it may be seen that both anode surfaces are porous. One distinction that can be made from the two SEM images is the large amount of agglomerates present on the anode in Figure 5.21. These agglomerates are a result of the NiO paste that is applied to the PSOFC anode before being operated as described in Section 4.4. Figure 5.22 presents another SEM image of the PSOFC anode at 1430X.

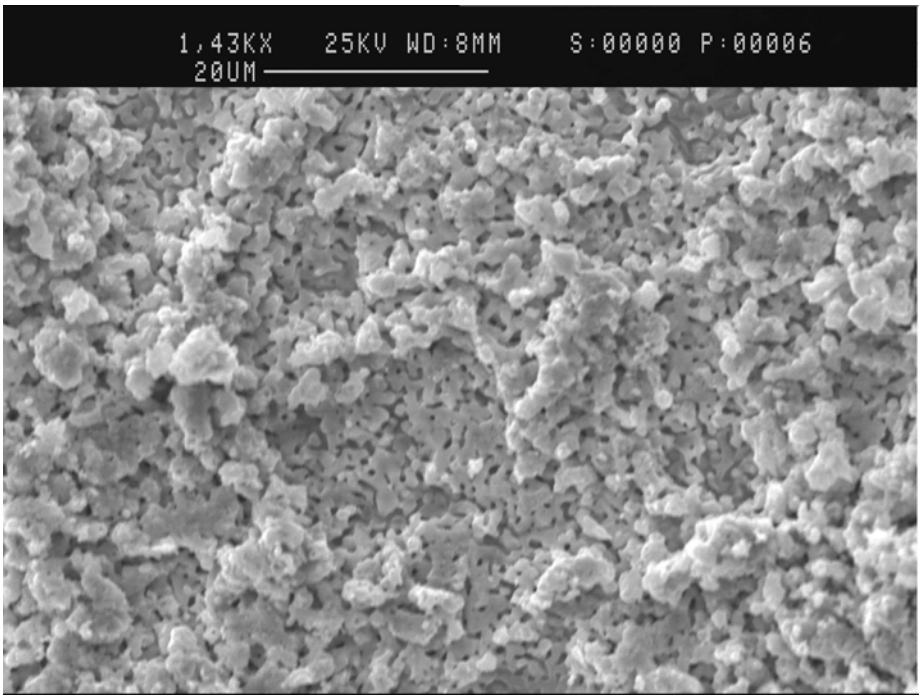

Figure 5.22 SEM Image of Trial 5 Anode at 1430X.

Figure 5.22 also shows that the anode of the PSOFC is still porous after utilizing the simulated coal syn gas.

EDXS analyses were completed on several areas of the PSOFC KS1S040210-43's anode. A representative spectrum and the spectrum obtained from the baseline PSOFC anode is shown in Figure 5.23.

(a)

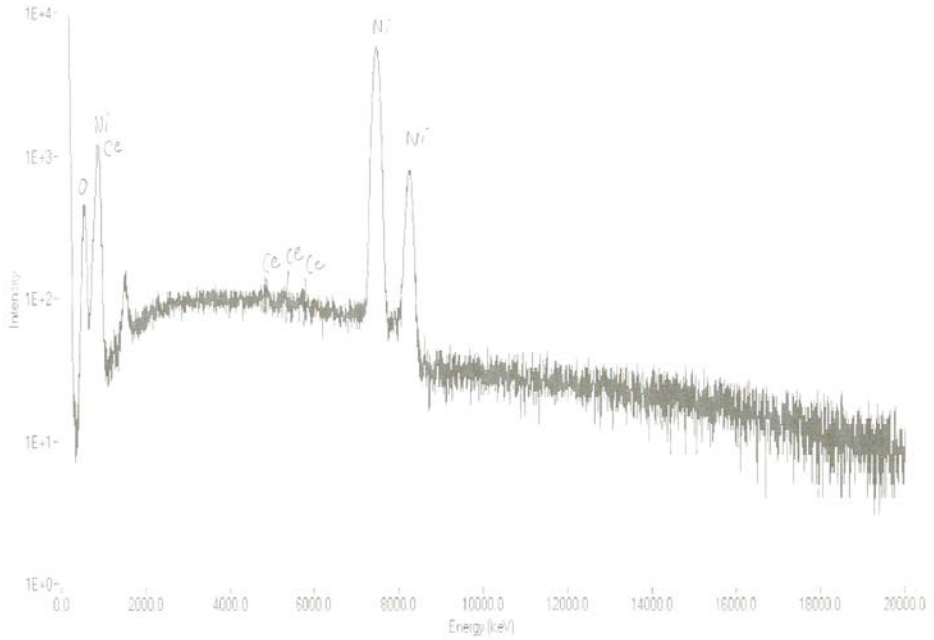

(b)

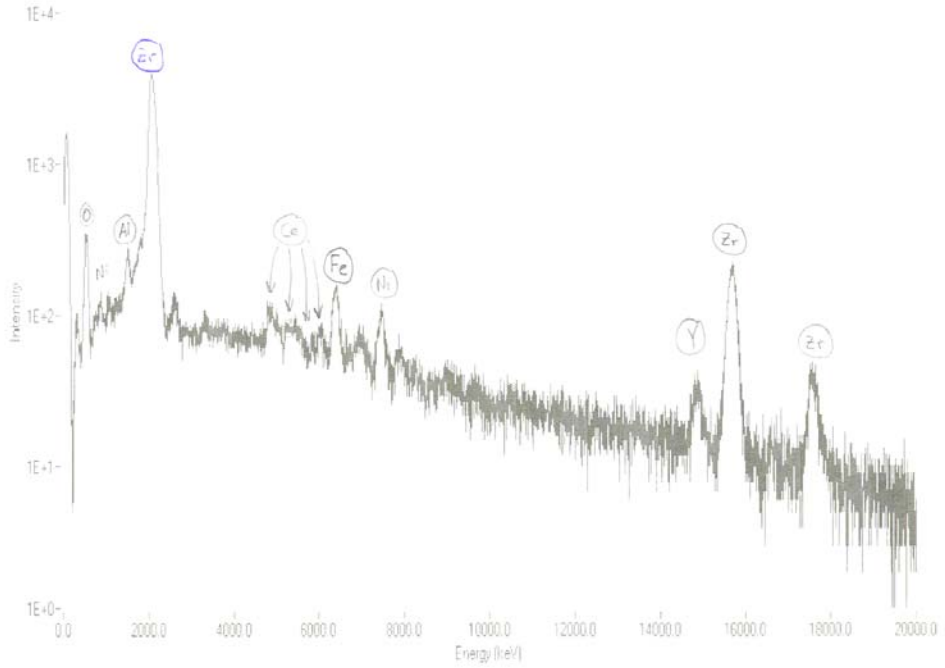

Figure 5.23 Anode EDXS Spectrums
(a) Baseline PSOFC Anode and (b) Trial 5 PSOFC Anode.

From Figure 5.23 it can be seen that the anode of PSOFC KS1S040210-43 contains Ni, Ce, Gd, O, Y, and Zr which were all found in the baseline PSOFC. The iron was determined to be from a small rust spot on the anode of the PSOFC. It is believed that the rust was caused by the H_2O that was in contact with the steel tubing that is used to transport the simulated coal syn gas from the gas delivery system to the single cell test stand during the PSOFC's cool down cycle. The EDXS spectrum in Figure 5.23 also shows no sign of carbon deposition as did Figure 5.14 from trial 4.

Several XRD analyses were conducted using the same testing parameters described in section 5.4.3 on the anode of the PSOFC. A representative spectrum is shown in Figure 5.24.

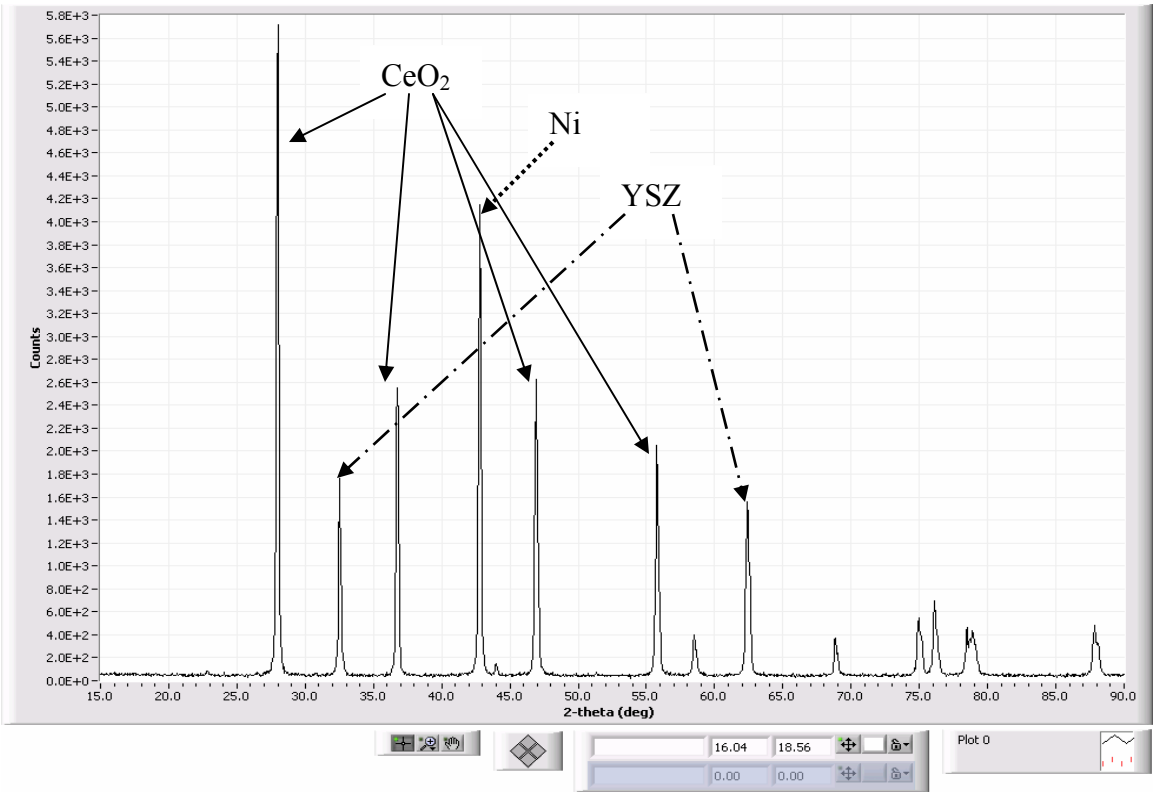

Figure 5.24 Trial 5 PSOFC Anode XRD Spectrum.

From Figure 5.24 the XRD spectrum showed the anode of PSOFC KS1S040210-43 contained Ni, CeO_2, and yttria stabilized zirconia (YSZ). These compounds coincide with the elements that were found from the EDXS spectrum shown in Figure 5.23.

5.6. Trial Six

Trial 6 was designed to determine the sulfur tolerance of the InDEC PSOFCs. The PSOFC was initially operated utilizing the initial H_2/N_2 anode fuel gas mixture. Next the anode fuel gas was switched to the same simulated coal syn gas mixture used in trial 5 and after steady operation with the baseline coal syn gas mixture was established the contaminant H_2S was added to the anode fuel gas mixture.

5.6.1. Trial 6 Initial PSOFC Operation

The operation of InDEC ESC PSOFC KS1S040318-5 was initiated in the same manner as in trials 4 and 5. Once the PSOFC reached its operating temperature of 850°C it was allowed to operate in open cell condition, no electrical load was applied, for approximately 1 hr. The initial open cell potential of the PSOFC was found to be 0.964±0.004 Volts compared to a theoretical open cell potential of 0.93 Volts. Because it is not possible for the measured open cell potential of a PSOFC to be greater than the theoretical open cell potential of the PSOFC the assumed H_2O content of the anode fuel gas was incorrect. In order to determine the actual H_2O content of the anode fuel gas the Nernst equation along with the measured open cell potential was used to calculate the H_2O content of the anode fuel gas. From this calculation the H_2O content of the fuel gas was found to be 18.4±1.1 mole percent H_2O. The calculation used to determine the H_2O content of the anode fuel gas is attached in Appendix 2. The resulting characteristic

curve resulting from the initial VI scan on PSOFC KS1S040318-5 is shown in Figure 5.25.

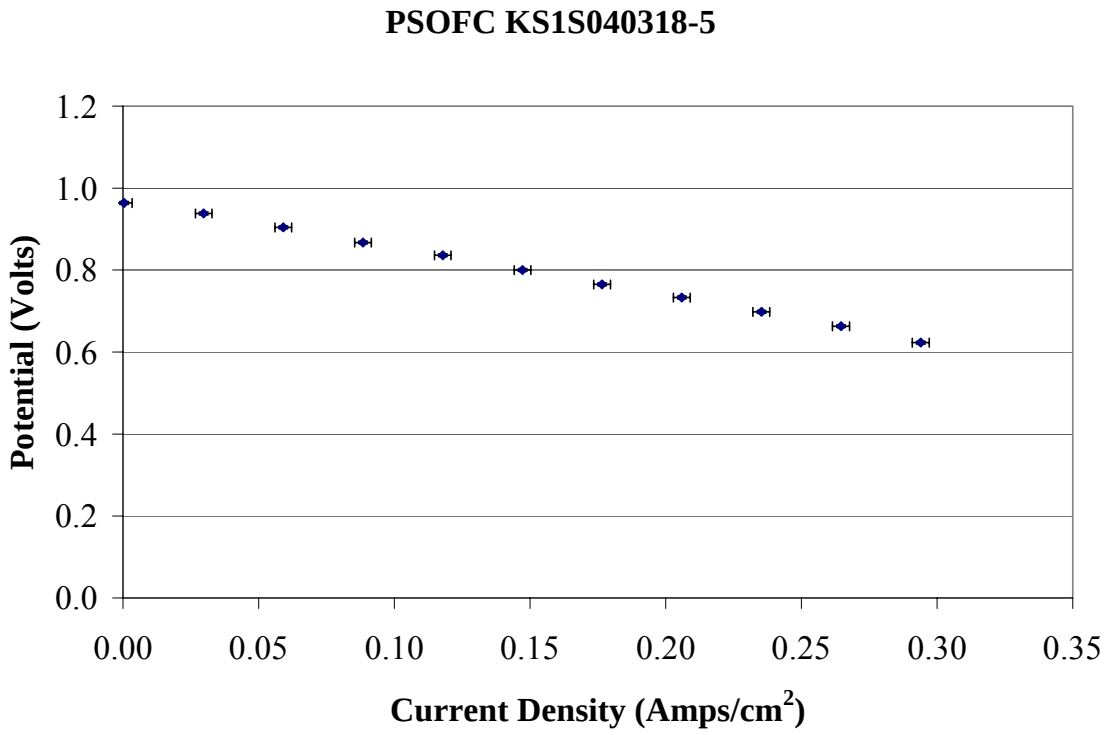

Figure 5.25 Trial 6 Initial VI Scan.

A least squares linear regression was then completed on the ohmic loss data to determine the slope of the line. The statistical equations used in the calculations are shown in Appendix 2. Figure 5.26 shows the initial ASR data and results from the ASR calculation for PSOFC KS1S040318-5 in trial 6.

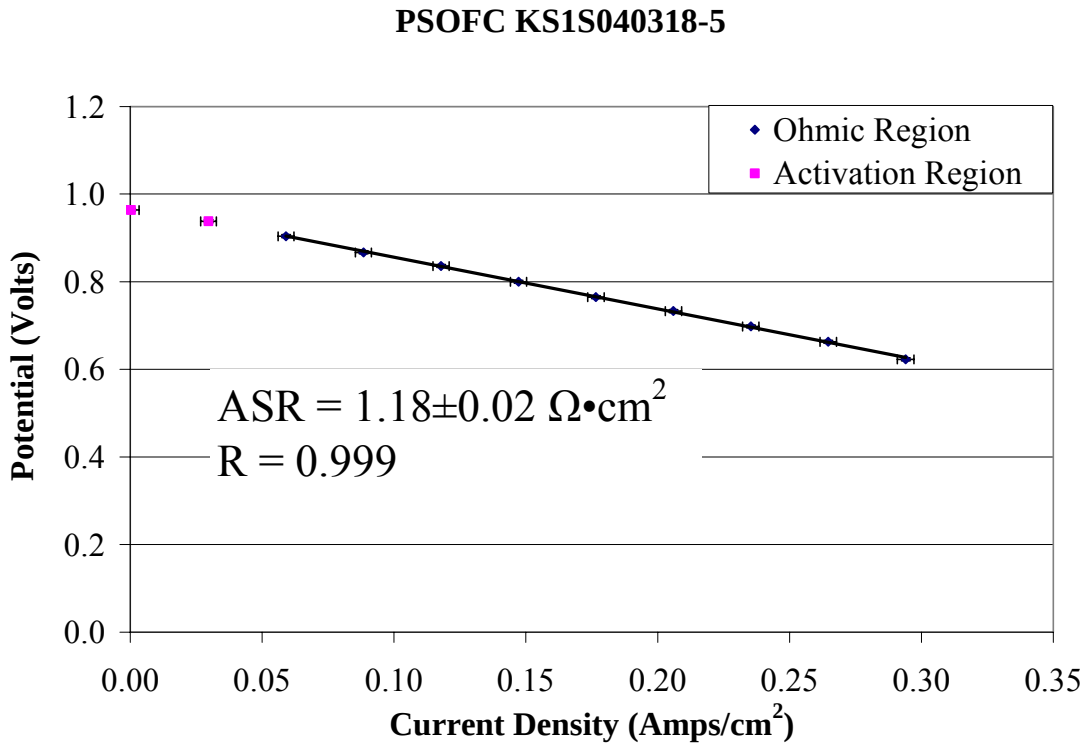

Figure 5.26 Trial 6 Initial ASR Regression.

As shown in Figure 5.26 the initial ASR measurement of PSOFC KS1S040318-5 resulted in a value of 1.18±0.02Ω/cm^2, which is within ±30 percent of 1.20 Ω/cm^2, so normal operation was established. A simulated baseline coal syn gas mixture was then delivered to the single cell test stand. The composition of the simulated coal syn gas is shown in Table 5.11.

Table 5.11 Trial 6 Simulated Coal Syn Gas Composition

Anode Gas Composition (Mole %)
21.6±0.9 H_2
32.8±0.7 CO
27.2±1.2 N_2
18.4±2.8 H_2O

The fuel gas was utilized by the PSOFC for approximately 68.4 hours during which three additional VI scans were completed. The resulting ASR values from VI scans two through four are shown in Table 5.12.

Table 5.12 Trial 6 Calculated PSOFC ASRs Utilizing Baseline Simulated Coal Syn Gas.

VI Scan	Operation Time (Hours)	ASR ($\Omega \cdot cm^2$)
2	23.0	1.23±0.01
3	49.9	1.18±0.02
4	68.4	1.16±0.03

The results shown in Table 5.12 shows that the ASR of the PSOFC decreased 1.7±2.5 percent over 68.4 hours of operation from VI scan one to four.

5.6.2. PSOFC Operation with Simulated Coal Syn Gas Containing H_2S

Once the steady state operation of the PSOFC utilizing the baseline simulated coal syn gas was established the effect of H_2S contamination was tested. H_2S was added to the system by replacing the CO portion of the baseline simulated coal syn gas with a mixture of CO and 758±4ppm H_2S. Using the partial pressure calculated from the Nernst equation (0.184 atm) the simulated coal syn gas composition is shown in Table 5.13.

Table 5.13 Simulated Coal Syn Gas Containing H_2S Composition.

Anode Gas Composition (Mole %)
21.6±0.9 H_2
32.8±0.7 CO
27.2±1.2 N_2
18.4±2.8 H_2O
249±9 ppm H_2S

The error associated with the H_2S was found by summing the variability in the open cell potential from the Agilent potentiostat. The initial open cell potential of the PSOFC was used since it is believed that it would yield a more accurate result than using the open cell potential when the coal syn gases were injected since the CO and H_2S may degrade the open cell potential. SOFCo EFS fuel cell engineers reported that the simulated coal syn gas contained 212±4 ppm H_2S, however it is believed this calculation was done using the open cell potential of the PSOFC once the simulated coal syn gas containing H_2S was injected into the system. VI scan five was completed 3.6 hours after the initial injection of H_2S into the system. Figure 5.27 shows the results from VI scan five.

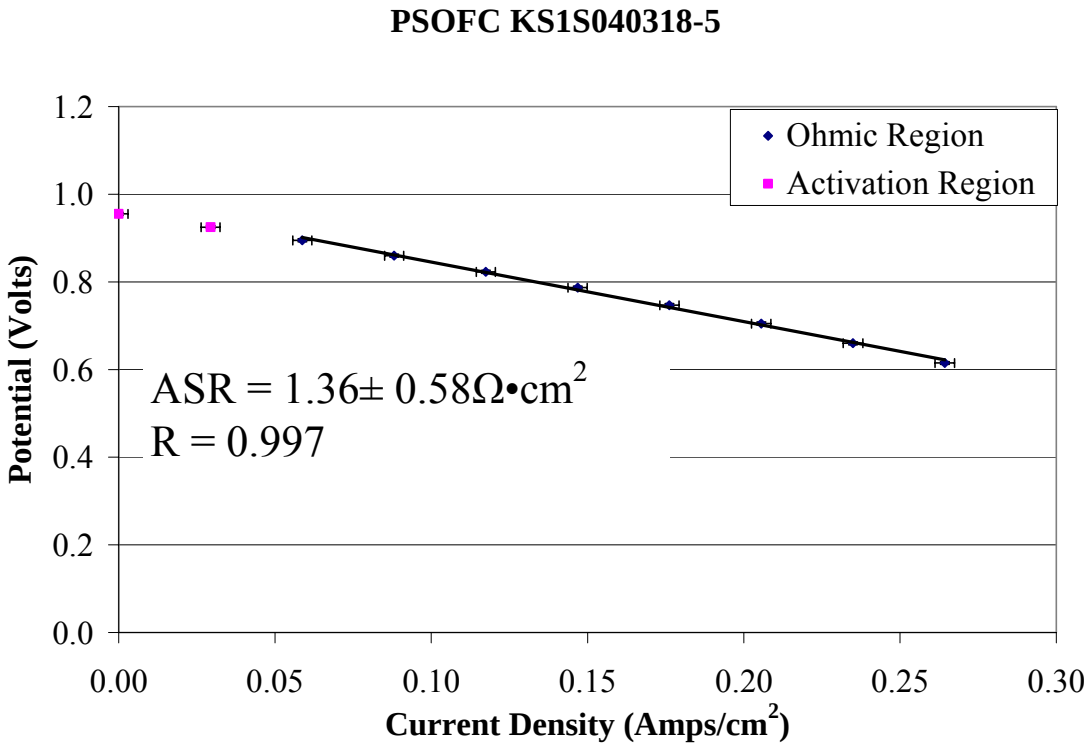

Figure 5.27 Initial ASR Regression After Injection of H_2S.

From the least squares linear regression the ASR of PSOFC KS1S040318-5 was found to be 1.36±0.58 $\Omega \cdot cm^2$. The confidence interval calculated from the ohmic region data showed that greater variability was present in the data collected than in previous VI scans resulting from the addition of H_2S which interferes in the electrochemical oxidation of H_2 and CO.

After the ASR value of PSOFC KS1S040318-5 for VI scan 5 was calculated the PSOFC was operated under an electrical load of 14.00±0.01 Amps for 525.6 hours with the same anode and cathode gas compositions and flow rates stated above. Nine additional VI scans were completed over the specified time period and the ASR of the PSOFC was calculated in the same manner as explained above. The results from VI

scans 4 through 12 that were completed on PSOFC KS1S040318-5 are shown in Table 5.14.

Table 5.14 Trial 6 Calculated PSOFC ASRs Utilizing Simulated Syn Gas Containing H_2S.

VI Scan	Operation Time (Hours)	ASR ($\Omega \cdot cm^2$)
6	141.5	1.47±0.55
7	165.8	1.50±0.54
8	189.9	1.56±0.51
9	189.9	1.60±0.51
10	306.7	1.63±0.50
11	337.7	1.62±0.50
12	360.8	1.64±0.51
13	410.4	1.64±0.50
14	477.6	1.72±0.50
15	501.6	1.70±0.49
16	525.6	1.69±0.48

As can be seen from Table 5.7 the ASR of PSOFC KS1S040318-5 continued to degrade over the length of the trial due to the H_2S contaminant. The variability in the data collected from PSOFC KS1S040318-5 was much greater once H_2S was added to the system. This is believed to be caused by the formation of Ni_2S_3 which reduces the number of reaction sites on the PSOFC anode. Trial 6 was shut down shortly after VI scan 16 was completed since the trial goal of 500 hours of operation was achieved.

After trial 6 was completed the ASR history of PSOFC KS1S040318-5 was plotted and studied. Figure 5.28 shows the ASR history from trial 6.

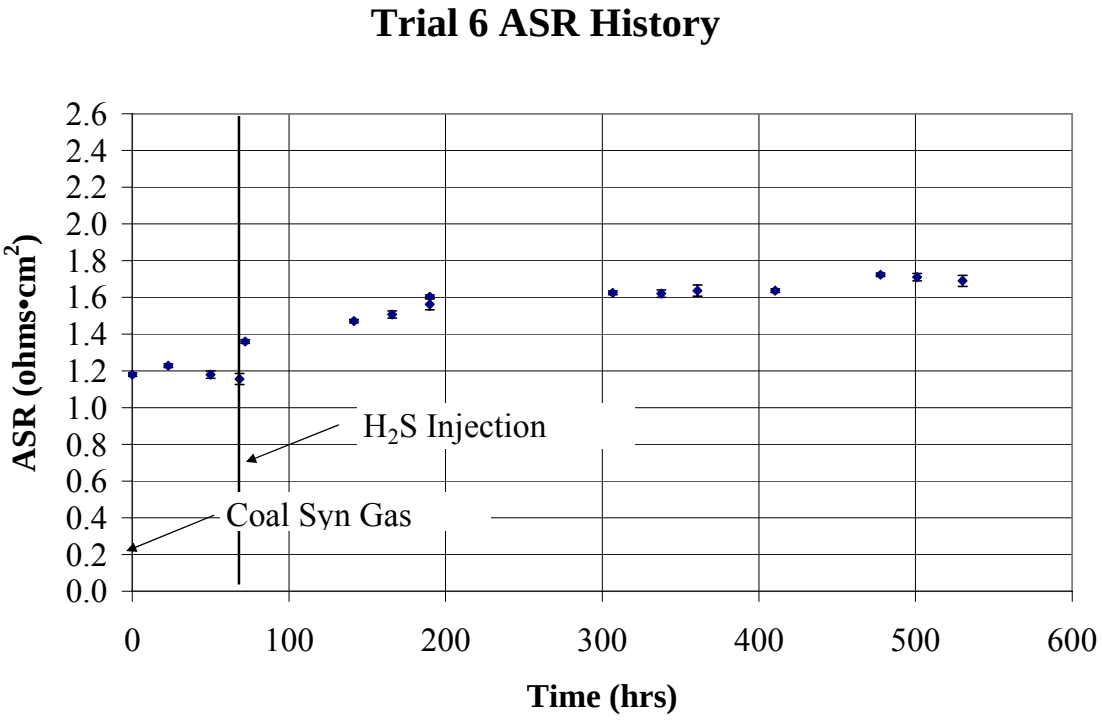

Figure 5.28 ASR History of Trial 6.

From Figure 5.28 three distinct trends can be seen in the ASR of PSOFC KS1S040318-5 after H_2S was added to the simulated coal syn gas mixture. The first trend can be seen as the large ASR degradation of the PSOFC from VI scan four to five. The second trend shows a linear degradation of the PSOFC ASR from VI scan 6 to 9. The third trend that can be seen is the ASR of PSOFC KS1S040318-5 reached a semi steady state value over VI scans 10 through 16. The initial ASR degradation of the PSOFC was found to be 17.6±4.2 percent over 4 hours of operation. The second ASR degradation trend found (VI scans 7 through 9) in trial 6 after the injection of H_2S was found to be 15.2±2.4 % per 100 hours of operation. The third ASR degradation rate (VI scans 10 through 16) was found to be 1.9±0.9 % per 100 hours of operation. Least squares linear regression

was completed on the data from the second and third ASR degradation trends but the data resulted in ASR degradation rates that were statistically insignificant. Better ASR degradation determination methods will be discussed in the recommendations section.

5.6.3. Trial 6 Anode Mateial Analyses

Once trial 6 was completed material analyses (SEM, EDXS, and XRD) were completed on PSOFC KS1S040318-5. Figure 5.29 shows an SEM image of the anode of PSOFC KS1S040318-5 at a magnification of 570X.

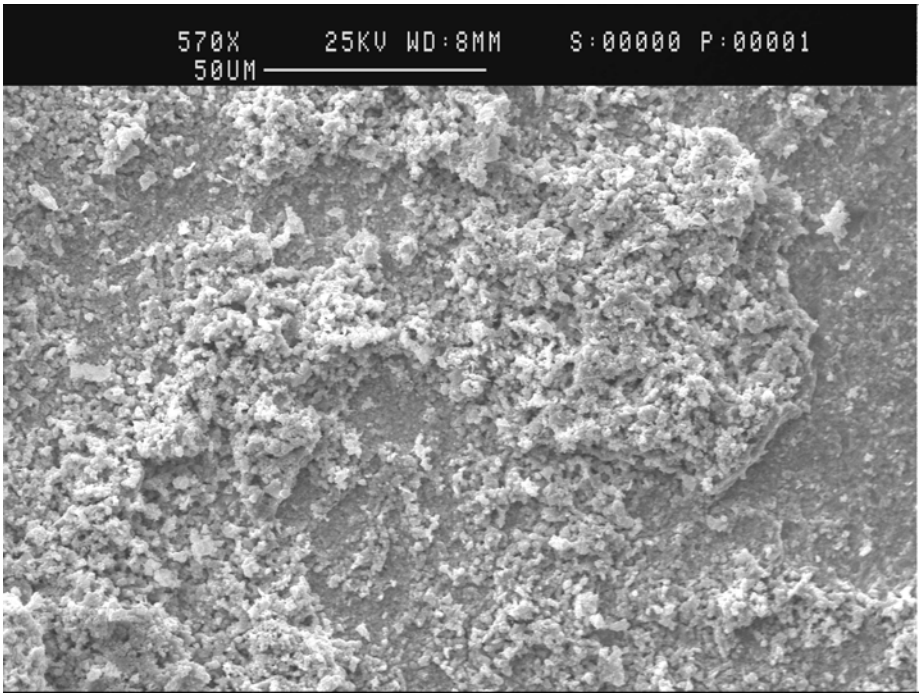

Figure 5.29 Trial 6 PSOFC Anode at 570X.

Inspecting Figure 5.29 it can be seen that the anode of PSOFC KS1S040210-43 is still porous after utilizing coal syn gas containing H_2S. This observation supports the conclusion that H_2S detrimentally affects the anode of the PSOFC by the formation of

Ni_2S_3 rather than blocking of gas flow channels. Another SEM image of the Trial 6 anode is shown in Figure 5.28 at a magnification of 1440X.

(a)

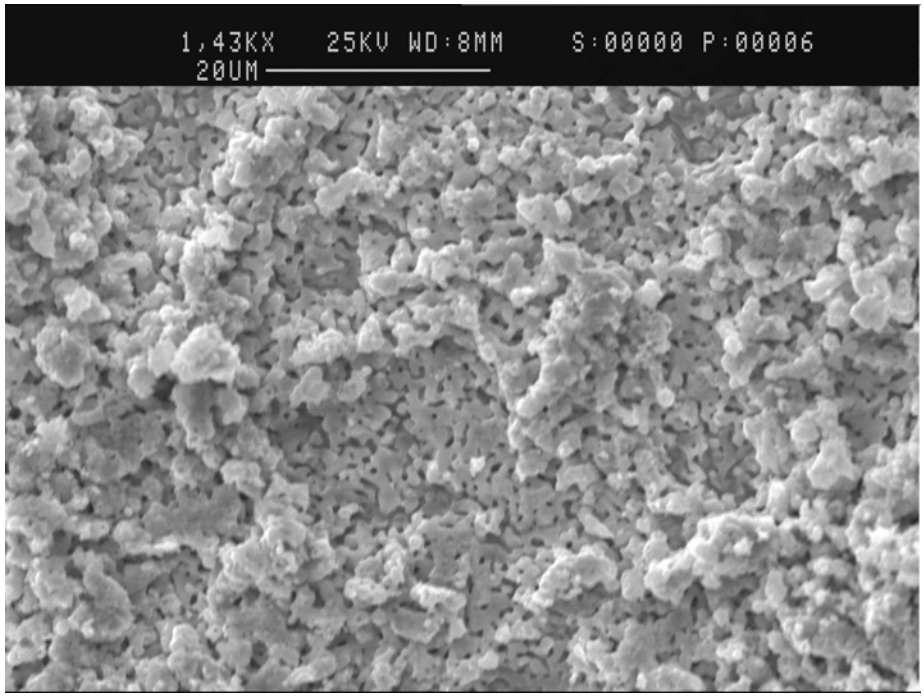

(b)

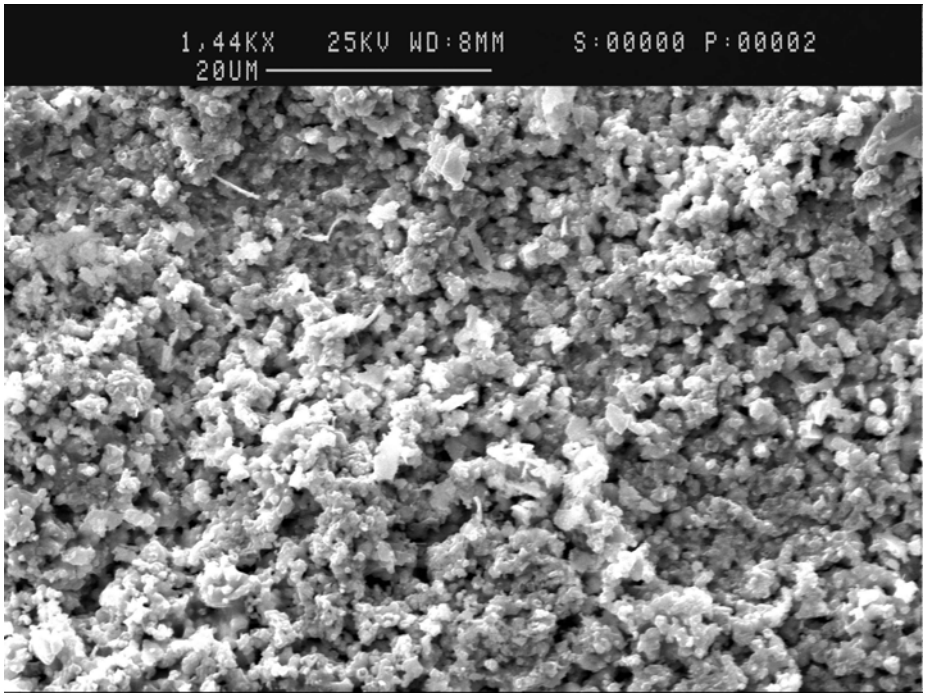

Figure 5.30 High Magnification SEM Images of PSOFC Anodes
(a) Baseline PSOFC Anode and (b) Trial 6 PSOFC Anode.

No discernable differences can be distinguished between the SEM images shown in Figure 5.30. Again this supports the conclusion that it is the formation of Ni_2S_3 and not the blockage of gas flow channels by the material that causes the degradation in the performance of the PSOFC.

EDXS analyses were completed on several areas of the PSOFC KS1S040318-5's anode. A representative spectrum is shown in Figure 5.31.

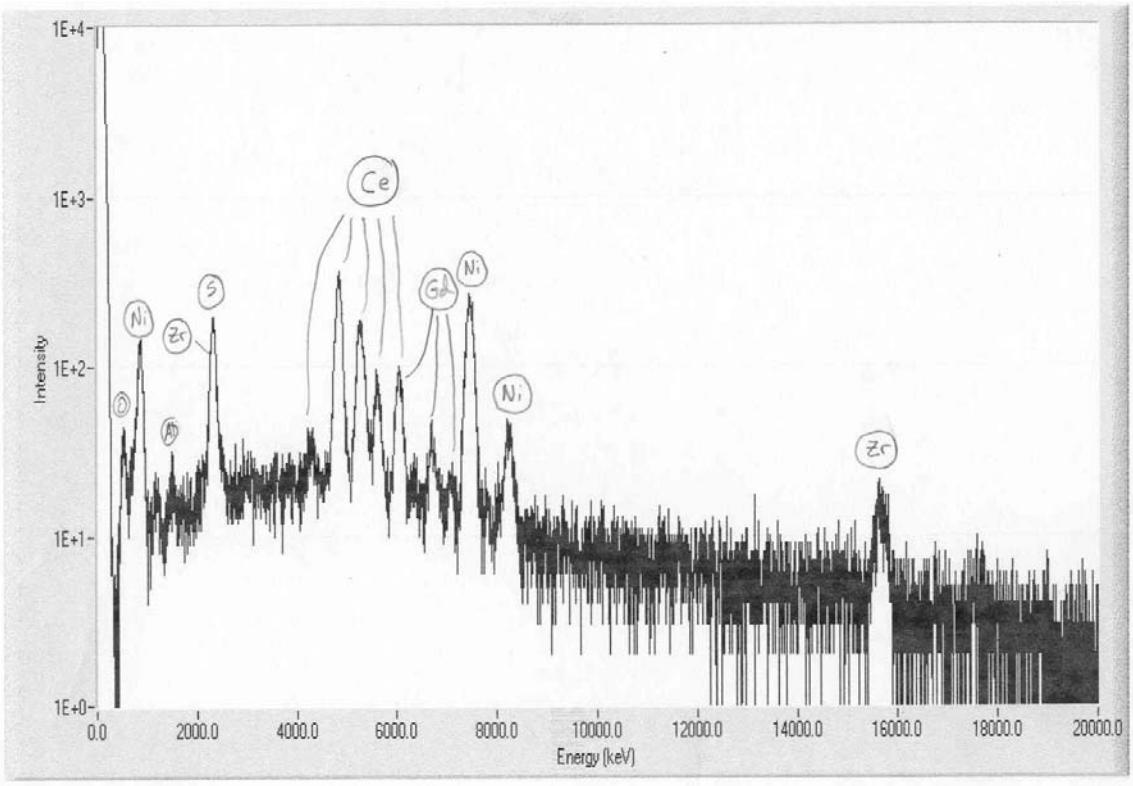

Figure 5.31 Trial 6 Anode EDXS Spectrum.

From Figure 5.31 it can be seen that the anode of PSOFC KS1S040318-5 contains Ni, Ce, Gd, O, Y, Zr and S. The sulfur in the PSOFC anode is from the formation of Ni_2S_3

when H_2S was added to the system. The EDXS spectrum in Figure 5.31 also shows no indication of carbon deposition.

Several XRD analyses were conducted using the same testing parameters described in section 5.4.3 on the anode of the PSOFC used in trial 2. A representative spectrum is shown in Figure 5.32.

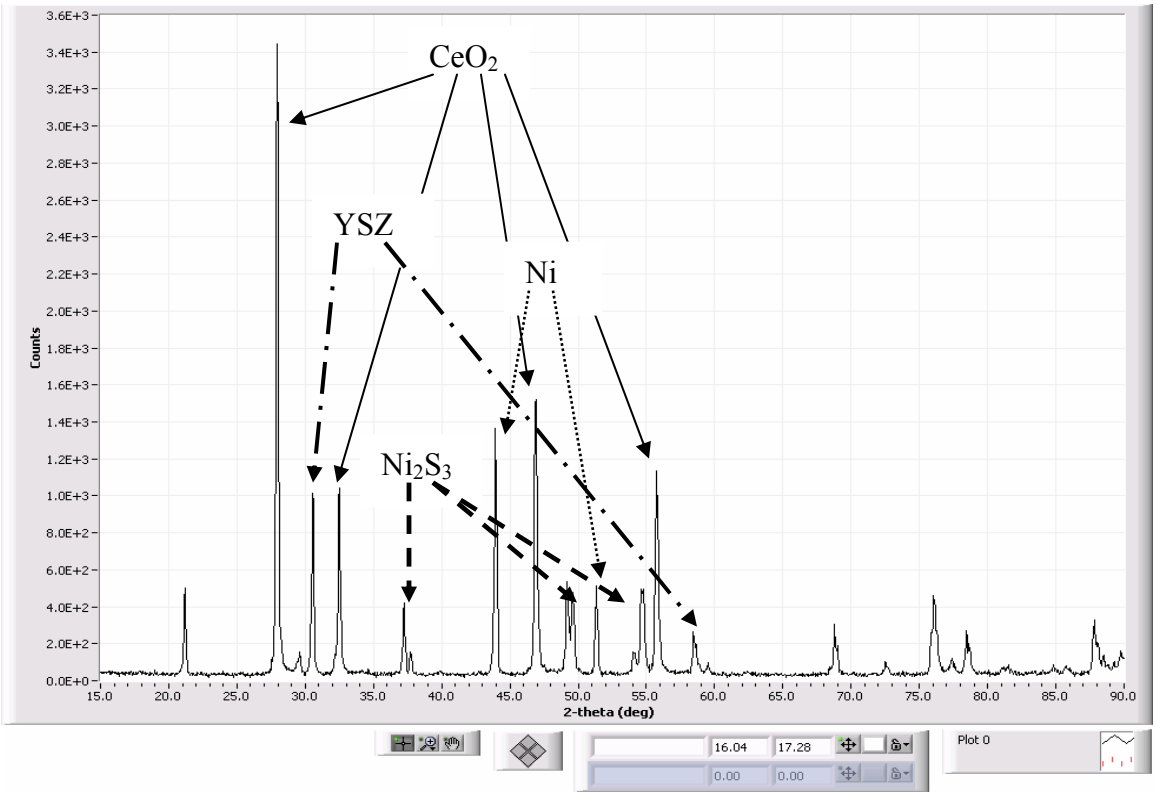

Figure 5.32 Trial 6 Anode XRD Spectrum.

The same compounds that were found in the PSOFC anodes from trials 4 and 5 were also found in the PSOFC anode of trial 6 as shown in Figure 5.32. However the compound Ni_2S_3 was also found and was expected based on literature sources [17]. It has been concluded that the nickel sulfide found in the anode trial 6 is the cause of the degradation

in performance of the PSOFC when H_2S was added to the baseline coal syn gas mixture. A calculation was completed to determine the worst case formation rate of Ni_2S_3 in the anode of the PSOFC and is attached in Appendix 2. The calculation was completed to compare the operation time of the PSOFC utilizing the coal syn gas mixture containing H_2S to the time that is available for the PSOFC to operate if all of the nickel in the anode of the PSOFC reacted with H_2S in the simulated coal syn gas. The calculation revealed that all of the nickel contained in the anode of the PSOFC would be converted to Ni_2S_3 after approximately 17.4 hours of operation which reveals that the other mechanisms are in control of the formation of Ni_2S_3.

5.7. Overview of Results

The overall results from trials 4 through 6 resulted in information that may be used to further engineering knowledge of PSOFCs. Figure 5.33 presents VI scans from trials 4 and 5 using the initial anode fuel gas and the simulated baseline coal syn gases.

(a)

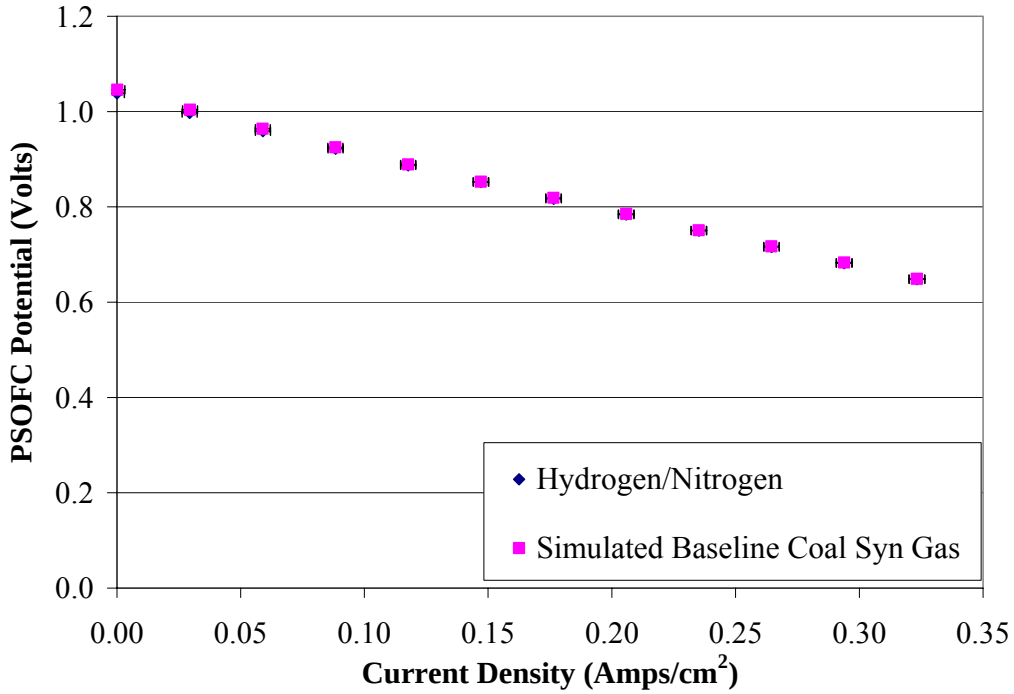

(b)

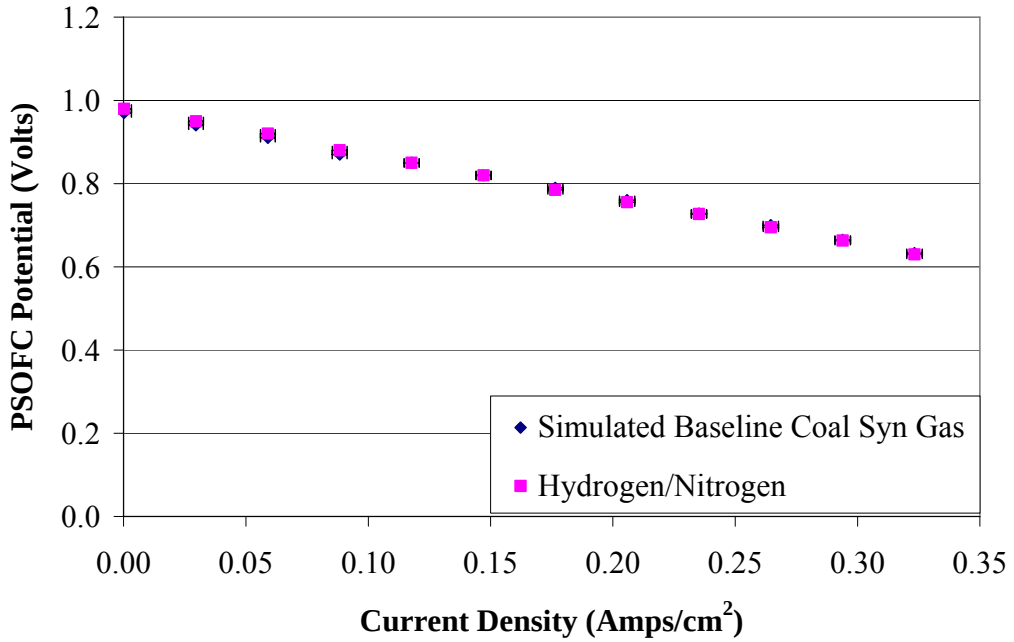

Figure 5.33 VI Scans for PSOFCs Utilizing H_2/N_2 and Simulated Baseline Coal Syn Gas (a) Trial 4 and (b) Trial 5.

From Figure 5.33 little to no difference may be distinguished between the VI scans of the PSOFC utilizing the H_2/N_2 fuel gas or the simulated baseline coal syn gas. These results show that the mixture of utilizable fuels contained in a coal syn gas (H_2 and CO) may be used to power a PSOFC. Figure 5.34 presents a plot of past SOFCo EFS InDEC PSOFC ASR histories and the ASR histories of trials 4 and 5.

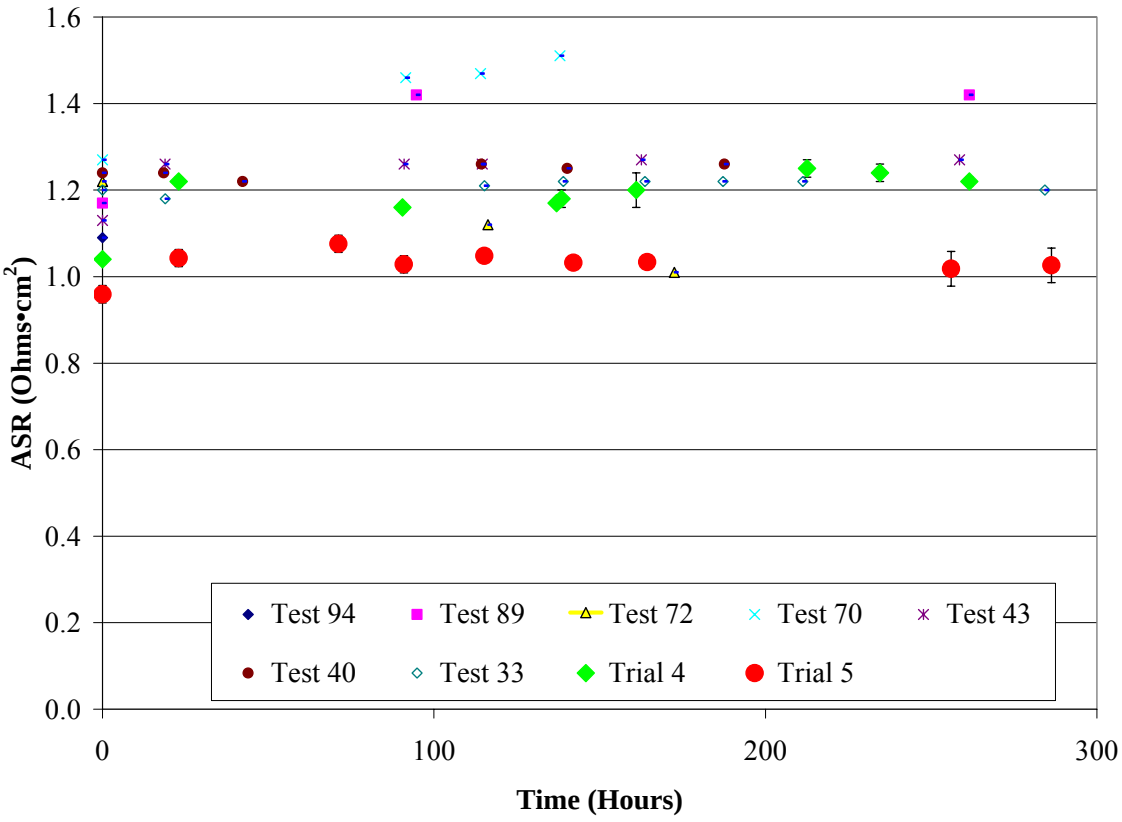

Figure 5.34 In DES PSOFC ASR History Comparison.

From Figure 5.34 it may be seen that the ASR trends from trials 4 and 5 are very similar to past SOFCo EFS PSOFC data. The low PSOFC ASR values that were found in trial 5

were deemed to be caused by a difference in the structure or morphology of PSOFC KS1S040210-43's anode. However the operation trend shown by the PSOFC behaves similarly to the ASR history of trial 5 and the past SOFCo EFS trials. Since the ASR values of the PSOFCs tested in trials 4 and 5 were found to be within 30 percent of 1.20 $\Omega \cdot cm^2$ the trials were considered to have established repeatability of the system. The results presented in Figure 5.33 also establish that a simulated coal syn gas with out H_2S may be utilized as a fuel source for the PSOFCs.

The detrimental effect that H_2S has on the PSOFC anode was shown in trial 6. Figure 5.35 presents the ASR histories from the three trials that were completed in the research.

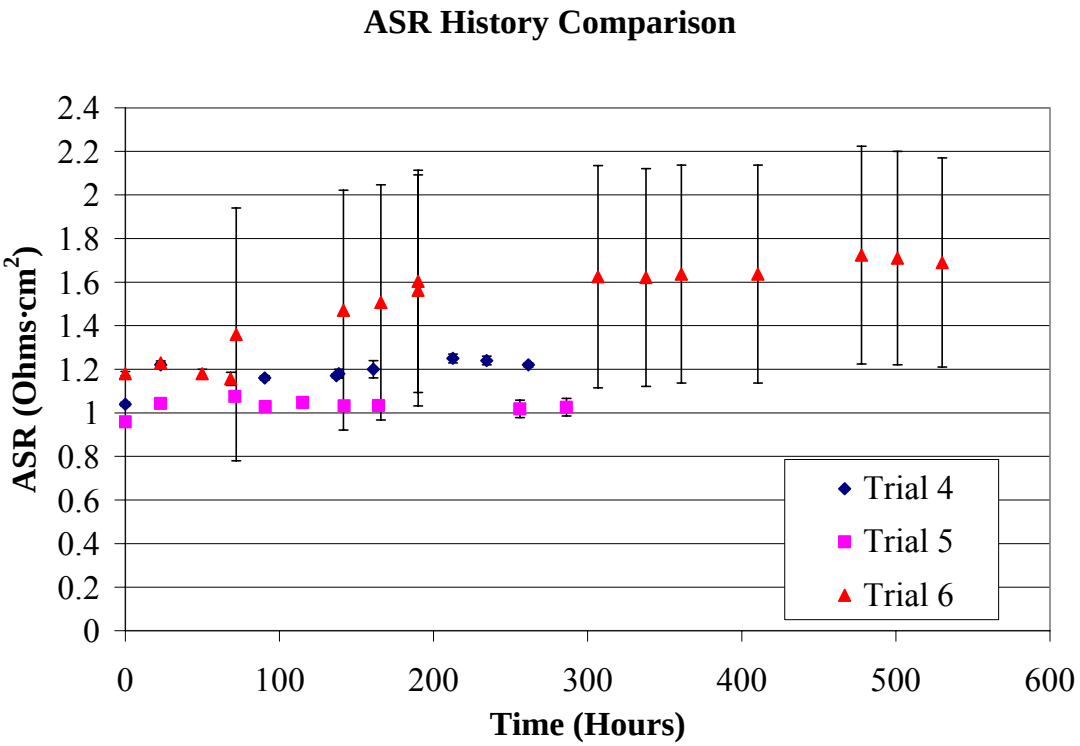

Figure 5.35 Trial 4 Through 6 ASR History Comparison.

From Figure 5.35 the detrimental effect that H_2S has on the PSOFC anode can easily be seen. The H_2S in the simulated coal syn gas reacts with the nickel of the PSOFC anode cermet forming Ni_3S_2 which is an electrical insulating material increasing the resistance of the PSOFC anode and therefore increasing the ASR of the PSOFC.

Chapter - 6

Conclusions

6.1. Introduction

Over the past year only three trials of a proposed six to investigate the effect of coal syn gas on the operation of PSOFCs were completed. Although the original goal of the thesis work was to investigate the effect of ambient and elevated pressure (50 psig) coal syn gas containing H_2S on the operation of a PSOFC was not accomplished useful information has been gained. The information that has been gained from the research presented in this thesis may be used to draw conclusions upon to further engineering knowledge. The following sections will present the conclusions that have been made as well as the justification for these conclusions.

6.2. Operation of PSOFC Utilizing Simulated Baseline Coal Syn Gas

Trials 4 and 5 were designed to demonstrate the InDEC PSOFC's ability to operate utilizing a simulated O_2 blown Pittsburgh No.8 coal syn gas. During trials 3 and 4 when coal syn gas with the composition shown in Table 5.4 was used an anode back pressure of 20 psig or more developed in the anode fuel gas line. The anode back pressures required the tests to be shut down to avoid damaging any test equipment. After trial 4 the development of the high anode back pressure was found to be caused by coking that was taking place in the inlet tube of the anode fuel manifold. In order to prevent the coking from taking place the H_2O content of the fuel gas was increased by increasing the H_2O bubbler temperature from 25°C to 70°C. This allowed the simulated coal syn gas to have a greater H_2O content by increasing the maximum partial pressure of H_2O. No

further coking was found to take place so it has been concluded that the increased H_2O content prevented the coking that was taking in the inlet tube of the anode manifold. Although the simulated coal syn gas mixtures for trials 4 and 5 contained different compositions the actual utilizable fuel available in both trials remained the same (212.1±4.5 smL/min CO and 139.2±6.0 smL/min H_2). Because both of these trials contained the same amount of usable fuel for the PSOFC both could be used to establish repeatability and compare with past SOFCo EFS data for InDEC PSOFCs. From Figure 5.33 no distinguishable difference can be seen between the potential and current data in trials 4 and 5. The information shown in Figure 5.33 allows the conclusion that PSOFCs may readily utilize the simulated baseline coal syn gas as readily as the H_2/N_2 fuel gas mixture. This idea is very important because it expands the fuel diversity of the PSOFC from H_2 to many more economically feasible fuels such as coal syn gas that has been cleaned of H_2S. Also the VI scans shown in Figure 5.33 (a) and (b) also show that H_2 is the more readily oxidized fuel. This conclusion may be drawn because the open cell potential of a CO/CO_2 atmosphere is higher compared to that of an H_2/H_2O atmosphere due to the higher Gibb's free energy of reaction for the CO/CO_2 system. From Figure 5.34 the ASR degradation of the PSOFCs used in trials 4 and 5 can be seen to be less than the ASR degradation than those for the past SOFCo EFS trials. The average ASR degradation from the past SOFCo EFS trials was 10% per 1000 hours of operation where the ASR degradation for trials 4 and 5 was -1.0±2.5 % per 1000 hours and -5.7±3.8 % per 1000 hours respectively. Although it would not be possible to actually have a declining ASR value during long periods of operation the data shows that the baseline simulated

coal syn gases of trials 4 and 5 caused little to no degradation to the PSOFC anodes. Another important conclusion that was made is the fact that the InDEC PSOFC anodes that were used in the research showed good resistance to carbon deposition. This was proven by the resulting EDXS and XRD spectrums of the PSOFC anodes from trials 4 through 6 which showed no signs of carbon deposition. These results indicate that the PSOFCs may be operated for a long periods of time utilizing carbonaceous fuels without pore blockage due to coking.

6.3. Operation of PSOFC Utilizing Simulated Coal Syn Gas Containing H_2S

Trial 6 was designed to investigate the InDEC PSOFCs ability to operate while utilizing a simulated coal syn gas containing approximately 249±9 ppm H_2S. The information that was obtained from this trial has been enough to make conclusions as to the PSOFC anode's sulfur tolerance compared to PSOFC anodes made of a Ni/YSZ cermet and the ability of PSOFC to be used in a distributed power generation system utilizing gasified coal as its fuel source. In Trial 6 the ASR of the PSOFC increased from 1.16±0.03 $\Omega \cdot cm^2$ to 1.36±0.58 $\Omega \cdot cm^2$, which is an initial ASR increase of 17.2±50.0 percent. In literature it has been reported that an instantaneous PSOFC ASR increase of 200 percent or more takes place with the addition of as little as 5 ppm H_2S in a PSOFC using an Ni/YSZ cermet anode [26]. At the conclusion of Trial 6 the final ASR value of the PSOFC was found to be 1.69±0.48 $\Omega \cdot cm^2$ which is a total increase in the ASR of the PSOFC from its initial steady state ASR value (1.23±0.01 Ω·cm2) of 37.4±39.0 percent after approximately 458 hours of operation. This increase in the ASR of the PSOFC is still drastically less than instantaneous increase of 200 percent for an Ni/YSZ cermet

anode utilizing a fuel gas containing 5 ppm H_2S. This information leads to the conclusion that the InDEC PSOFC anodes show some tolerance compared to Ni/YSZ cermet anodes. This tolerance is believed to be caused by the expansion of the TPB with the addition of CeO_2 to the anode compared to the Ni/YSZ cermet anode. However the InDEC PSOFC anodes still show too high of an ASR degradation to elevated concentrations of sulfur (200 to 300 ppm H_2S) to be used for a distributed power generation system using coal syn gas as a fuel source.

6.4. Recommendations

Upon the completion of the research that has been presented many recommendations for future research have been made and will be discussed in the following sections. Many failures and inadequacies that had taken place during the research have caused the need for change in order for future research to take place in a more efficient manner. The recommendations that will be presented will entail suggested changes in the determination of the ASR degradation rate, the PSOFC testing setup procedure, operation of the single cell test stand, modifications to the pressurized testing chamber, and more sulfur tolerant anodes materials.

6.4.1. ASR Degradation Determination

More accurate methods to determine the ASR degradation rate of the PSOFCs over time must be used in future research work. The trials that were completed in the research presented in this thesis resulted in statistically insignificant ASR degradation rates when using least squares linear regression and Equation 3.1 only represents the degradation rate of the PSOFC ASR at two points in time rather than over time. Least

squares linear regression will results in better ASR degradation determination but more VI scans must be completed to ensure that statistically significant ASR degradation rates are found. In order to do this it is recommended that the VI scan rate be increased to two to three times daily while completing a least square linear regression on the ASR/time data after each VI scan has been completed. The VI scans should be completed until an acceptable statistically significant ASR degradation rate for the PSOFC has been established. This method should be used both when H_2/N_2 and simulated coal syn gas mixtures are being used by the PSOFC. The anode gas mixture should not be switched until the ASR degradation of the PSOFC has been established. Also the rate at which VI scans are completed should also be investigated to determine the optimal VI scan rate that will establish a statistically significant ASR degradation rate.

6.4.2. PSOFC Testing Setup

During the PSOFC testing setup procedure many problems were encountered including incorrectly wired solenoid valves, incorrect installation of fuel cells, undersized MFCs, and incorrect manifold setups. Many trials were lost due to these problems that had taken place during the PSOFC testing setup procedure and recommendations to the current setup procedure will be discussed below in order to eliminate the associated problems and decrease lost testing time.

The first problem that was encountered with the PSOFC testing setup occurred during the setup of the initial single cell test stand trial. The anode gas manifold was found to be incorrectly wired which caused a high pressure slug of H_2O to travel to the

PSOFC damaging it during its heating cycle. Two measures have been recommended to prevent this from taking place again. The first recommendation is to check all the wiring that is completed during the construction of the PSOFC test stand. This should be done during the construction of the test stand to avoid problems associated by completing the inspection upon the completion of the test stand. The second recommendation is to plan for an initial setup trial in the testing matrix that is to be completed. The initial trial in every new test matrix may be used to determine if the testing system has any inadequacies that may detrimentally affect the research that is co be completed. If no inadequacies are found in the testing system then the initial trial may then be used to as the first trial in the research test matrix. This added trial will allow testing system inadequacies to be identified at the beginning of the research to reduce lost trials and testing time.

The next recommendation for the PSOFC testing setup procedure is for the engineer who is completing the research to install the PSOFC or be present when the installation is taking place. This is especially important when personnel from outside of the Ohio Coal Research Center are completing the installation work. This will avoid problems that were encountered when the PSOFC was mistakenly installed upside down and when ceramic insert tubes that were to be used with the anode fuel manifold were not used. In order to avoid these problems the engineer should install the PSOFC or help the technician that is installing the PSOFC to ensure the PSOFC is installed correctly and avoid wasting PSOFCs and testing time.

The next recommendation is to complete MFC calibrations with a bubble meter before every new test matrix is to be completed with the single cell gas delivery system. In order to complete the calibrations safely N_2 or air should be used as the calibration gas and the measurements can then be converted for the respective MFC gas density. The calibrations will allow the engineer operating the single cell gas delivery system to better account for the variation in the MFC flow rates and ensure the MFCs are capable of providing the anode and cathode fuel gases that are required for the testing.

Another possible problem that was encountered during the PSOFC setup procedure is the application of the inks to the anode and cathode of the PSOFC. It is very important that the inks used on the anode and cathode of the PSOFC do not touch the edge of the PSOFC so they do not come into contact with one another during testing. The crossover of the inks from one side of the PSOFC to the other will cause a short circuit to form. It is recommended that the engineer setting up the PSOFC use masking tape to tape of the edges of the PSOFC electrolyte so that no electrode inks will travel across the edge of the electrolyte and short circuit the PSOFC. The masking tape may then be removed after the respective ink has been applied.

6.4.3. Operation of Single Cell Test Stand

Recommendations to more safely operate the single cell testing system have been made. The first recommendation is to always have the anode gas cabinet blower operating at all times. This blower produces a negative pressure in the anode gas cabinet and ensures that air from the room is always being drawn through the anode gas cabinet

preventing leakage of toxic gases into the room. Even if the toxic gases (CO and H_2S) are not present the anode gas cabinet blower should still be operated as a safety habit.

The next recommendation for engineers operating the single cell test stand during operation is to be very careful when refilling the H_2O bubbler of the single cell test stand. The H_2O bubbler should be filled at a very slow rate to ensure that the column is not overfilled and floods the anode of the PSOFC during operation. Upon this recommendation it may be advisable to add an overfill safety device that will not allow the H_2O level in the column to rise above a predetermined height.

6.4.4. Pressurized PSOFC Testing Chamber

Many problems were encountered when the pressurized testing chamber was used at the operational temperature of 850°C. The pressurized testing chamber was found to develop a large leak around the sealing face of the chamber and was not capable of building a back pressure greater than 20 psig. After discussions with engineers in the Ohio Coal Research Center the conclusion that the face to face metal sealing that is being used in the current pressure chamber is not capable of withstanding the back pressures that are desired for testing (50 psig). In order to accomplish the desired back pressure it is recommended that an o-ring be added to the face to face seal of the pressurized test chamber in order to build the back pressure that is desired for testing.

6.4.5. Sulfur Tolerant Anode Materials

The results that were obtained from trial 6 have led to the conclusion that more sulfur tolerant anode materials are needed for the development of a PSOFC distributed

power generation system utilizing gasified coal as fuel. The desired capabilities of a PSOFC anode for the distributed power generation system are to have current densities very similar to PSOFC anodes utilizing only H_2 as a fuel source, resistant to coking, and show very high tolerance to sulfur impurities. Two of the desired capabilities have been demonstrated in the research that has been conducted with simulated coal syn gases. However the degradation of the PSOFC ASR caused by 249±9 ppm H_2S is too high. A desirable level of PSOFC ASR degradation is 3 percent per 1000 hours of operation or less. Although some materials have been found to be sulfur tolerant and have the capability of electrochemically oxidizing H_2 their performance is not as good as typical PSOFC anode materials [33]. Because of this it is recommended that more research be completed to develop a sulfur tolerant anode that is capable of being used as a PSOFC anode for the distributed power generation system that is being developed. Also it is recommended that the capabilities of multi layer anodes using sulfur tolerant materials be investigated.

References

1. United States Department of Energy, "Short Term Energy Outlook – November 2004," http://www.eia.doe.gov/emeu/steo/pub/contents.html, November 2, 2004.

2. United States Department of Energy,, "Annual Coal Report 2003," http://www.eia.doe.gov/cneaf/coal/page/acr/acr_sum.html, Novemer 2, 2004.

3. R. Peltier, "Power Magazine's Top Plants of 2003," Platts Power, 147, 6, 42 (2003).

4. D.J. Jacob, Atmospheric Chemistry, Princeton University Press, 1999, pp. 172, 249.

5. R. Wilson and J. Spengler, Particles in Our Air: Concentrations and Health Effects, p. 212, 1999.

6. United States Environmental Protection Agency, "US Power Plant Total Emissions by Year," Resource and Generation Resource Integrated Database, December 10, 2003.

7. United States Environmental Protection Agency, "Acid Rain Program," http://www.epa.gov/airmarkets/arp/, November 15, 2004.

8. Clean Air Task Force, Death, Disease, and Dirty Power: Mortality and Health Damage Due to Air Pollution from Power Plants, p. 5, 2000.

9. K. Krist, J.D. Wright, and K.J. Gleason, "Solid Oxide Fuel Cell Residential Cogeneration," 1999 Joint DOE/EPRI/GRI Fuel Cell Technology Review Conference, Chicago, IL, August 3-5, 1999.

10. D. Hart, and G. Hormandinger, "Environmental Benefits of Transport and Stationary Fuel Cells," Journal of Power Sources, 71, pp. 352 (1998).

11. A. B. Stambouli and E. Traversi, Solid oxide fuel cells,: a review of an environmentally clean and efficient source of energy, Renewable and Sustainable Energy Reviews, 6, p.433-455 (2002).

12. A. Bauen and D. Hart, Assessment of the environmental benefits of transport and stationary fuel cells, Journal of Power Sources, 86, p.482-494 (2000).

13. M. Williams, "Status of SOFC Development and Commercialization in the US," Solid Oxide Fuel Cells VI, pp. 3-9 (1999).

14. EG&E Services, Parsons, Inc. and Science Applications International Corporation (eds.), Fuel Cell Handbook, 5th ed., 2000. pp. 2.3-2.8, 2.11, 8.3, 8.13-8.15.

15. C. Fisher, "Solid Oxide Fuel Cells," http://www.spice.or.jp/~fisher/sofc.html, December 10, 2003.

16. K. Kordesch and G. Simander, Fuel Cells and Their Applications, VCH Publishing, 1996, pp. 23-30, 140.

17. Y. Matsuzaki and I. Yasuda, "Effect of a Sulfur-Containing Impurity on Electrochemical Properties of a Ni-YSZ Cermet Electrode," Solid Oxide Fuel Cells VII, pp. 769-777 (2001).

18. Y. Jiang and V. Virkar, "Fuel Composition and Diluent Effect on Gas Transport and Performance of Anode-Supported SOFCs," Journal of the Electrochemical Society, 150 (7), p. A942 (2003).

19. H. Yakabe et al., "Evaluation and Modeling of Performance of Anode-Supported Solid Oxide Fuel Cells," Journal of Power Sources, 86, p. 423 (2000).

20. Y. Matasuzaki and I. Yasuda, "Electrochemical Oxidation of H_2 and CO in a H_2-H_2O-CO-CO_2 System at the Interface of a Ni-YSZ Cermet Electrode and YSZ Electrolyte," Journal of the Electrochemical Society, 147, p. 1630 (2000).

21. A. Weber et al., "Oxidation of H_2, CO and Methande in SOFCs with Ni/YSZ Cermet Anodes," Solid State Ionics, 152-153, p.543 (2002).

22. K. Sasaki et al., "Current-Voltage Characteristics and Impedance Analysis of Solid Fuel Cells for Mixed H_2 and CO Gasesm," Journal of the Electrochemical Society, 149, p. A227 (2002).

23. J.Sfeir, J. Van Herle and A.J. McEvoy, in Proceedings of the 3rd European Solid Oxide Fuel Cell Forum, p. 267 (1998).

24. E.P. Murray and S.A. Barnett, "A Direct Methane Fuel Cell with a Ceria Based Anode," Nature, 400, p. 649, (1999).

25. S. Park, J.M. Vohs, and R.J. Gorte, "Direct Oxidation of Hydrocarbons in a Solid Oxide Fuel Cell," Nature, 404, p.265 (2000).

26. Y. Matsuzaki and I. Yasuda, "Effect of a Sulfur-Contain Impurity on Electrochemical Properties of a Ni-YSZ Cermet Electrode," Solid Oxide Fuel Cells VII, pp. 769-777 (2001).

27. E.H. Edwin, H. Karoliussen, and R. Odegard, "H_2S in Natural Gas Fuel Reduces Mechanical Stress in Solid Oxide Fuel Cells," Solid Oxide Fuel Cells V, p. 839 (1997).

28. N.J. Maskalisk, and E.R. Ray, "Contaminant Effects in Solid Oxide Fuel Cells," Fourth Annual Fuel Cells Contractors Review Meeting, Morgantown, WV, May 5-6, pp. 4-7 (1992).

29. J. Geyer et al., "Investigations into the Kinetics of the Ni-YSZ Cermet Anode of a Solid Oxide Fuel Cell," Solid Oxide Fuel Cells V, p. 587 (1997).

30. SOFCo EFS, Testing and Evaluation of an Advanced High Performance Planar SOFC Stack, SOFCo EFS, SOFCo EFS, 1999, pp. 2-6.

31. E. Batawi et al., "Cell Manufacturing Processes at Sulzer Hexis," Solid Oxide Fuel Cells VII, pp. 143-144 (2001).

32. S. Primadahl and M. Mogensen, "Limitation in the Hydrogen Oxidation Rate of Ni/YSZ Anodes," Solid Oxide Fuel Cells VI, pp. 533-535 (1999).

33. R. Mukundan et al., "Sulfur Tolerant Anodes for SOFCs," Electrochemical and Solid State Letters, 7, pp. A5-A7 (2004).

34. K. Kordesch and G. Simander, Fuel Cells and Their Applications, VCH Publising, 1996, pp. 23-30, 140.

35. R. Kikuchi et al., "Characteristics of Anodic Polarization of Solid Oxide Fuel Cells Under Pressurized Condition," Solid Oxide Fuel Cells VIII, p. 720 (2003).

36. EG&E Services, Parsons, Inc. and Science Applications International Corporation (eds.), Fuel Cell Handbook, 5th ed., 2000, pp. 2.3-2.8, 2.11, 8.3, 8.13-8.15.

37. S.C. Singhal, "Progress in Tubular Solid Oxide Fuel Cell Technology," Solid Oxide Fuel Cells VI, pp. 39-51 (1999).

Appendix 1

Past SOFCo EFS trial data with InDEC ESC fuel cells with an active electrode area of 68.1 cm^2 is presented below in Figure A.1. All of the PSOFC trial data presented below was operated with 350 smL/min H_2 and 350 smL/min N_2 when VI scans were taken from the PSOFCs and operated with 214 smL/min H_2 and 214 smL/min N_2 when the cells were operated under a constant load of 14.00±0.01 Amps. The cathode air flow rate to the PSOFCs was kept constant at 2500±45 smL/min Air.

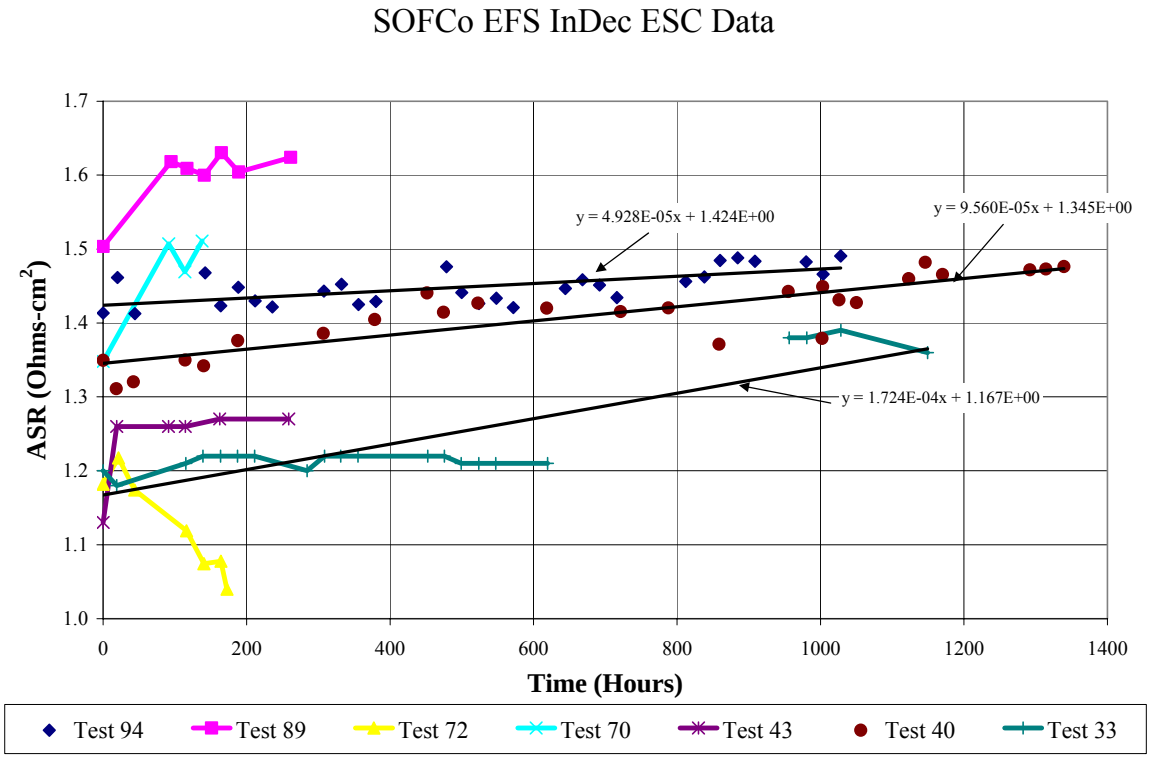

Figure A.1 Past SOFCo EFS InDEC ESC Trial Data.

Appendix 2

In order to determine the theoretical open cell potential of the PSOFCs the Nernst equations presented by Jiang and Virkar were used and are shown below Equation A.1 and A.2 [18].

$$E = \frac{RT}{4F}\ln\left(\frac{P_{O_2(Cathode)}}{P_{O_2(Anode)}}\right) \qquad \text{Equation A.1}$$

$$\ln\left(P_{O_2(Anode)}\right) = \frac{2\Delta G}{RT} + 2\ln\left(\frac{P_{H_2O}}{P_{H_2}}\right) \qquad \text{Equation A.2}$$

Where E is the theoretical open cell potential of the PSOFC (Volts), R is the ideal gas constant (8.314J/mol·K), T is the reactijon temperature (1123K), F is Faraday's constant (96485 Coulombs/e^-), $P_{O_2(Cathode)}$ is the partial pressure of oxygen at the cathode (0.21 atm), $P_{O_2(Anode)}$ is the partial pressure of oxygen at the anode found from Equation A.2, ΔG is the Gibb's free energy of reaction (-185875 J/mol for Equation 1.2, P_{H_2O} is the partial pressure of H_2O at the anode of the PSOFC, and P_{H_2} is the partial pressure of H_2 at the anode of the PSOFC.

Determination of Theoretical Open Cell Potential for Trial 4:

In order to determine the theoretical open cell potential of the PSOFC for the operating conditions of the PSOFC utilizing 350 smL./min H_2 and 350 smL./min N_2 that is bubbled through a column containing H_2O at 25°C Equations A.1 and A.2 were used. Since the H_2O content of the anode fuel gas could not be measured it was assumed that the anode fuel gas became saturated after traveling through the column. The saturation

pressure of H_2O at 25°C is approximately 3.13 atm. This value was used along with Equations A.1 and A.2 to calculate the theoretical open cell potential of the PSOFC as shown below.

$$\ln\left(P_{O_2(Anode)}\right)=\frac{2\left(-185875\frac{J}{mol}\right)}{\left(8.314\frac{J}{mol\cdot K}\right)(1123K)}+2\ln\left(\frac{.0313atm}{0.484atm}\right)$$

Solving for $P_{O_2(Anode)}$ yielded 2.13×10^{-20} atm. Using this value along with Equation A.1 yielded the theoretical open cell potential for the PSOFC in trial 4.

$$E=\frac{\left(8.314\frac{K}{mol\cdot K}\right)(1123K)}{4\left(96485\frac{C}{e^-}\right)}\ln\left(\frac{0.21atm}{2.13\times10^{-20}}\right)=1.05V$$

No error was quantified with theoretical open cell potential because the variability in the H_2O content of the anode fuel gas is unknown at this time.

Determination of the H_2O content of the anode fuel gas for Trial 5:

Assuming the H_2O content of the anode fuel gas was equal to the saturation pressure of H_2O at 70°C (0.308 atm) yielded at theoretical open cell potential that was lower than the actual open cell potential of the PSOFC (0.956±0.004 V). Because it is impossible for the actual open cell potential of the PSOFC to be greater than the theoretical open cell potential the actual H_2O content of the anode fuel gas is below saturation. In order to quantify the actual H_2O content of the anode fuel gas the measured

open cell potential was used along with Equation A.1 and A.2 to calculate the actual H_2O content of the fuel gas as shown below.

$$0.956 \pm 0.004V = \frac{\left(8.314\frac{K}{mol \cdot K}\right)(1123K)}{4\left(96485\frac{C}{e^-}\right)} \ln\left(\frac{0.21atm}{P_{O_2(Anode)}}\right)$$

Solving the equation above yielded $P_{O_2(Anode)}$ of $1.45\times10^{-18}\pm0.22\times10^{-18}$ atm. This value was then used along with Equation A.2 to solve for the H_2O content of the anode fuel gas as shown below.

$$\ln(1.45\times10\text{-}18 \pm 0.22\times10\text{-}18\ \text{atm}) = \frac{2\left(-185875\frac{J}{mol}\right)}{\left(8.314\frac{J}{mol \cdot K}\right)(1123K)} + 2\ln\left(\frac{P_{H_2O}}{\frac{1-P_{H_2O}}{2}}\right)$$

Solving the equation above yielded P_{H_2O} of 0.21±0.01 atm. This H_2O content was then used along with the baseline simulated coal syn gas flow rates to determine the overall composition of the simulated baseline coal syn gas mixture.

Determination of H_2S content of simulated coal syn gas in trial 6:

In order to calculate the H_2S content of the simulated coal syn gas mixture used in trial 6 the H_2O content of the fuel gas had to first be found before a mass balance could be completed to determine the actual H_2S content of the fuel gas. The initial open cell potential of the PSOFC was used to determine the actual H_2O content of the simulated

coal syn gas. The initial open cell potential was used rather than the open cell potential of the PSOFC at the time of H_2S because no degradation of the PSOFC anode could have taken place at this time. It is believed that the CO or H_2S portions of the simulated coal syn gas mixture could lower the measure open cell potential of the PSOFC than would normally be seen so the initially measure open cell potential of the PSOFC was used in this calculation to be conservative. The initially measure open cell potential of the PSOFC when the H_2/N_2 mixture was utilized by the PSOFC was 0.964±0.004 V. This value along with Equation A.1 was used to determine $P_{O_2(Anode)}$ as shown above. This calculation resulted in a $P_{O_2(Anode)}$ of $1.04\times10^{-18}\pm0.16\times10^{-18}$ atm. This value was then used along with Equation A.2 to solve for the H_2O content of the anode fuel gas. The result from this calculation was P_{H_2O} of 0.184±0.110 atm. Using this value and the stated simulated coal syn gas flow rates for H_2, CO, and N_2 a mass balance yielded a simulated coal syn gas mixture that contained 249±9 ppm H_2S.

Least Squares Linear Regression Equations:

The ohmic region data that was obtained from each VI scan was fitted to a simple linear equation shown below as Equation A.3.

$$V = (ASR \times CD) + y_{\text{int}} \qquad \text{Equation A.3}$$

where V is the PSOFC potential (Volts), ASR is the average sum resistance of the PSOFC ($\Omega\cdot cm^2$), CD is the PSOFC current density ($Amps/cm^2$), and y_{int} is the potential intercept determined from regression.

In order to determine then two modeling parameters ASR and y_{int} Equations A.4 and A.6 were used along with the ohmic region data found from each VI scan.

$$ASR = \frac{\sum\left(CD_i - \bar{CD}\right)\left(V_i - \bar{V}\right)}{\sum\left(V_i - \bar{V}\right)^2} \qquad \text{Equation A.4}$$

where ASR is the slope of the regressed line ($\Omega \cdot cm^2$), CD_i is the current density point, $\bar{CD}$ is average current density value of the set of ohmic region data, V_i is the potential data point, and $\bar{V}$ is the average potential value of the ohmic region data. The y-intercept is solved for using Equaition A.5

$$y_{\text{int}} = \sum \frac{CD_i}{n} - ASR \sum \frac{y_i}{n} \qquad \text{Equation A.5}$$

where n is the number of data points.

Once the regressed slope or ASR of the PSOFC was obtained the negative of this number was accepted as the ohmic resistance of the PSOFC for the VI scan that was completed. In order to determine the confidence interval on the ASR value that was calculated Equation A.6 through A.8 were used. In order to determine the precision in which the calculated ASR value described the relationship of the ohmic region data the standard deviation (σ) was calculated with Equation A.6.

$$\sigma = \sqrt{\frac{\sum_{i=1}^{n} (ASR_i - ASR)^2}{n - DOF}} \qquad \text{Equation A. 6}$$

where ASR_i was calculated using Equation A.8, and DOF is the degrees of freedom in the linear model (2).

$$ASR_i = \frac{(y_{\text{int}} - V_i)}{(0 - CD_i)} \qquad \text{Equation A.7}$$

Because the ASR value is a curve-fit relationship the confidence interval is calculated will use σ_{mean}, Equation A.8, because 10 data points are used in each ASR calculation.

$$\sigma_{mean} = \frac{\sigma}{\sqrt{n}} \qquad \text{Equation A. 8}$$

The confidence interval on the calculated ASR value is then found with Equation A.9.

$$CI = t \times \sigma_{mean} \qquad \text{Equation A. 9}$$

where t is obtained from a cumulative t-distribution table for a confidence interval of 95%.

Formation rate of Ni_2S_3 in the PSOFC anode:

The following calculation is an estimate of the worst case situation where all H_2S entering the PSOFC anode will form nickel sulfide without kinetic limitations.

PSOFC Area = 68.1 cm^2
Top Layer = 10μm (40 % porous, 100 volume % Ni)
Second Layer = 25μm (40 % porous, 50 volume % Ni)

$$Ni_{Vol} = \left(0.00681 m^2\right)\left(10\times10^{-6} m\right)(0.4) + \left(0.00681 m^2\right)\left(25\times10^{-6} m\right)(0.4)(0.5) = 6.1\times10^{-8} m^3 Ni$$

$$Ni_{Wt} = \left(6.1\times10^{-8} m^3 Ni\right)\left(8908\frac{kg}{m^3}\right) = 0.55 gNi$$

$$Ni_{moles} = \left(0.55 gNi\right)/\left(58.69\frac{g}{mol}\right) = 0.009 molesNi$$

$$H_2S \text{ Flow Rate} = \left(646.6\frac{smL}{\min}\right)\left(\frac{249 ppmH_2S}{1\times10^6}\right) = 0.161\frac{smLH_2S}{\min}$$

$$H_2S \text{ Molar Flow Rate} = \frac{\left(101 kPa\right)\left(1.61\times10^{-4}\ \frac{L}{\min}\right)}{\left(8.314\frac{kPa\cdot L}{mol\cdot K}\right)\left(273 K\right)} = 7.2\times10^{-6}\ \frac{molH_2S}{\min}$$

$$\text{Time for Ni depletion} = \frac{\left(0.009\frac{molNi}{\min}\right)}{\left(7.2\times10^{-6}\frac{molH_2S}{\min}\right)\left(\frac{1 molS_2}{2 molH_2S}\right)\left(\frac{2 molNi}{1.5 molS_2}\right)} \approx 32 hrs$$